*I bequeath myself to the dirt to grow from grass I love,*
*If you want me again look for me under your boot-soles.*

*-Walt Whitman*

# University of Alberta

Influence of Soil Capping Depth on Water Dynamics in Phosphogypsum Stack Reclamation

by

Andre Forrest Christensen

A thesis submitted to the Faculty of Graduate Studies and Research
in partial fulfillment of the requirements for the degree of

Master of Science
in
Soil Science

Department of Renewable Resources


Fall 2013
Edmonton, Alberta

# Dedication

To my family, friends and love. Thank you for the encouragement and support, without which I would not have succeeded.

# Abstract

The influence of capping soil depth on water dynamics was investigated at a decommissioned phosphogypsum (PG) stack in Fort Saskatchewan, Alberta. PG is a byproduct in phosphoric acid production, a necessary component of phosphorus fertilizer. Currently, there are no environmental regulations governing the depth of capping soil required for PG stack reclamation. Time Domain Reflectometry (TDR), MPS-1 matric potential sensors and conservative tracer application were used to assess water balance across capping soil depths. Results from the varying experiments indicated that an increase in capping soil depth contributed to greater infiltration of spring snowmelt water resulting in deeper penetration of the advective water front into the reclaimed system. Percolation estimates for capping soil depths < 46 cm were < 3% of annual precipitation; however, the temporal variation in downward flux estimates suggest spring snowmelt is the dominant event contributing to percolation.

# Acknowledgements

Dr. Miles Dyck, supervisor, mentor and friend. Thank you for everything you have taught me and your ongoing support. Thank you for the opportunities you have given and continue to give. Thank you to Dick Puurveen. I can't imagine this could have been completed without your help and support. You are a friend, a mentor and a teacher. Words are not enough to express my gratitude to you both. Thank you!

Thank you to Dr. Connie Nichol for all of your support, encouragement and guidance, and thank you for always having some time for a casual conversation, those were the best moments of all. Thank you to Dr. Anne Naeth and Dr. David Chanasyk for your guidance and recommendation throughout the years. I have had the pleasure of knowing Dr. Naeth since my 2nd year of my undergraduate degree and I have come to admire and appreciate all she does for her students and her tenacious teaching style. Thank you, I really do believe you make good students better. A special thank you to Dr. Guillermo Hernadez-Ramirez for taking the time to review my thesis as my external examiner.

Thank you to Hailong He and Amanuel Weldeyohannes for everything each of you have done for me. You are two of the smartest and most driven people I have ever had the pleasure of knowing. Special thanks go out to Giovanna Dragonetti, Pam Sabbagh, Syed Mostafa, Ju Zhang, Amy Gainer, Kelly Kneteman, Lenore Turner, Cory Kartz, Leah Predy, Manjila Shahidi, Tina Harms, Mekonnen Giweta, Sheryl Ramnarine and Jenn Martin for their support and friendship. Thank you to Neeta Gurnani for your friendship, encouragement and support. PG!

To my family, Joel, Tiffany, Lee, Evy, Mecailla, Grant and Laurianne. Your support and encouragement meant everything. Thank you Athena for putting up with me and for all the support, encouragement, laughs and love you provide.

To Alan Harms, Xin (Jean) Zhang and Donna Friesen, thank you for all of your help over the years and the conversations during extractions. To Christie Nohos, Amanda Brown, Mike Abley, Nash Goonewardena and all support staff for everything they do to keep the wheels turning. Christie, you are one of the major reasons for me to ever check my mailbox, thank you for everything you are.

# Table of Contents

# List of Tables

# List of Figures

## 1.0 INTRODUCTION

Phosphogypsum (PG) is a by product of the production of phosphoric acid, a necessary component of phosphorus fertilizers (Luther et al. 1993; Rutherford et al. 1994). The production of phosphoric acid involves the digestion of phosphate rock with sulfuric acid and water. The resulting solution is a combination of gypsum ($CaSO_4 \cdot 2H_2O$), hydrogen fluoride (HF) and phosphoric acid ($H_3PO_4$) (Luther et al. 1993). Once the gypsum material has been filtered from the solution, it is mixed with water to form a slurry which can be pumped into settling ponds (wet stacking). These settling ponds grow as the gypsum material settles out, forming large stacks referred to as PG stacks (Wissa 2002).

Global demand for phosphoric acid-based fertilizers reached 39,785,000 tonnes in 2009, resulting in approximately 180 million tonnes of PG by product (Abril et al. 2009). In Canada, there are PG stacks in Ontario, Quebec, New Brunswick, British Columbia and Alberta (Thorne 1990). Currently the only operational PG stack in Canada is located in Redwater, Alberta, accruing 1.5 million tonnes of PG per year. Upon completion, the Redwater PG stack will occupy a land base of approximately 300 ha and will have a height of 40 m (Nichol 2009). There are numerous naturally occurring impurities in the phosphate source rock including, but not limited to, radium ($^{226}Ra$), uranium ($^{238}U$), arsenic (As), barium (Ba), cadmium (Cd), chromium (Cr), lead (Pb), mercury (Hg), selenium (Se) and fluoride ($F^-$) (Rutherford et al. 1995).

These trace elements can potentially accumulate in the PG by product, and in the water held within its pore space, depending on the chemical and physical nature of the elements. The introduction of precipitation into the PG stack can facilitate the mobility of these trace elements as well as dissolve the gypsum material (SENES 1987); therefore, the objective for PG stack reclamation is to minimize interaction between percolating water and the PG material. Currently, there are no environmental regulations governing the reclamation of PG stacks; however, within the context of an approval process proponents are required to provide comparative results to the Nominal Base Case Reclamation Plan which includes, but is not limited to; 1) removal of infrastructure; 2) erosion control; 3) final use of reclamation area; 4) revegetation; 5) reclamation sequence and schedule; 6) pre-reclamation and post-reclamation water management; and 7) soil replacement of at least 1 m (Alberta Environment 2008).

The default recommendation of 1 m of cover soil is subject to evaluation if a shallower depth is found to be adequate for fulfilling the reclamation objectives. The purpose of this research is to investigate differing topsoil thicknesses to further understand the dynamics of water percolation and infiltration and their role in the overall hydrological environment within the context of PG stack reclamation.

## 1.1 Phosphogypsum Production and Physiochemical Characteristics

### 1.1.1 Production

Phosphoric acid (PA) is a necessary component in the production of phosphate fertilizers. The most common technique used in PA production involves a wet process of digesting phosphate rock with sulfuric acid and water to produce calcium sulfate dihydrate (gypsum), phosphoric acid and hydrogen fluoride according to the following reaction (Becker 1989; Rutherford et al. 1994):

$$Ca_{10}(PO_4)6F_2 + 10H_2SO_4 + 20H_2O \rightarrow 10CaSO_4 \cdot 2H_2O + 6H_3PO_4 + 2HF$$

The gypsum material that is produced in the wet process reaction is filtered from the liquid phase and mixed with water to form a slurry which is then pumped to a disposal or holding area (Becker 1989). In most cases the slurry material is transferred to settling ponds where the gypsum material settles out of suspension and the processed water is recycled. These settling ponds grow as the gypsum material settles out forming large stacks, referred to as PG stacks (Wissa 2002).

Approximately 4 to 5 tonnes of PG are produced for every tonne of PA (Thorne 1990). The amount of PA produced and the form of gypsum depends on the operating acid concentration and reaction temperature. The most common PA process (dihydrate) produces 28-30% acid and is the most widely used method in North America (Becker 1989; Kouloheris

1980). In 2009, global estimates of annual PG production had reached 180 million tonnes (Abril et al. 2009). In Canada, conservative projections estimate total PG production to date to be approximately 100 million tonnes (Rutherford et al. 1994). In Alberta there are PG stacks located in Medicine Hat, Calgary, Fort Saskatchewan, and Redwater accounting for 60% of the nation's total PG stockpile. Currently the only operational PG stack in Canada is located in Redwater, Alberta, and is growing by approxiamately 1.5 million tonnes of PG per year (Nichol 2009).

### 1.1.2 Chemical Characteristics

The source material for PA production is phosphate ore which can be of sedimentary, or of igneous and metaphoric origins. Sedimentary phosphates represent 85% of known phosphate rocks and are the most easily mined deposits (Becker 1989; Habashi 1980). Chemical composition of sedimentary phosphate rock deposits vary widely due to geographic location and the nature of their depositional environment. Major components include calcium oxide (CaO) (29-54%), phosphorus pentoxide ($P_2O_5$) (24-40%), silicon dioxide($SiO_2$) (0.1-14%), fluorine(F) (1.3-4.1%), carbon dioxide ($CO_2$) (0.2-7.3%), sulfur trioxide ($SO_3$) (0.0-3.3%), aluminum oxide ($Al_2O_3$) (0.2-1.8%), iron(III) oxide ($Fe_2O_3$) (0.1-2.6%), magnesium oxide (MgO) (0.0-2.2%) and sodium oxide ($Na_2O$) (0.2-1.5%) (Rutherford et al. 1994). $P_2O_5$ is the conventional form describing the phosphorus component in phosphate mineral; however, the primary

form of phosphate minerals that occur in nature include fluor-apatite ($Ca_{10}(PO_4)_6F_2$), hydroxyl-apatite ($Ca_{10}(PO_4)_6(OH)_2$), carbonate-hydroxy-apatite ($Ca_{10}(PO_4,CO_3)_6(OH)_2$) and francolite ($Ca_{10-x-y}Na_xMg_y(PO_4)_{6-z}(CO_3)_zF_{0.4z}F_2$) (van Straaten 2002).

Currently, the only producer of PA in Canada, Agrium Inc., had until recently received its supply of phosphate source material from its mine in Kapuskasing, Ontario. The majority of these deposits consisted of unconsolidated apatite sands, with minor components consisting of phosphate rich cemented material. These deposits range in purity from 0 to > 40% $P_2O_5$ and are grouped into categorical grades which are dependent upon their phosphate and iron content. Typically the highest grade material, A Grade, is defined by high phosphate and low iron content (> 30 wt% $P_2O_5$ and 0 to 8 wt% $Fe_2O_3$) (Pressacco 2001).

PG is primarily comprised of Ca and $SO_4$ in the form of gypsum (Berish 1990). Impurities which may be present in PG include quartz, fluorides, phosphates, organic matter, and aluminum (Al) and iron (Fe) minerals (Collings 1980; Luther et al. 1993). Trace elements such as As, Ba, Cd, Cr, $F^-$, Pb, Hg, Se, silver (Ag), manganese (Mn) and $^{238}U$ decay products can be elevated within the PG material as well the pore water (Wissa 2002). The chemical composition of PG is highly dependent upon numerous factors including source rock composition, chemical signature of acids used during digestion, process efficiency, post production

contamination and environmental impurities in the form of rainwater (Arman and Seals 1990).

PG is an acidic substance due to the acidic byproducts (i.e. HF) which are inherent given the production process. PG typically has an average pH between 3 and 4; however, this will depend on the production process (Collings 1980). Studies observed pH between 2.1 and 5.5 for Florida PG (May and Sweeney 1984), while PG from Alberta was reported as less than 4 (Luther et al. 1993). PG material that has been aged and leached can reach pH approaching neutrality (SENES 1987). PG that is stored at lower pH is susceptible to migration of mobile trace elements under conditions favorable to transport, which can have significant environmental implications (Rutherford et al. 1994).

### 1.1.3 Physical Characteristics

The chemical composition of PG is dominated (>90%) by gypsum ($CaSO_4 \bullet 2H_2O$) and therefore shares similar physical characteristics to gypsum. PG is weakly soluble (2.81 – 2.63 g $L^{-1}$) and has a particle density between 2.27 and 2.40 g $cm^{-3}$ (Rutherford et al. 1994; Seifert et al. 2002). Typical gypsum crystals are characterized as medium to fine with an average diameter of < 0.075 mm (May and Sweeney 1984; SENES 1987; Wissa 2002). Size and morphology of crystal structure depends on numerous parameters including particle size of pre-digested phosphate rock, operating acid concentration, chemical impurities in source material,

reaction temperature and excess acid in post-digestion slurry (Becker 1989; Rutherford et al. 1994). Bulk density of PG varies between 0.9 and 1.7 g $cm^{-3}$ (Keren and Shainberg 1981; May and Sweeney 1984; Vick 1977).

Free water content of PG following filtration on the production line is between 25 and 30% (Wissa 2002). Free water content within the PG stack however, varies greatly on depth of sample, temporal variability of sampling interval, allowable drainage duration and weathering (Rutherford et al. 1994). SENES (1987) reported the vertical hydraulic conductivity of PG to range between 1.0 X $10^{-3}$ and 2.0 X $10^{-5}$ cm $s^{-1}$. Hydraulic properties within PG stacks are influenced by processes such as overburden compression, which increases the density and decreases the permeability (Wissa 2002).

### 1.1.4 Mineralogical and Geomorphic Characteristics

The crystal morphology of PG is highly influenced by the production process. Factors that control the shape and dimensions of crystal formation include: (1) type of phosphate source material; (2) particle size of phosphate source material; (3) concentration of operation acid; (4) solids content and sulfuric acid content in process slurry; (5) chemical impurities in phosphate source material; and (6) variability in fertilizer production process such as temperature, stock ratios, recirculation and agitation (Becker 1989). Common gypsum shapes include needles,

rhombic and X-shaped swallowtail twins, flat table-like, clusters and thick rhombic types (Figure 1.1). Table-like elongated crystals are the most common (Becker 1989); however, May and Sweeney (1984) reported PG from Florida as exhibiting tabular diamond-shaped morphology, and Luther et al. (1993) observed larger crystals with dimension 8:6:1.The mineralogical characteristics of PG are dependent upon the nature of the phosphate source material, type of reaction used, operational efficiency, stockpile age, and post production environmental contamination (Arman and Seals 1990).

### 1.1.5 Radiological Characteristics

Relative to most geological and soil materials, PG is more radioactive due to the naturally occurring radionuclides contained within the phosphate source material (Rutherford et al. 1994; Santos et al. 2006a). The two dominant radionuclides present in phosphate rock are uranium-238 ($^{238}$U) and thorium-232 ($^{232}$Th). The decay series for $^{238}$U and $^{232}$Th within the phosphate rock material partitions during the PA process reaction. The resulting daughter products of radium ($^{226}$Ra) and polonium ($^{210}$Po) for uranium and thorium, respectively, accumulate in the PG material due to their integration with insoluble sulphates of the crystalline structure, while $^{238}$U, $^{232}$Th, and Lead ($^{210}$Pb) distribute into the PA (Abril et al. 2009; Dueñas et al. 2007; Hanson and Laird 1990; Rutherford et al. 1994; Santos et al. 2006a).

$^{226}$Ra and $^{210}$Po have half-lives of 1620 years and 138 days, respectively. The daughter product of $^{226}$Ra is Radon ($^{222}$Rn), a highly mobile gas with a half-life of 3.8 days, which in turn will eventually decay to $^{210}$Pb and $^{210}$Po (Hull and Burnett 1996; Rutherford et al. 1994). As a result of the extended half-life of $^{226}$Ra the environmental implication of the PG stack reclamation is an ongoing concern (Abril et al. 2008; May and Sweeney 1994; Roessler et al. 1979; Rutherford et al. 1993; Rutherford et al. 1994; Rutherford et al. 1996).

## 1.2 Phosphogypsum Uses and Disposal Methods

### 1.2.1 Disposal Methods

Globally, there are four methods that are utilized in the disposal of excess PG material including: (1) discharge to open bodies of water; (2) back filling of exhausted mine pits; (3) dry stacking; and (4) wet stacking (Wissa 2002). The last two mentioned methods might be more appropriately referred to as long term storage options, as the term “disposal” would infer the absence of future utilization.

Discharging PG into open bodies of water is restricted due to environmental, political and biological factors. The method involves the addition of PG material with water to form a slurry which can be discharged into large bodies of water that are uninhabited and have strong currents (Wissa 2002). In Morocco, for example, fertilizer producers can

discharge 9.1 million tonnes of PG material into the Atlantic Ocean annually (Becker 1989). The bodies of water that can receive the PG material have to be of saline nature and constantly in motion to prevent sedimentation; however, most active phosphate fertilizer operations are not located near such bodies of water (Wissa 2002).

Backfilling of exhausted mine pits is becoming an attractive option for disposal of PG material because it has the advantage reducing cost and creating an environmentally acceptable means of disposal. The method would involve blending overburden material or mine tailings with PG to fill the pits that were created during mining activity. Currently this method is limited by the properties of the PG material such as compressibility, solubility, and radioactivity (Dippel 2004; Wissa 2002). Other issues associated with this method involve the political ramification of transferring one province's "waste product" to another. While the goals of each active party are potentially fulfilled, the public's perception of the material as a waste product will limit its uses in reclamation across provincial boundaries.

Dry stacking of PG material is predominantly used in areas where water availability is scarce. This method requires the transport of filtered PG material from the production plant to a storage area by means of either vehicles (trucks, trains, loaders, etc.) or by a system of conveyor belts. Once the PG material is transferred to the storage area it is reworked by machines to level the piles into more manageable stacks (Wissa 2002).

While this method does have advantages in water scarce locations, it does create circumstances that can lead to environmental contamination in the form of air emissions. When PG material is left undisturbed it will form a thin crust that prevents wind erosion; however, when this crust is disturbed by mechanical means the PG material can become air borne and hazardous to the environment (Wissa 2002).

Wet stacking is the dominant method used for storing PG material and is widely used in Europe and North America. The method involves mixing water (salt or fresh) with the filtered PG material to form a slurry, which can be pumped through pipes from the production plant to settling ponds. As the PG settles from solution the process water is decanted and reused in the transport system or discharged into bodies of water depending on the plants operational demands. The ponds are engineered to retain vast amount of PG material and can grow to immense scales, occupying hundreds of acres of land. Historically regulatory guidelines for PG stack construction were limited; however, currently most stacks in North America are required to have a high density polyethylene liner (HDPE) installed as a barrier between the PG stack and the underlying substrate (Alberta Environment 2004; Florida Department of Environmental Protection 2006).

### 1.2.2 Current Utilization of Phosphogypsum

According to May and Sweeney (1984), PG cannot be classified as toxic waste because it is neither corrosive nor is the average total elemental concentration above the acceptable limit for toxic hazardous waste; however, utilization of PG is limited due the presence of radionuclides and the radiological emissions that are a result of the decay process inherent in the phosphate source material (Rutherford et al. 1994). While commercially viable solutions are not at present available for reutilization in North America, a number of other uses are being tested and implemented in various industrial sectors including environmental restoration, agriculture and construction (Dippel 2004; Degirmenci et al. 2007; Kazman et al. 1983; Rechcigl et al. 1993; Rutherford et al. 1994).

Agriculturally, PG is used as a soil conditioner and amendment to enhance the various physical and chemical properties of the soil to a more desirable state. Kazman et al. (1983) concluded that the addition of PG to sodic soils increased infiltration rates which could be useful in combination with liming to decrease exchangeable sodium. In general crop yields have been found to be higher in soils that have been amended with PG (Beretka 1990; Novikov et al. 1990). However, another study investigated the response of PG to plant growth and the results did not support any positive response of plant growth to PG applications at either 2.2 Mg $ha^{-1}$ or 4.4 Mg $ha^{-1}$(Rechcigl et al. 1993). In terms of plant nutrients, PG has been used as an effective source of Ca, S, and P due to its expedited

dissolution rate and its capacity to delivery soluble nutrients during crop growth (Bianco et al. 1990; Gascho and Alva 1990; Malavolta et al. 1987; Singh et al. 1990).

PG uses in the construction and engineering fields have been explored in great detail. Studies have investigated the use of PG for erosion control (Agassi et al. 1985; Agassi et al. 1990; Agassi and Ben-Hur 1991; Frenkel et al. 1989; Gal et al. 1984), soil stabilization (Degirmenci et al. 2007; Degirmenci 2008), construction aggregate (Foxworthy et al. 1994; Ghafoori and Chang 1993; Qiao et al. 2010), and mine backfill (Dippel 2004). In Alberta the most supported alternative uses for PG include: landfill cover system, cementing agent, compost conditioner, road base building material, and tailings flocculant (AMEC 2006). Partnership between Agrium and Syncrude in the late 1990s explored the beneficial uses of PG for accelerated densification of oil sands tailings that would utilize 80,000 tonnes per year; however, the effectiveness of the pilot project was hindered by the introduction of locally generated source of gypsum material therefore eliminating the need for PG (AMEC 2006).

## 1.3 Environmental Implications Associated with Phosphogypsum

Environmental contamination resulting from PG production, transport, and storage may occur in the form of the following: (1) atmospheric contamination from emission of $F^-$ or other toxic elements; (2)

groundwater contamination from PG leachate; (3) $^{226}Ra$ emissions; (4) exposure of radioactive dust and other airborne elements; (5) direct exposure to gamma radiation from PG material (Rutherford et al. 1994); and (6) water and wind erosion (Rydzynski 1990).

### 1.3.1 Erosion Potential

Water and wind erosion can be a potential environmental hazard associated with PG disposal and storage. While PG material is primarily comprised of Ca and $SO_4$ it can contain up to 4% of $F^-$, which is isolated as a potential concern for environmental contamination (Rutherford et al. 1994). Physical redistribution of PG can be achieved by mechanical means on active PG stacks by operational equipment such as transport vehicles (Norlander 1998; Wissa 2002). Wind can expedite the transport of particulate matter off site and greatly increase the area of impact. Elevated levels of $F^-$ have been found in plant material within close proximity to PG stacks; however, the source of $F^-$ is unclear as it may be traced to the pond water and not the PG material directly (McLaughlin 1986; Rutherford et al. 1994). The leading concern regarding plant uptake of $F^-$ is the transfer function of this contaminant to other biological vectors including wildlife and possibly human consumption which can lead to fluorosis (Weinstein and Davidson 2004; Wissa 2002).

The introduction of water into the surficial system of a PG stack can have profound impacts on erosion potential. Most notably is the potential

for PG dissolution in the presence of water which can lead to sinkholes and solution cavities (Rutherford et al. 1995; SENES 1987). While PG is weakly soluble in water it can have profound impacts on larger scales. Deep cavities can create direct conduits for subsurface contamination and structural instability (Wissa 2002); furthermore, overland flow of water that has been contaminated by PG can migrate to open bodies of water and impact the biological community (Haridasan et al. 2001; Pérez-Lopéz et al. 2010).

### 1.3.2 Groundwater Contamination

Groundwater contamination may occur as a result of process water seepage in active stacks or by downward leaching of infiltrating precipitation on inactive stacks (Rutherford et al. 1994; SENES 1987). Hydrogen fluoride contaminant that may be present in the PG material can interact with the silicate minerals ($MAlSiO_2$) resulting in dissolution and the formation of silicon tetrafluoride ($SiF_4$) as described by the equation:

$$H_2O + HF + MAlSiO_2 \rightarrow M^+ + AlF_2^+(4H_2O) + SiF_4 + nH_2O$$

In some instances $SiF_4$ may undergo hydrolyses to form fluorosilicic acid ($H_2SiF_6$) resulting in the dissolution of clay particles within the subsoil matrix, allowing accelerated movement of contaminants into the groundwater (Motalane and Strydom 2004; Rutherford et al. 1995).

Acidic seepage through the protective liners or subsoil bases can negatively impact groundwater resources by increasing the mobility of

trace elements and radionuclides that are detrimental to human health and the general environment (Cañete and Palad 2008; Rutherford et al. 1994; Rutherford et al. 1995). The presence of alkaline subsoil and groundwater may act to buffer the effects of acid seepage, thereby minimizing the mobility of heavy metals including nickel (Ni), cobalt (Co) and copper (Cu) (Pérez-López et al. 2007; SENES 1987); however, $SO_4^{2-}$ and $F^-$ are marginally affected by pH changes and therefore are still of environmental concern (Rutherford et al. 1994).

Rutherford et al. (1994) summarized several groundwater studies conducted in North America as well as Africa. The findings varied greatly with respect to the magnitude and spatial distribution of contaminants including $F^-$, Fe, $SO_4^{-2}$, Ca, Cr, Mg, molybdenum (Mo), Cu, zinc (Zn) and $^{226}Ra$ due to the climatic and geologic variability. Other studies on the presence of natural radionuclides in aquatic environmental near PG disposal area concluded that elevated levels of $^{226}Ra$ where present in river water adjacent to a PG stack and that concentrations were influenced by seasonal variability (Azouazi et al. 2001; Haridasan et al. 2002). A review of groundwater studies conducted in southern Alberta concluded that $SO_4^{-2}$ and $F^-$ concentrations were elevated with respect to background levels and that heavy metals were not of a concern because of the elevated groundwater pH of the surrounding area would limit their mobility (SENES 1987 in Rutherford et al. 1994).

### 1.3.3 Radiological Emissions

Natural occurring radionuclides such as $^{238}U$ and $^{232}Th$ are present within the phosphate rock source material which is used in the production of phosphate based fertilizers. The exact proportion of each parent radionuclide is dependent upon the geologic formation from which the source material was obtained and varies greatly from region to region (Rutherford et al. 1994; Silva et al. 2010). According to the decay series for $^{238}U$ the most active radionuclides include $^{226}Ra$, $^{222}Rn$, $^{210}Pb$ and $^{210}Po$ all of which can be found within the PG material. Notably $^{226}Ra$ is of concern for its elevated presence in the PG material, its longer half-life (1620 years), and its alpha decay product, $^{222}Rn$. While $^{222}Rn$ has a half-life of 3.8 days its radiotoxicity and expedited mobility elevates the seriousness of the potential exposure pathways (Abril et al. 2008; Dueñas et al. 2007; Rutherford et al. 1994; Santos et al. 2006b). Studies have indicated that emission of $^{222}Rn$ is directly related to $^{226}Ra$ concentrations, porosity, bulk density of soil and daily evapotranspiration potential (Abril et al. 2008; Dueñas et al. 2007).

Gamma radiation and $^{222}Rn$ emissions all contribute to the overall hazards associated with radiation exposure. Gamma radiation from PG stacks are a function of stack size, exposure distance from stack and concentration of gamma emitting radionuclides (FDEP 2006). Direct radiation from PG stack exposure is primarily a concern for individuals who work and/or live near the stacks due to the fact that gamma radiation diminishes with

distance from the source (Berish 1990). Major health concerns with gamma radiation include damage to blood forming organs and the central nervous system, skin burns, hair loss and even death (Argonne National Laboratory, Environmental Science Division 2005). Radiological emissions that are generated from $^{222}Rn$ are dependent on $^{226}Ra$ concentrations, porosity within PG stack, water content and potential evapotranspiration. Since $^{222}Rn$ is gaseous in nature it will never be eliminated completely as a source for radioactive contamination and therefore needs to be minimized with the use of cover systems that have lower permeability (SENES 1987).

## 1.4 Cover Systems for Waste Isolation

Currently, the most widely accepted management strategy for large volume isolation of low-value waste material is based on the philosophy of containment rather than remediation and is reliant on the fundamentals of risk management. The purpose of containment is to prevent or minimize the movement of waste to and through various environmental receptors. Ultimately the objective of a cover system is to 1) minimize interaction between precipitation and the waste material; 2) isolate the waste; and 3) control the release of gases produced by the waste (Hauser 2009). In the context of risk management the objective of a containment system is to minimize the risks associated with environmental liability.

These cover systems vary in their functionality and can be grouped into two categories including conventional and alternative cover systems. In general a cover system should work in harmony with the other functional components of a containment system (i.e. liners and drainage systems) to satisfy the overall isolation objectives; however, in order to fulfill these objectives consideration needs to be focused on the physical and biological factors pertaining to the cover design as well as the abiotic environmental factors that will define the boundary condition applied to the cover system (Hauser 2009).

### 1.4.1 Conventional Cover Designs

Waste cover systems are typically separated into either conventional cover systems, or alternative cover systems. Currently, most landfill cover systems in place are conventional in design and generally employ barrier technology. These conventional cover systems typically include several layers placed above the waste material (Koerner and Daniel 1997; US EPA 1991) (Figure 1.2).

The top layer, also known as the cover layer, consists of a cover soil and is in place to provide a medium for plant growth which provides control for wind and water erosion as well as provides protection to the underlying layers. The cover layer can range between 15 and 100 cm in thickness (Alberta Environment 2010; Hauser 2009); however, the thickness of the cover layer is generally regarded as dependent upon the

climate, soil properties, and vegetative type (Hauser and Gimon 2004). Various manipulations to the cover layer might be required depending on the specific nature of the site. For example, high wind erosion potential might require coarse textured material to be mixed into the cover layer, or cobble stones to prevent animal intrusion (Hauser 2009).

The second layer is known as the drainage layer. This layer typically consists of a highly permeable substrate material usually sand, gravel, or some geosynthetic material. The function of the drainage layer is to remove the excess precipitation that percolates through the cover layer (Albright et al. 2004). By removing the water that has percolated from the cover layer, the drainage layer effectively removes or reduces the hydraulic head that would otherwise be present on the next layer, the barrier layer. The drainage layer also provides slope stability by minimizing pore water pressure within the matrix of the material directly above the barrier layer (Hauser 2009).

The third layer is the barrier layer and is the central component of conventional cover systems. The barrier layer can consist of a single material or a combination of several materials. In general this layer minimizes percolation by creating a physical barrier which opposes the natural downward gravitational flow of water. Compacted clay layers (CCLs) are the most widely used barrier layer, typically 60 cm in thickness (Alberta Environment 2010; Hauser 2009); however, other materials that can be used include: geosynthetic clay (GC), high-density polyethylene

(HDPE), linear low-density polyethylene (LLDPE), polypropylene (PP), and polyvinyl chloride (PVC) (Hauser 2009). According to Federal regulation in the United States, to satisfy the requirements for a barrier layer the material must have a saturated hydraulic conductivity of < 1.0 X $10^{-7}$ cm $s^{-1}$ (US EPA 1991); however, in Alberta the standards for landfills only require a saturated hydraulic conductivity of < 1.0 X $10^{-6}$ cm $s^{-1}$ (Alberta Environment 2010).

The fourth layer is the gas collection layer and is ubiquitous with a barrier layer such that the barrier layer will often trap and accumulate potentially harmful gasses below the cover layer. While this layer is not always required for all types of waste isolation facilities, it is required for waste materials that are susceptible to decomposition, or evaporation of organic compounds (Hauser 2009). The collection of the gasses can be either passive (i.e. venting to the atmosphere) or active (i.e. collected for reuse). Similarly to the drainage layer, the gas collection layer should have high permeability characteristics to expedite the movement of landfill gasses (Albright et al. 2004).

The final layer is known as the foundation layer and its function is to provide separation between the various functional layers and the waste material. The foundation layer also established the necessary surface grade and provides a stable working surface (Hauser 2009).

### 1.4.2 Alternative Cover Design

The alternative to the conventional cover designs entail the removal of the barrier layer and requires more emphasis be placed on the natural water holding properties of the soil and the closed loop continuum of evapotranspiration (Figure 1.3). These alternative cover designs usually employ a layer of soil which acts as a reservoir temporarily storing infiltrating precipitation until evapotranspiration can remove the water from the system (Hauser 2009). Various alternative cover designs have been proposed including modified surface runoff (MSR), infiltrate-stabilize-evapotranspire (ISE), and vegetative covers (Albright et al. 2004; Hauser 2009). Under MSR cover systems the goal is to divert precipitation into rain gutters in an attempt to minimize the amount of water available for infiltration. In a study by Schulz et al. (1997) the researchers concluded that approximately 70% of observed annual precipitation (> 1000 mm) was diverted from the site and 30% was removed through evapotranspiration.

The success of this system was noted to be used with caution due to the costs associated with maintenance and repairs. Furthermore, the site location was specific to an underground nuclear waste storage facility of minimal size in comparison to the land base required for other landfills (Schulz et al. 1997). Other studies concluded that MSR cover systems are hindered by low oxygen levels within the soil due to compaction, resulting in limited root development; furthermore, vegetation might also reduce the

effectiveness of the system due to unforeseen disturbances to the rain gutters (Chittaranjan 2005; Karr et al. 1999).

ISE cover systems as introduced by Blight (2006) are described as non-vegetated, compacted soil covers that promote a continuous wetting of the waste material to facilitate waste decay in areas of low precipitation. The system function solely by evaporation since no vegetation is present. The ISE cover system while effective in areas of extremely low precipitation is impractical in areas where precipitation is not limited (Blight 2006).

The vegetative cover system, also referred to as an evapotranspiration (ET) cover system, employs a layer of soil which acts as a water reservoir effectively retaining precipitation until the natural process of evapotranspiration is able to remove the water (Anderson 1997). The ET cover system is a cost effective alternative to conventional waste isolation methods; however, considerations regarding the biological and physical nature of the environment need to be address on a site specific criteria.

### 1.4.3 Factors Influencing Effectiveness of ET Cover Systems

Several considerations need to be addressed when designing a ET cover system including: 1) climate; 2) hydrogeology; 3) gas production; 4) cover soil characteristics; 5) vegetation characteristics; 6) seismic environment; and 7) end land use (Hauser 2009), of which the physical

and biological attributes of the soil and plant community as well as climatic variability are of the utmost importance.

#### 1.4.3.1 Climate

Various climatic variables greatly influence the effectiveness of an ET cover system, of which precipitation (i.e. rain and snow), ambient air temperature, wind, relative humidity, and solar radiation are the dominant factors (Hauser 2009). Temporal and spatial distribution of precipitation will greatly impact infiltration of water into and potentially through the ET cover system. For example, the average annual precipitation in Fort Saskatchewan is 459.5 mm, 104.6 mm of which is deposited as snow (Environment Canada 2012).

Given that snow accounts for 23% of the annual precipitation in Fort Saskatchewan, it is paramount to realize that when the water stored in the snowpack becomes available to the environment in the form of snowmelt, the plant communities are still inactive and unable to transpire that amount of water. The result of this scenario is an excessive amount of free water that is potentially available for infiltration, percolation, runoff, or evaporation. Under this circumstance it is clear that seasonal climatic variation can greatly impact the effectiveness of an ET cover system; however, daily climatic variation can have just as strong an impact. For example, if 40 mm of rain was to fall on a given area over a week time period in mid-July the potential for deep percolation might be far less than

if 40 mm of rain had fallen at the same location during a single storm event.

Within the context of these examples precipitation is the dominant factor; however, precipitation alone is but one climate variable. Relative humidity, air temperature, solar radiation and wind will influence ET rates (Hauser et al. 2001; US EPA 2003); so while precipitation will govern the amount of water that will be available to the environment, the other climatic variables will govern how well the ET cover system will potentially function.

#### 1.4.3.2 Cover Soil Characteristics

Local soil characteristics and availability are important considerations for determining the potential effectiveness of an ET cover system (Hauser 2009). Texture, soil fertility, storage capacity, hydraulic conductivity, bulk density, and soil thickness are some of the key elements that are used in designing an ET cover system. Typically, finer textured materials (i.e. silts and clayey silts) are more favorable for their greater storage capacity in comparison to sandier materials; however, sandy soils can be used as a bottom layer to create a capillary barrier which can provide contrast in unsaturated hydraulic properties between the two layers (US EPA 2011).

In general, the effectiveness of an ET cover system is reliant on the physical characteristics of the cover layer; therefore, use of a readily

available soil with inadequate water holding capacity, for example, may be impractical (Hauser 2009). Other physical properties of soil, such as hydraulic conductivity and water retention characteristics, will impact such parameters as infiltration and water redistribution, both of which will greatly influence the effectiveness of an ET cover system. For example, a cover soil with extremely low hydraulic conductivity will inhibit long term infiltration and result in increased potential for runoff; conversely, a cover soil with an extremely high hydraulic conductivity and low water holding capacity will expedite the flow of water from the surface to depth and potentially result in an positive head boundary condition on the waste material interface.

Other soil physical properties, such as bulk density, texture and soil thickness, will impact not only the hydraulic properties mentioned, but the biological features that will ultimately provide the ET component of the cover system. For example, soils that have high bulk densities might inhibit root development and limited water holding capacity which will limit the growth of the plant and result in limited ET potential (Hauser 2009). The thickness, or depth, of the cover soil is a critical parameter for balancing the costs of the system with the physical and biological requirements for the cover system. In general, the depth of the cover soil will depend on the storage capacity requirements, which will be determined by the specific location's water balance (US EPA 2011). For example, a thin cover soil in a humid environment, while relatively

inexpensive with respect to transportation and generation costs, might not provide adequate storage capacity and rooting volume, resulting in an ineffective ET cover design.

#### 1.4.3.3 Vegetation Characteristics

Vegetation selection for ET cover systems is primarily based on whether the plant species is native to the area as well as the physiological and aesthetic characteristics. The function of the plant community in the context of a cover system is to promote transpiration and provide erosion control for the cover soil. Vegetation including grasses, shrubs, and trees are commonly used on ET cover systems; however, the specific selection of each will depend on the overall ET cover system objective. For example, deep rooting perennials might be appropriate if the cover soil is thick and the penetration of roots into the waste material is advantageous; however, if the philosophy of isolation and containment is to be observed than the use of a shallow fibrous rooting perennial might be more appropriate.

According to Jackson (2009), plant species selection for PG stack reclamation was based on characteristics including: 1) high germination and establishment rates; 2) root development that would provide erosion control; 3) resilient to fluctuation in climatic conditions that were present on site; 4) low nutrient requirements; and 5) tolerance to acidic environments.

## 1.5 Phosphogypsum Stack Reclamation

### 1.5.1 General Reclamation Objectives

Common reclamation objectives in North America include: (1) prevention of contaminated water from entering the environment by means of surface or groundwater flow; (2) sustain structural integrity of PG stack; (3) minimize radionuclide emissions from PG stack; and (4) minimize interaction between precipitation and PG material (Alberta Environment 2008; FDEP 2006). Other reclamation objectives that are more specifically engaged towards end land use will be subject to the various proponents involved. In general, a cover system is the most suited strategy for fulfilling the desired objectives.

Final cover systems for PG stack reclamation are generally comprised of two main components. The first component is a physical barrier constructed of a low-permeable soil or amended PG, or a synthetic barrier, such as a HDPE liner. The purpose of this barrier is to physically limit precipitation from infiltrating into the PG stack. The second component is the biological element, or the living organisms that will effectively manage the precipitation that is able to infiltrate and limit the amount of water available for percolation into the PG stack (FDEP 2006). These biologically engineered cover systems can be effective at preventing wind and water erosion, minimizing infiltration and percolation,

limiting radionuclide emissions, and adequately providing a medium for plant growth (Jackson 2009; Hallin 2008).

### 1.5.2 Regulatory Framework

The *Canadian Guidelines for the Management of Naturally Occurring Radioactive Materials* (NORM) were set in place as a means for identification, classification, handling, and materials management of NORM in Canada; however, these guidelines are only applicable to PG in terms of reuse limits and not inclusive of reclamation standards (Health Canada 2000). Regulatory guidelines for PG stack reclamation do not exist in Canada at the federal level and therefore are addressed at the provincial level on a case-by-case basis.

In 2008 Alberta Environment issued an approval for the construction, operation and reclamation of the Redwater fertilizer manufacturing plant. Within the terms and conditions of the approval, Agrium Products Inc. must provide a comparison of research results to the Nominal Case Reclamation Plan which includes at a minimum: (1) the final use of the reclaimed area; (2) removal of infrastructure; (3) soil replacement of at least 1 m; (4) erosion control; (5) revegetation; (6) reclamation sequence and schedule; and (7) water management prior to and after reclamation. Under this approval the replacement of at least 1 m of soil is subject to investigation by the active parties to evaluate the

suitability of a shallower depth of cover soil in the fulfillment of the reclamation objectives (Alberta Environment 2008).

## 1.6 Previous Research Conducted on Decommissioned PG Stack in Fort Saskatchewan

Three studies were conducted at the Agrium Nitrogen Operation facility in Fort Saskatchewan between the years of 2006 and 2012 (Jackson 2009; Hallin 2009; Turner 2013). In these studies researchers investigated several aspects of PG stack reclamation including: (1) chemical and physical evaluation of substrate; (2) response of capping soil thickness on plant development; (3) evaluation of water quality and quantity; and (4) response of capping soil thickness on $^{222}Rn$, gamma radiation and HF emissions (Jackson 2009; Hallin 2009; Turner 2013).

### 1.6.1 Evaluation of Capping Soil on Plant Development

Plant health and vigor were not affected by capping soil depth and were not influenced by root development into PG material. Capping depths of 8 to 15 cm were sufficient in providing an adequate medium for plant development (Jackson 2009; Hallin 2009; Turner 2013); however, the control plots that contained 0 cm of capping soil had minimal plant growth present (Jackson 2009). Post reclamation plant community was highly influenced by predisposed plant community present within the seed bank of the capping soil (Jackson 2009; Hallin 2009). Plant communities

that were present on the plots were sufficient in preventing erosion of substrate; however, further investigation into localized soil/PG anomalies need to be addressed (Hallin 2009). Maximum rooting depth increased with capping depth; however, total biomass did not increase for capping depths > 8 cm (Turner 2013). Fluoride, Co and Ni concentration were elevated in some plant material located on site relative to reference plant material; furthermore, F and Co concentrations were positively associated with decreases in capping depth (Turner 2013).

### 1.6.2 Water Quality and Quantity within PG Stack and Near Surface Pathways

Water percolation as represented by an increase in PG water content below soil/PG interface was generally negligible regardless of rainfall event magnitude and infiltration (Jackson 2009; Hallin 2009). Water content below soil/PG interface declined marginally during the growing season and generally was between field capacity and permanent wilting point for all treatment depths (Jackson 2009). Soil water content was lower in the 91 cm plots when compared to other treatment; therefore, capping depth < 46 cm was recommended to maintain adequate moisture for plant growth (Turner 2013).

Quality of runoff water exceeded aquatic life guidelines for Cd, Cu, Se, Zn, and nitrate ($NO_3$), but were below drinking water guidelines. Total dissolved P, $SO_4^{-2}$, total dissolved solids (TDS) and electrical conductivity

(EC) had the highest levels of exceedance, but could be attributed to the contamination from PG dust that would otherwise not be present post reclamation (Hallin 2009; Hallin et al. 2010). Soil and PG pore water quality exceeded criteria outlined by the Canadian Council of Ministers of the Environment (CCME) and Alberta Environment for Al, Ni, Cd and $F^-$ (Jackson 2009).

### 1.6.3 Influence of Capping Soil Depth on Radon Gas, Gamma Radiation and HF Emissions

Gamma radiation for the decommissioned stacks was documented as below guideline levels (Hallin 2009) and decreased with increasing capping depth (Jackson 2009). There was no relationship found between HF gas emission and cap depth and emission levels were reported as well below emission standards. $^{222}Rn$ emissions were consistently below guideline levels for radon exposure; however, further research is needed to confirm the presence of a relationship between capping soil depth and radon gas emissions (Jackson 2009).

## 1.7 Research Objectives

The overall objective of this research program is to contribute to the reclamation plan for PG stack closure by determining the effective depth of soil needed as a cover system in order to provide the necessary requirements for plant establishment and growth while providing a

sufficient amount of biological, chemical and physical separation between the PG material and the environment. In order to fulfill the overall reclamation objectives specific focused will be placed on the hydrological boundary conditions and subsequent transport of water within the reclaimed system.

Specific research objectives include:

I. Quantification of water movement in the topsoil cap.

II. Evaluation of potential drainage of water from topsoil into the underlying PG material.

III. Quantification of the rate at which water moves through the topsoil and PG material.

IV. Evaluation of water distribution in soil profile.

## 1.8 References

Abril, J.M., R. García-Tenorio, S.M. Enamorado, M.D. Hurtado, L. Andreu, and A. Delgado. 2008. The cumulative effect of three decades of phosphogypsum amendments in reclaimed marsh soils from SW Spain: 226Ra, 238U and Cd contents in soils and tomato fruit. Science of the Total Environment 403:80-88.

Abril, J.M., R. García-Tenorio and G. Manjón. 2009. Extensive radioactive characterization of a phosphogypsum stack in SW Spain: 226Ra, 238U, concentrations and 222Rn exhalation rate. Journal of Hazardous Materials 164:790-797.

Agassi M., I. Shainberg and J. Morin. 1985. Infiltration and runoff in wheat fields in semi-arid region of Israel. Geoderma. 36:263-276.

Agassi, M., I. Shainberg and J. Morin. 1990. Slope, aspect, and phosphogypsum effects on runoff and erosion. Soil Science Society of America Journal 54:1102-1106.

Agassi, M. and M. Ben-Hur. 1991. Effect of slope length, aspect and phosphogypsum on runoff and erosion from steep slopes. Australian Journal of Soil Research 29:197-207.

Alberta Environment, 2004. Amending Approval Environmental Protection and Enhancement Act R.S.A. 2000, c.E-12. Approval No. 210-01-11. Approval holder: Agrium Products Inc., Redwater AB. Effective date November 19, 2004. 21 pp.

Alberta Environment, 2008. Amending approval Environmental Protection and Enhancement Act R.S.A. 2000, c.E-12. Approval No. 210-02-00. Approval holder: Agrium Products Inc., Redwater AB. Effective date April 4, 2008. 41 pp.

Alberta Environment. 2010. Standards for landfills in Alberta. ISBN: 979-0-7785-8826-9. [Online] Available: http://environment.gov.ab.ca/info/library/7316.pdf. [2013 July 10].

Albright, W.H., C.H. Benson, G.W. Gee, A.C. Roesler, T.A.P. Apiwantragoon, B.F. Lyles and S.A. Rock. 2004. Field water balance of landfill final covers. Journal of Environmental Quality 33:2317-2332.

AMEC. 2006. The beneficial uses of waste. Prepared by: AMEC Earth and Environmental. Calgary, Alberta.

Anderson, J.E. 1997. Soil-plant cover systems for final closure of solid waste landfills in arid regions. In: Landfill capping in the semi-arid west: problems, perspectives, and solutions. Reynolds, T.D. and R.C. Morris, Eds. Environmental Science and Research Foundation. Idaho falls, ID.

Argonne National Laboratory- Environmental Science Division. 2005. Ionizing radiation: human health fact sheet. http://www.ead.anl.gov/pub/doc/ionizing-radiation.pdf. Accessed July 31, 2012.

Arman, A. and R.K. Seals. 1990. A preliminary assessment of utilization alternatives for phosphogypsum. In: Proceedings of the third international symposium on phosphogypsum. Volume II. Publication No. 01-060-083. December, 1990. FIPR. Orlando, FL. Pp. 562-575.als 1990.

Azouazi, M., Y. Ouahidi, S. Fakhi, Y. Andres, J.Ch. Abbe and M. Benmansour. 2001. Natural radioactivity in phosphates, phosphogypsum and natural waters in Morocco. Journal of Environmental Radioactivity 54:231-242.

Becker, P. 1989. Phosphates and Phosphoric Acid: raw materials, technology, and economics of the wet process. Fertilizer Science Technology Ser., Second edition. Vol. 6. Marcel Dekker, Inc., New York. p.752.

Beretka, J. 1990. The current state of utilization of phosphogypsum in Australia. In: Proceedings of Third International Symposium on Phosphogypsum. Orlando, FL. FIPR Publication No. 01-060-083. Vol. 2. pp. 394-401.

Berish, C.W. 1990. Potential environmental hazards of phosphogypsum storage in central Florida. In: Proceedings of the Third International Symposium on Phosphogypsum. Orlando, FL, FIPR Publication No. 01-060-083, Vol. 2. pp. 1-29.

Bianco, C.W., Ruggiero, G.C. Vitti, and P.R.R.S. Santos. 1990. Effects of phosphogypsum and potassium chloride on nutritional status, production, and organoleptical quality of pineapple fruits. In: Proceedings of the Third International Symposium on Phosphogypsum. Orlando, FL. FIPR Publication No. 01-060-083. Vol. 1. pp. 348-361.

Blight, G.E. 2006. The infiltrate-stabilize-evapotranspire or ISE landfill cover. In Proceedings of the forth international conference on unsaturated soils. Geotechnical special publication 147. American Society of Civil Engineers. pp. 753-764.

Cañete, S.J.P. and L.J.H. Palad. 2008. Leachable 226Ra in Philippine phosphogypsum and its implication in groundwater contamination in Isabel, Leyte, Philippines. Environmental Monitoring and Assessment 142:337-344.

Chittaranjan, R. 2005. The next best thing. Civil Engineering Magazine 75(7):58-63.

Collings, R.K. 1980. Phosphogypsum in Canada. In: Proceedings of the international symposium on phosphogypsum. Publication No. 01-001-017.November 5-7, 1980. FIPR. Lake Buena Vista, FL. pp. 583-596.

Degirmenci, N., A. Okucu and A. Turabi. 2007. Application of phosphogypsum in soil stabilization. Building and Environment 42:3393-3398.

Degirmenci, N. 2008. The using of waste phosphogypsum and natural gypsum in adobe stabilization. Construction and Building Materials 22:1220-1224.

Dippel, S.K. 2004. Mineralogical and geochemical characteristics of phosphogypsum waste material and its potential for use as a backfill at WMC fertilizers'' mine site, Phosphate Hill, N-W Queensland. M.Sc. Thesis. James Cook University. Douglas, QL. 336pp.

Dueñas, C., E. Liger, S. Cañete, M. Pérez and J.P. Bolívar. 2007. Exhalation of $^{222}$Rn from phosphogypsum piles located at the

Southwest of Spain. Journal of Environmental Radioactivity 95:63-74.

Environment Canada. 2012. National climate data and information archive. [Online] Available: http://www.climate.weatheroffice.gc.ca/advanceSearch/searchHistoricDataStations_e.html?searchType=stnName&timeframe=1&txtStationName=fort+saskatchewan&searchMethod=contains&optLimit=yearRange&StartYear=1840&EndYear=2012&Month=9&Day=21&Year=2012&selRowPerPage=25&cmdStnSubmit=Search. [2012 Mar. 20].

Florida Department of Environmental Protection. 2006. Chapter 62-673 phosphogypsum management. http://www.floridadep.org/legal/rules/shared/62-673.pdf. Effective date: July 19, 2006. 15 pp. Last accessed November 29, 2008.

Frenkel, H., M.V. Fey, G.H. Goodal and W.B. Russel. 1989. Effects of soil surface amendments on runoff and erosion from simulated rain applied to a sesquioxidic soil. South African Journal of Plant and Soil 6:197-202.

Foxworthy, P.T., E. Ott and R.K. Seals. 1994. Utilization of phosphogypsum-based slag aggregate in Portland cement concrete mixtures. Transportation research record 1437, Transportation Research Board, National Research Council, National Research Council, Washington, D. C. pp.19-26.

Gal, M., L. Arcan, I. Shainberg and R. Keren. 1984. Effects of exchangeable sodium and phosphogypsum on crust structure-scanning electron microscope observations. Soil Science Society of America Journal 48:872-878.

Gascho, G.J. and A.K. Alva, 1990. Beneficial effects of gypsum for peanut. In: Proceedings of the Third International Symposium on Phosphogypsum. Orlando, FL. FIPR Publication No. 01-060-083. pp. 376-393.

Ghafoori, N. and W.F. Chang. 1993. Investigation of phosphate mining waste for construction materials. Journal of Materials in Civil Engineering 5:249-264.

Habashi, F. 1980. The recovery of uranium from phosphate rock: progress and problems. In: Proceedings of the Second International Congress of Phosphorus Compounds. Boston, MA. pp. 629.

Hallin, I.L. 2009. Evaluation of a substrate and vegetation cover system for reclaimed phosphogypsum stacks at Fort Saskatchewan, Alberta. MSc Thesis. University of Alberta, Edmonton, AB. 107 pp.

Hallin, I.L., M.A. Naeth, D.S. Chanasyk and C.K. Nichol. 2010. Assessment of a reclamation cover system for phosphogypsum

stack in Central Alberta, Canada. Journal of Environmental Quality 39:2160-2169.

Hanson, W.K. and D. Laird. 1990. Characteristics of by-product slag from phosphogypsum. In: Proceedings of the Third International Symposium on Phosphogypsum. Volume I. Publication No. 01-060-083. December, 1990. FIPR. Orlando, FL. pp. 225-239.

Haridasan, P.P., A.C. Paul and M.V.M. Desai. 2001. Natural radionuclides in aquatic environment of a phosphogypsum disposal area. Journal of Environmental Radioactivity 53: 155-165.

Haridasan, P.P., C.G. Maniyan, P.M.B. Pillai and A.H. Khan. 2002. Dissolution characteristics of $^{226}$Ra from phosphogypsum. Journal of Environmental Radioactivity 62:287-294.

Hauser, V.L. 2009. Landfill remediation with covers. Pages 7-13 *in* Evapotranspiration covers for landfills and waste sites. CRC Press, Boca Raton, FL. USA.

Hauser, V.L., B.L. Weand and M.D. Gill. 2001. Natural covers for landfills and buried waste. Journal of Environmental Engineering 127(9). pp. 8.

Hauser and Gimon. 2004. Evaluating evapotranspiration (ET) landfill cover performance using hydrological models. Prepared for: Air force center for environmental excellence. Brooks City-Base, TX. 118 pp.

Health Canada. 2000. Canadian guidelines for the management of naturally occurring radioactive material (NORM). First Edition. pp. 47.

Hull, C.D. and W.C. Burnett. 1996. Radiochemistry of Florida phosphogypsum. Journal of Environmental Radioactivity. 32:213-238.

Jackson, E. M. 2009. Assessment of soil capping for phosphogypsum stack reclamation at Fort Saskatchewan, Alberta. MSc Thesis. University of Alberta, Edmonton, AB. 162 pp.

Karr, L., B. Harre and T.E. Hakonson. 1991. Infiltration control landfill cover demonstration at Marine Corps Base, Hawaii. Technical report TR-2108-ENV, Naval Facilities Engineering Services Center. Port Hueneme, CA.

Kazman, Z., I. Shainberg, and M. Gal. 1983. Effects of low levels of exchangeable sodium and applied phosphogypsum on the infiltration rate of various soils. Journal of Soil Science 135:184-192.

Keren, R. and I. Shainberg. 1981. Effects of dissolution rate on the efficiency of industrial and mined gypsum in improving infiltration of sodic soil. Soil Science Society of America Journal 45:103-107.

Koerner, R.M. and D.E. Daniel. 1997. Final covers for solid waste landfills and abandoned dumps. ASCE Press. Reston, VA. 256 pp.

Kouloheris, A.P. 1980. Chemical nature of phosphogypsum as produced by various wet process phosphoric acid process. In: Proceedings of International Symposium on Phosphogypsum. Lake Buena Vista. FL. FIPR Publication No. 01-001-017. pp. 9-33.

Luther S.M., M.J. Dudas and P.M. Rutherford. 1993. Radioactivity and chemical characteristics of Alberta phosphogypsum. Water, Air, and Soil Pollution 69:227-290.

Malavolta, E., G.C. Vitti, C.A. Rosolem, N.K. Fageria, and P.T.G. Guimaraes. 1987. Sulphur response of Brazilian crops. Journal of Plant Nutrients 10:2153-2158.

May, A. and J.W. Sweeney. 1984. Assessment of environmental impacts associated with phosphogypsum in Florida. In: R.A. Kuntze (Ed.). The Chemistry and Technology of Gypsum. ASTM Special Technical Publication No. 861. pp. 116-139.

McLaughlin, D.L. 1986. Phytotoxicity assessment surveys in the vicinity of Eldorado Resources Ltd. Port Hope, 1984 and 1985. Air Resources Branch. Ontario Ministry of the Environment. ARB-115-86-Phyto.

Motalane, M.P. and C.A. Strydom. 2004. Potential groundwater contamination by fluoride from two South African phosphogypsums. Water SA 30:465-468.

Nichol, C.K. 2009. Environmental Scientist, Agrium Inc. Personal communication. Fort Saskatchewan, AB. March 4, 2009.

Norlander, G.W. 1988. The decommissioning of phosphogypsum tailings in Alberta. MSc Thesis. University of Calgary. Calgary, Alberta. 143 pp.

Novikov, A.A., P.V. Klassen, and S.D. Evenchik. 1990. The status and trends of phosphogypsum utilization in the USSR. In: Proceedings of the Third International Symposium on Phosphogypsum. Orlando, FL. FIPR Publication No. 01-060-083. Vol. 2. pp. 594-601.

Pérez-López, R., Álvarez-Valero, A., Nieto, J.M., 2007. Changes in mobility of toxic elements during the production of phosphoric acid in the fertilizer industry of Huelva (SW Spain) and environmental impact of phosphogypsum wastes. Journal of Hazardous Materials 148:745–750.

Pérez-Lopéz, R., J.M. Nieto, I. López-Coto, J.L. Aguado, J.P. Bolívar and M. Santisteban. 2010. Dynamic of contaminants in phosphogypsum of the fertilizer industry of Huelva (SW Spain): from phosphate rock ore to the environment. Applied Geochemistry 25:705-715.

Pressacco, R. 2001. Geology of the Cargill township residual carbonatite-associated phosphate deposit, Kapuskasing, Onatrio. Exploration and Mining Geology 10:77-84.

Qiao, D., J. Qian, Q. Wang, Y. Dang, H. Zhang and D. Zeng. 2010. Utilization of sulfate-rich solid wastes in rural road construction in Three Gorges Reservoir. Resources, Conservation and Recycling 54:1368-1376.

Rechcigl, J.E., P. Mislevy and A.K. Alva. 1993. Influence of limestone and phosphogypsum on Bahiagrass growth and development. Soil Science Society of America Journal 57: 96-102.

Roessler, C.E., Z.A. Smith, W.E. Bolch, and R.J. Prince. 1979. Uranium and radium-226 in Florida phosphate materials. Health Physics 37: 269-277.

Rutherford, P.M. and M.J. Dudas. 1993. Radium-226 uptake by plants growing in Alberta phosphogypsum. In: AERT Final Report Leachate Chemistry of Phosphogypsum By-Product. Technical Report PG-93-2. Department of Soil Science, University of Alberta. Edmonton, Alberta. 13 pp.

Rutherford, P.M., M.J. Dudas, and R.A. Samek. 1994. Environmental impacts of phosphogypsum. The Science of the Total Environment 149:1-38.

Rutherford, P.M., M.J. Dudas and J.M. Arocena. 1995. Radioactivity and elemental composition of phosphogypsum produced from three phosphate rock sources. Waste Management and Research 13:407-423.

Rutherford, P.M., M.J. Dudas and J.M. Arocena. 1996. Heterogeneous distribution of radionuclides, barium and strontium in phosphogypsum by-product. The Science of the Total Environment 180:201-209.

Rydzynski, R. 1990. Pollution loads from a large chemical plant and phosphogypsum stack. In: Proceedings of the Third International Symposium on Phosphogypsum. Orlando, FL. FIPR Publication No. 01-060-083. pp. 64-73.

Santos, A.J.G., B.P. Mazzilli, D.I.T. Fávaro and P.S.C. Silva. 2006a. Partitioning of radionuclides and trace elements in phosphogypsum and its source materials based on sequential extraction methods. Journal of Environmental Radioactivity 87:52-61.

Santos, A.J.G., P.S.C. Silva, B.P. Mazzilli and D.I.T. Fávaro. 2006b. Radiological characterization of disposed phosphogypsum in Brazil: evaluation of the occupational exposure and environmental impact. Radiation Protection Dosimetry 121:179-185.

Schultz, R.K., R.W. Ridky and E. O'Donnell. 1997. Control of water infiltration into near surface low-level waste disposal units. U.S. Nuclear Regulatory Commission. Washington, DC. Report no. NUREG/CR-4918, Vol. 10.

Seifert, K., A. Moska and F. Domka. 2002. The effect of waste phosphogypsum on the denitrification and desulfurication processes. Physicochemical Problems of Mineral Processing 36:209-216.

SENES. 1987. An analysis of the major environmental and health concerns of phosphogypsum tailings in Canada and methods for their reduction. Prepared by: SENES Consultants Limited. Willowdale, ON.

Silva, L.F.O., J.C. Hower, M. Izquierdo and X. Querol. 2010. Complex nanominerals and ultrafine particles assemblages in phosphogypsum of the fertilizer industry and implications on human exposure. Science of the Total Environment 408:5117-5122.

Singh, A.L., Y.C. Joshi, V. Chaudhari and P.V. Zala. 1990. Effects of different sources of iron and sulfur on leaf chlorosis, nutrient uptake and yield of groundnut. Fertilizer Research 24:85-96.

Thorne, W. E. R. 1990. Reclamation of a phosphogypsum tailings pond: an examination of the relevant issues. MEDes thesis. University of Calgary, Calgary, AB. 330 pp.

Turner, E. L. 2013. Influence of soil cap depth and vegetation on reclamation of phosphogypsum stacks in Fort Saskatchewan, Alberta. M.Sc. Thesis. University of Alberta, Edmonton, AB. 172 pp.

US EPA. 1991. Design and construction of RCRA/CERCLA final cover. EPA/625/4-91/025. Office of Research and Development. Washington, DC.

US EPA. 2003. Evapotranspiration landfill cover systems fact sheet. EPA 542-F-03-015. Office of Solid Waste and Emergency Response. Cincinnati, OH.

US EPA. 2011. Fact sheet on evapotranspiration cover systems for waste containment. EPA 542-F-11-001. Office of Solid Waste and Emergency Response. Cincinnati, OH.

van Straaten, P. 2002. Rocks for Crops: Agrominerals of sub-Saharan Africa. ICRAF, Nairobi, Kenya. 338 pp.

Vick, S.G. 1977. Rehabilitation of a gypsum tailings embankment. In: Proceedings of the Conference on the Geotechnical Disposal of Solid Waste Materials. Ann Arbor, MI. pp. 679-714.

Weinstein, L.H. and A.W. Davison. 2004. Fluorides in the environment. CABI Publishing. Oxon, UK. Pp. 12, 37-39, 47, 53, 58, 88, 92, 93.

Wissa, A.E.Z. 2002. Phosphogypsum disposal and the environment. In: J.J. Schultz and D.R. Waggoner (eds.). Proceedings of international workshop on current environmental issues of fertilizer production. June 7-9, 1999. Prague, Czech Republic. IFDC. Muscle Shoals, AL. Pp. 195-205.

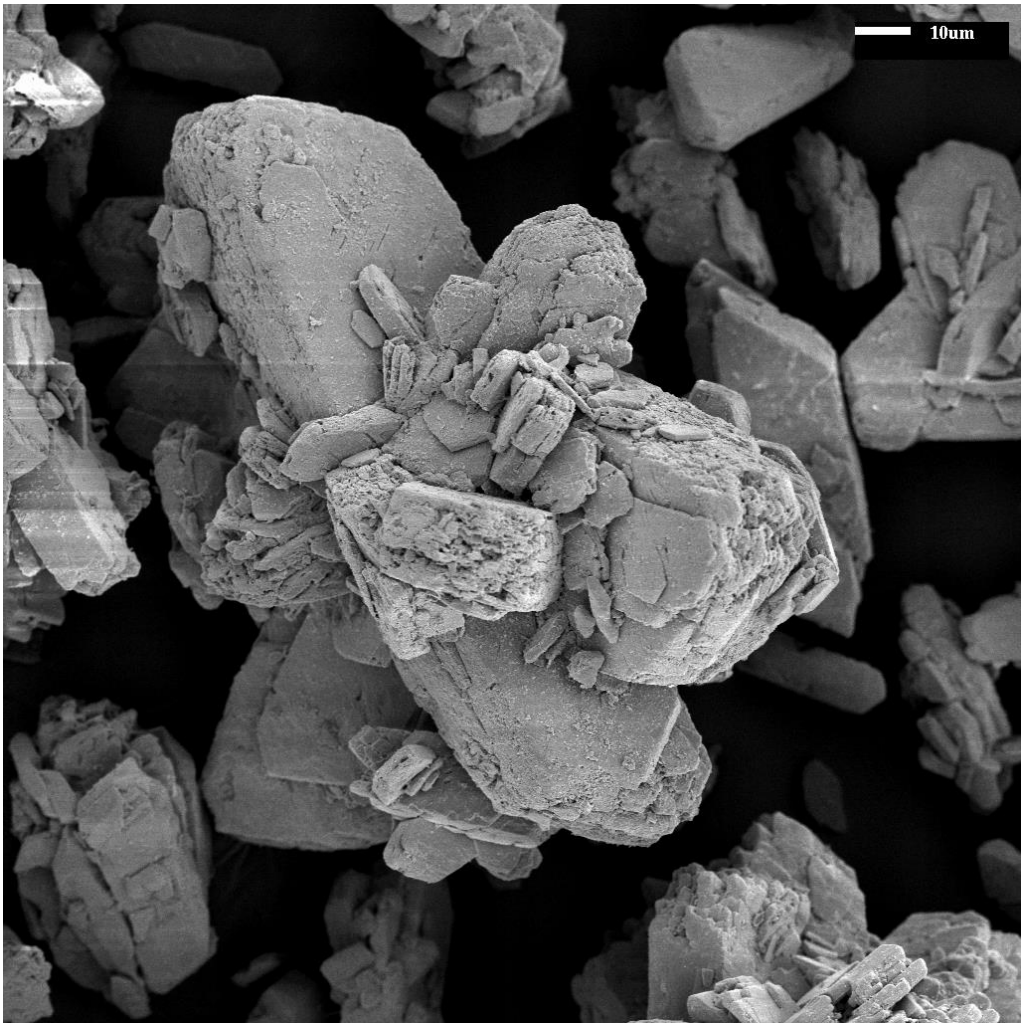

Figure 1.1: Scanning Electron Microscope (SEM) image of phosphogypsum crystal from Fort Saskatchewan, AB (Nichol 2009).

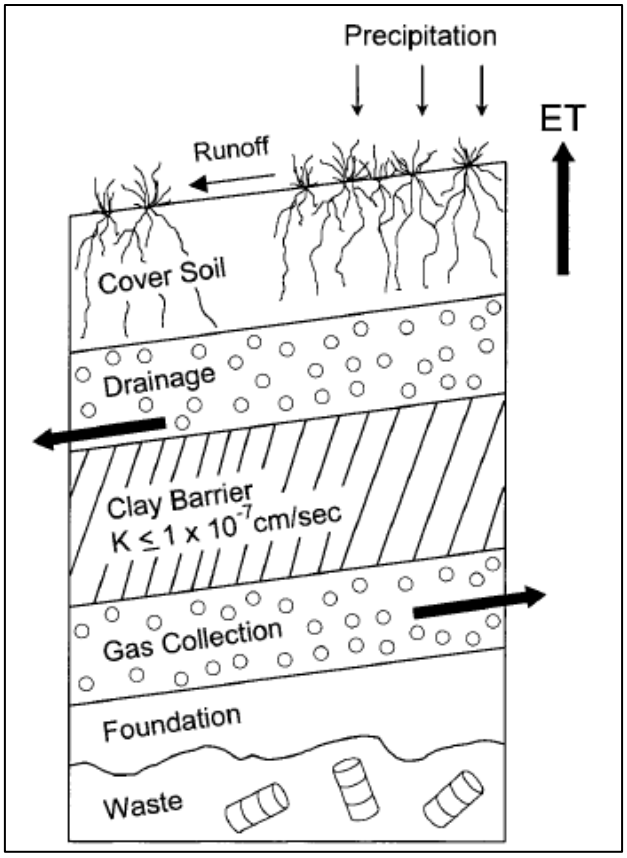

Figure 1.2: Cross section of Resource Conservation and Recovery Act (RCRA) landfill cover (conventional cover) from Hauser et al. (2001).

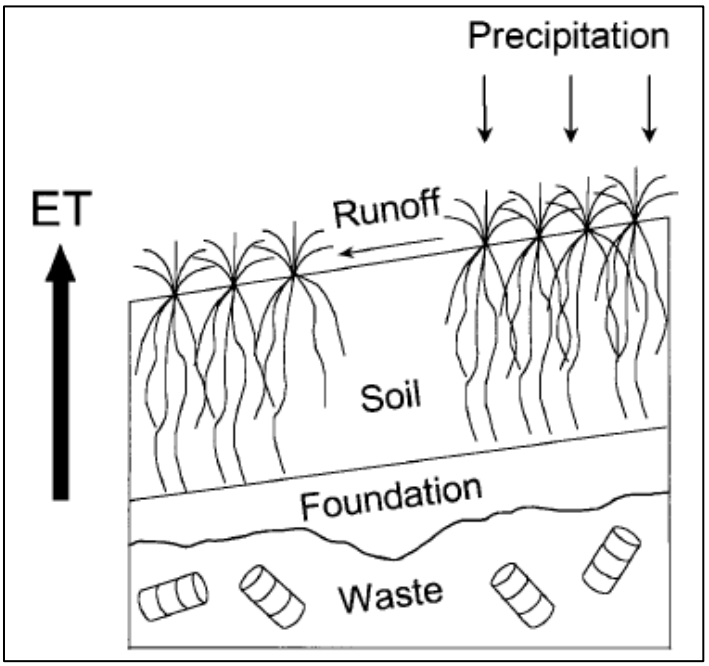

Figure 1.3: Cross section of evapotranspiration cover system from Hauser et al. (2001).

## 2.0 INFLUENCE OF CAPPING SOIL DEPTH ON WATER DYNAMICS IN PHOSPHOGYPSUM STACK RECLAMATION

[A version of this chapter is in press in the Canadian Journal of Soil Science]

### 2.1 Introduction

Phosphogypsum (PG) is a byproduct in the production of phosphoric acid (PA), a necessary component in phosphorus fertilizers. The production of PA involves the digestion of phosphate ore with sulfuric acid and water according to the reaction:

$$Ca_{10}(PO_4)_6F_2 + 10H_2SO_4 + 20H_2O \rightarrow 10CaSO_4{\bullet}2H_2O + 6H_3PO_4 + 2HF$$

Where, gypsum ($CaSO_4{\bullet}2H_2O$), PA ($H_3PO_4$), and hydrogen fluoride (HF) are the products (Rutherford et al. 1994; Luther et al. 1993). The gypsum material that precipitates out of solution is referred to as PG. Once the PG is filtered from the PA product it is mixed with water to form a slurry which can be pumped to settling ponds. The process water is then decanted and recycled within the transport system while the PG material settles, forming large stacks referred to as PG stacks (Wissa 2002).

Globally the demand for PA based fertilizers in 2009 reached approximately 40 million tonnes, resulting in an annual accumulation of PG of over 180 million tonnes (Abril et al. 2009). In Canada there are PG stacks located in Ontario, Quebec, New Brunswick, British Columbia and Alberta; however, the only operational stack in Canada is located in Redwater, Alberta (Thorne 1990). The PG stack in Redwater accumulates

approximately 1.5 million tonnes of PG annually and is predicted to occupy an area of 300 ha upon closure (Nichol 2009).

Environmental implications associated with PG production, transport and disposal are not limited to the vast amount of PG accumulation but also by the impurities integrated into the PG material. These impurities include, but are not limited to, radium ($^{226}Ra$), uranium ($^{238}U$), arsenic (As), barium (Ba), cadmium (Cd), chromium (Cr), lead (Pb), mercury (Hg), selenium (Se) and fluoride ($F^-$) (Rutherford et al. 1995). These trace elements can enter the environment through atmospheric contamination from emission of $F^-$ or other toxic elements, groundwater contamination from PG leachate, $^{226}Ra$ emissions, exposure of radioactive dust and other airborne elements, direct exposure to gamma radiation from PG material (Rutherford et al. 1994), and water and/or wind erosion (Rydzynski 1990).

The introduction of precipitation into the PG stack can facilitate the mobility of the mentioned trace elements as well as dissolve the gypsum material (SENES 1987); therefore, one of the objectives for PG stack reclamation is to minimize interaction between percolating water and the PG material. Other objectives include the prevention of contaminated water from entering the environment by means of surface or groundwater flow, sustain structural integrity of PG stack, and minimize radionuclide emissions from PG stack. To limit the possibility of environmental contamination through these sensitive vectors the use of a cover system is

necessary. The cover system as outlined by Alberta Environment, within the context of the approval that was issued to Agrium Products Inc., involves the replacement of at least 1 m of soil (2008). This recommendation is subject to investigation to determine whether a more sustainable amount of topsoil can be used to fulfill the general reclamation objectives.

## 2.2 Research Objectives

The overall objective of this research is to contribute to a reclamation plan for PG stack closure by estimating the optimal amount and hydraulic properties of topsoil needed to provide the necessary requirement for plant establishment, while minimizing the potential translocation and percolation of water into and through the PG material. Specific objectives include:

- Quantification of water movement in topsoil caps of various thicknesses.
- Evaluation of potential drainage of water from the topsoil into the underlying PG material.
- Quantification of the rate at which water moves through the topsoil and the PG material.
- Evaluation of water distribution in the soil profile.

## 2.3 Materials and Methods

### 2.3.1 Site Description

Experimental plots with varying topsoil cap thickness were constructed in 2006 at the Agrium Fort Saskatchewan facility to help identify an optimal capping depth for PG stack in Alberta. The research plots are located atop a decommissioned PG stack situated within the Agrium Nitrogen Operation facility in Fort Saskatchewan, Alberta, Canada (53$^{o}$44'11" N and 113$^{o}$11'34" W) (Figure 2.1). The area is described as belonging to the Central Parkland Natural Subregion within the Aspen Parkland Ecoregion.

Average annual precipitation for the area is 459.5 mm, with 354.9 mm in the form of rainfall and 104.6 mm in the form of snow water equivalence. The climate is described as semi-arid to humid continental with an average winter temperature of -10.2 $^{o}$C and an average summer temperature of 14.7 $^{o}$C (Environment Canada 2012; Natural Regions Committee 2006). Daily extreme rainfall events have ranged in magnitude from 6.4 mm in December of 1958 to 77.7 mm on June 26$^{th}$, 1965. In general the 100 year storm event magnitude, on a monthly average, is 150 mm (Environment Canada 2012).

Surficial geology of the Fort Saskatchewan area is dominated by alluvial deposits such as gravels, sands and silts along the North Saskatchewan River, as well as coarse glaciolacustrine deposits such as sands and silty sands. The bedrock material underlying the Pleistocene

deposits include sandstones, siltstones and mudstones all pertaining to the Belly River Formation of the Cretaceous period (Bayrock and Hughes 1962). The landform profile of the area is described as undulating with a limited slope of 4% with well to rapid drainage. Soils of the area are dominated by Orthic Black Chernozems of the Mundare series with a minor component (20%) falling within the Eluviated Eutric Brunisol of the Primula series (Agriculture and Rural Development 2011).

Production of phosphoric acid at the Fort Saskatchewan property commenced in 1965 and continued until 1991. During the 26 years of operation the phosphoric acid plant produced 4,971,000 tonnes of dry PG. The PG was placed in 5 stacks on the property and occupies a total basal area of 87 acres (Figure 2.2). Stacks #1 and #2 were commissioned in 1965 and stack #3 in 1974. These three stacks were built on natural clay liners; however, only Stack #3 at the time was built with a drainage system. Stack #4 was commissioned in 1983 and was built on a HPDE synthetic liner and designed with a drainage system. Finally, stack #5 was commissioned in 1986, but does not have a liner because it was used to store dry PG material from stacks #3 and #4 until June 1991 when the production of phosphoric acid was discontinued (Svarich 1999).

Upon decommissioning of the various PG stacks, 10 to 15 cm of soil was applied to the outer slopes of each stack and a seed mixture consisting of *Bromus inermis* and *Brassica napus* L. (canola) was broadcast (Nichol 2009). In 2006, the settling basin on top of Stack #4 was

selected as the site for an intensive research program put forth by Agrium Inc. in partnership with the University of Alberta. The settling basin atop stack #4 occupies an area of 4.7 ha and is relatively flat with a slight northeast aspect. The inner slopes of stack #4 were left bare as well as the basin, with the exception of a small area that had mushroom compost applied (Jackson 2009). Access to the site is available from the south and northeast where two access roads were constructed joining a road that follows the rim of the stack. Vehicle access is not advisable during the winter months due to heavy snow accumulation within the basin area, as well as during the spring melt periods when the PG material is pliable.

### 2.3.2 Experimental Design

The field site is located on top of a decommissioned PG stack that was operational for 8 years before its closure in 1991. The PG stack is approximately 15 m in height and occupies a base area of 9.3 ha. Eighteen (50 m x 10 m) plots were constructed atop the decommissioned PG stack in a complete randomized design during the fall of 2006 (Jackson 2009). The plots were arranged into three replicates each containing six topsoil capping depth treatments including 8, 15, 30, 46, and 91 cm, as well as a 0 cm control (Figure 2.3). The general topography on which the topsoil was placed was relatively flat with a slope of < 1%. Each topsoil depth treatment was further subdivided into 5 subplots (10 m x 10 m) that contained five different plant species treatments including

*Agropyron trachycaulum* (Link) Malte ex H.F. Lewis (slender wheatgrass), *Agrostis stolonifera* L. (redtop), *Deschampsia caespitosa* (L.) P. Beauv. (tufted hairgrass), *Festuca ovina* L. (sheep fescue) and a mixture of 54% redtop, 2% slender wheatgrass, 28% tufted hairgrass, 8% sheep fescue and 8% Alsike clover (Jackson 2009).

The 15, 30 and 46 cm treatments of replicate 2 were selected for soil water investigation were within the range recommendations made by previous studies (Jackson 2009; Hallin 2009), and because of the close proximity of each plot to one another which accommodated limited cable lengths of soil moisture sensors. All experimental measurements were conducted within the *Agropyron trachycaulum* subplots of the three soil treatments in order to establish a controlled plant community that would be representative of the final reclamation goals. Furthermore, the *Agropyron trachycaulum* species was selected for its dominancy with respect to weeds, salinity resiliency and the uniformity with which the plant grows. The vegetative subplots that were selected (i.e. the *Agropyron trachycaulum of the* 15, 30 and 46 cm of Replicate 2) will be hence forth referred to as the experimental plots.

### 2.3.3 Meteorological Measurements

An on-site weather station was used to measure and record routine meteorological data on an hourly basis using a CR 10X data logger (Campbell Scientific (Canada) Corp. 2007). Precipitation and solar

radiation were measured using a TE525WS Texas Electronic 0.254 mm tipping bucket rain gauge and a Kipp & Zonen silicon pyranometer (SP-Lite), respectively. Wind speed and direction were measured using a 05103-10 RM Young wind monitor. Finally, air temperature and relative humidity were measured using a HMP45C Vaisala probe housed in a radiation shield (Campbell Scientific (Canada) Corp. 2007). Snowfall data was measured at the Fort Saskatchewan meteorological station, located 1.79 km south of the field site (Environment Canada 2012).

### 2.3.4 Time Domain Reflectometry, Matric Potential, and Soil Temperature Measurements

Within each of the selected experimental plots Time Domain Reflectometry (TDR) probes, dielectric soil water potential sensors (MPS-1, Decagon Devices Inc., Pullman, WA, USA) and soil temperature sensors were installed (TMC50-HD, Onset Computer Corporation, Bourne, MA, USA; Table 2.1). The TDR probes and MPS-1 sensors were installed horizontally at the topsoil/PG interface as well as 7.5 cm above and below the interface. Additional TDR probes were installed horizontally at 15 cm increments from the topsoil/PG interface and a single vertical probe with a length equal to topsoil capping depth (15, 30 and 46 cm) was also installed into the topsoil cap (Figure 2.4). The horizontal TDR probes were installed into a 60 cm by 50 cm trench that was dug to a depth of approximately 1 m using a backhoe in November of 2010.

Once the TDR probes were installed, the substrate material was repacked in the order in which it was removed in order to avoid mixing. The soil temperature probes were installed vertically into a narrow hole that was created within 50 cm of the TDR probes in April of 2011. Soil temperature sensors were installed at depths corresponding to the horizontal TDR probes for each experimental plot and subsequently routed to HOBO U12 external data loggers and logged on an hourly basis. The MPS-1 probes were routed to a CR 1000 data logger and monitored every 2 hours (Campbell Scientific (Canada) Corp. 2007).

The TDR probes that were used during the experiment were constructed using 2 stainless steel rods spaced 4 cm apart, each with a diameter of 0.5 cm attached directly to a 10-m long RG 58/U coaxial cable. Vertically installed TDR probes varied in length corresponding to topsoil treatment depth (15, 30 and 46 cm), while the horizontally-installed TDR probes had a standardized length of 30 cm. The TDR probes that were installed were routed to 3, SDMX 50 multiplexers corresponding to the three experimental plots under investigation.

The 3-SDMX50 multiplexers were subsequently routed to a central multiplexer which was connected directly to a TDR 100 and CR 800 data logger (Campbell Scientific (Canada) Corp. 2007). In order to reduce signal loss along the length of the cable a RG 8/U coaxial cable was used to link the SDMX 50s to the central SDMX 50 multiplexer. During spring melt and fall freeze up electrical conductivity (EC) and the dielectric

permittivity ($\varepsilon_a$) were logged every 2 hours, while the individual wave forms were logged every 6 hours. During the mid-summer months the $\varepsilon_a$ was logged every 4 hours and waveforms were logged every 12 hours.

TDR measurements for volumetric water content were calibrated in a laboratory setting by packing oven dry topsoil and PG into 10.16 cm diameter polyvinyl chloride (PVC) pipes. Individual TDR probes were vertically installed into the column of dry substrate and logged to measure $\varepsilon_a$, electrical conductivity (EC) and waveforms every 10 seconds. During the calibration, tap water was ponded on the surface of the column and allowed to infiltrate into the dry substrate, thus saturating the column over time. The volume of water entering into the column was measured with a permeameter attached to the top of the column allowing the total amount of water in the soil at each time interval to be estimated. The calibration curve for each probe and soil are summarized in Figure 2.5. The TDR probes were individually calibrated according to the length of each probe and the material to which it was inserted; therefore, a total of 4 calibrations are present for the 15, 30 and 46 cm probe lengths for topsoil as well as a single 30 cm probe for the PG material.

### 2.3.5 Estimation of Unfrozen Water and Ice Content with TDR-Measured $\varepsilon_{eff}$

Water and ice content in soil can be estimated with TDR-measured effective dielectric permittivity ($\varepsilon_{eff)}$ of the soil. The TDR method estimates

the $\varepsilon_{eff}$ of the soil within the sampling volume of the TDR wave guides by introducing a fast rise (approximately 200 ps) step voltage into the soil system through wave guides. The reflected waveform is sent back to the signal generator and the apparent travel time of the waveform is computed to determine the $\varepsilon_{eff}$, which is a function of the dielectric permittivity's of the various components of soil (Dalton et al. 1984; Dalton and van Genuchten 1986; Dasberg and Dalton 1985; Topp et al. 1980). The $\varepsilon_{eff}$ of air, soil minerals, ice and water are 1, 3-5, 3.2 and 80, respectively; therefore, the bulk apparent $\varepsilon_a$ of soil is highly sensitive to water (Topp et al. 1980). Similarly, if the soil was to freeze under non-fluctuating total water content conditions the bulk apparent $\varepsilon_a$ would be sensitive to the presence of ice (He and Dyck 2012).

To compute the liquid water and ice content of the soil a dielectric mixing model was used. A mixing model is a physically-based or empirical mathematical expression that relates the $\varepsilon_{eff}$ of the soil to the dielectric permittivity of the individual soil constituents and their volumetric fractions (He and Dyck 2012; Jones and Friedman 2000; Sihvola and Lindell 1990).

These models, however, are dependent on the assumption that the amount of total water before freezing is equal to the amount of total water present during and after freezing. In other words the model is based on the assumption that during the freezing processes the total amount of water is unchanged, only the state of the water is changing (He and Dyck 2012). This assumption has been validated through observation of water

content data onsite during the fall of 2011 and 2012. During this period rainfall events were minimal (i.e. < 2 events of < 10 mm) and evapotranspiration demands were low, and as expected the estimated volumetric water content remained stable within the topsoil and PG material for approximately 1 month before the freezing processes began; therefore, it is regarded that the stable water dynamics that were observed in the fall should carry forth throughout the winter with minimal vertical drainage. Furthermore, it was observed that the topsoil caps had minimal water within the pore spaces leading into the fall as a result of their limited ability to retain water. As for the PG material, the limited water content fluctuations during the active growing season adds further evidence to the assumption that limited percolation/drainage would be occurring during the winter months.

### 2.3.6 Snow Depth Survey

Snow depth and density was measured on 26 February, 2011. A snow survey was not conducted in 2012 because of the lack of cumulative snowpack; however, snowfall data was obtained from the nearby meteorological station in Fort Saskatchewan for the winter of 2011 and 2012. For each 50 m by 10 m plot 12 locations were selected for snow depth measurements (D, cm) using a standard ruler. Within each *Agropyron trachycaulum* subplot (10 m x 10 m) a single snow core was collected using a clear PVC tube (2.38 cm radius). For soil treatments with

TDR probes installed the snow cores were collected within 50 cm of probes location. The snow cores were transferred to plastic sampling bags and weighed. The density of snow was used to compute snow water equivalent (SWE (mm)) measurements for the plots under investigation.

### 2.3.7 Physical Properties of PG and Topsoil

#### 2.3.7.1 Moisture Retention for the PG and Topsoil

Moisture retention curves were measured on the topsoil as well as the PG material to further understand the hydraulic dynamics of each material. Field cores were collected on 12 October, 2011 using aluminum cores that had an inside diameter of 4.8 cm. The aluminum cores were manually pounded into the topsoil/PG material until compaction was detected. The cores were carefully removed from the substrate material and stored in a refrigerator until further processing. All samples were collected from the 30 cm treatment plots to a depth of approximately 60 cm across all replicates.

The aluminum cores containing the undisturbed substrate material were subsequently cut into 3 cm segments above and below the estimated topsoil/PG interface location. The 3 cm sections were carefully retained in the core using cheese cloth. Pressures of 0.0015, 0.005, 0.01, 0.05, 0.1, 0.4, 1.0 and 1.5 MPa were selected in order to effectively estimate the curvature of the moisture retention curves for each substrate.

For the lower pressures (i.e. 0.0015 and 0.005 MPa) a hanging water column apparatus was used; however, for the higher pressures (i.e. 0.01, 0.05, 0.1, 0.4, 1.0, and 1.5 MPa) pressure chambers were used. The samples remained at each designated pressure until the amount of water that was released became negligible (4-14 days), upon which time they were weighed and set to a higher pressure. After completion of the last pressure potential the samples were oven dried at 55 $^{o}$C for 48 hours in order to minimize molecular water loss from within the crystalline structure of the PG material (Averitt and Gliksman 1990; Strydom and Potgieter 1999). Each core was represented by an undisturbed sample; therefore, the bulk density was also obtained and used to convert gravimetric water content to volumetric water content.

The data collected was subsequently used to fit the van Genuchten (VG) model:

$$\theta(hm) = \theta r + \frac{(\theta s - \theta r)}{[1+(-\alpha hm)^{n}]^{m}} \qquad \text{for } hm < 0\text{cm} \qquad [2.1]$$

where, θr and θs are the residual and saturated volumetric water contents ($cm^3\ cm^{-3}$) and *hm* is the matric potential (cm), while $\alpha$, n and m=1-1/n are parameter that will determine the shape of the moisture retention curve (1980). From Eq. 2.1 the volumetric water content (θ(*hm*)) can be obtained for any given matric potential. Water retention dynamics for the topsoil indicated that the air entry potential for the topsoil material was approximately -28 cm and that the residual water content at -15,000 cm was 0.11 $cm^3\ cm^{-3}$, while the water retention dynamics for the PG material

indicated that the air entry potential was approximately -186 cm and that the residual water content at -15,000 cm was 0.03 $cm^3$ $cm^{-3}$ (Figure 2.7).

#### 2.3.7.2 Hydraulic Conductivity for PG and Topsoil

The parameters that were obtained from fitting the VG model to the moisture retention data were also used to predict the hydraulic conductivity curves for the PG and topsoil materials according to the van Genuchten-Mualem model (van Genuchten 1980); however, the saturated hydraulic conductivity needed to be measured independently of the moisture retention curve to use this model. The saturated hydraulic conductivity was measured for each substrate material using PVC columns that had been packed with the substrate material to the desired field bulk density. The columns were 15 cm in height and had an inside diameter of 7.7 cm. The columns were subjected to varying boundary conditions to simulate ponding of water on the substrate surface. Once the material had become fully saturated and the outflow flux had stabilized, samples were collected over several minutes to determine the cumulative outflow.

Based on Darcy's Law:

$$Jw = -Ks \frac{\Delta H}{\Delta z} \qquad [2.2]$$

where, $\Delta H / \Delta z$ (cm $cm^{-1}$) is the hydraulic gradient and Jw ($cm^3$ $cm^{-2}$ $s^{-1}$) is the flux, the saturated hydraulic conductivity (Ks (cm $s^{-1}$)) can then be computed by rearranging Eq. 2.2. Each computation of Ks was repeated

several times over several different time intervals to obtain a representative value. The saturated hydraulic conductivity of the topsoil material was 7.4 X $10^{-3}$ cm $s^{-1}$ ±7.9 X $10^{-5}$, while the saturated hydraulic conductivity of PG material was 3.7 X $10^{-4}$ cm $s^{-1}$ ±6.6 X $10^{-6}$ (Table 2.2).

Based on these results the predicted unsaturated hydraulic conductivity curve was created to support our understanding of the hydraulic properties of the substrate materials using the following equation:

$$K(hm) = Ks\ \frac{\{1-(-\alpha hm)^{n-1}[1+(-\alpha hm)^{n}]^{-m}\}^{2}}{[1+(-\alpha hm)^{n}]^{\frac{m}{2}}} \qquad \text{for } hm < 0 \qquad [2.3]$$

where, Ks is the measured saturated hydraulic conductivity (cm $s^{-1}$), *hm (-cm)* is the matric potential of the soil and $\alpha$, n and m=1-1/n are parameter that were determined from fitting the VG model to the moisture release curve for each substrate type (van Genuchten 1980). Figure 2.8 details the complete hydraulic conductivity of each substrate material. From the predicted model it is clear that the saturated hydraulic conductivity of the topsoil is an order of magnitude higher than that of the PG material; however, under minimal matric potentials the trend is reversed and the PG material has a higher hydraulic conductivity than that of the topsoil material.

## 2.4 Results and Discussion

### 2.4.1 Water Content Distribution in Evapotranspiration Cover System

Engineered cover systems, including evapotranspiration (ET) cover systems, operate with the forces of nature as opposed to attempting to control them. In this context the soil provides a natural water reservoir while the plants and environment contribute to removing water from the reservoir by means of evaporation and transpiration (Hauser 2009). The soil water reservoir is a major feature of an ET cover system and therefore requires intensive investigations regarding the materials that will be used to maximize efficiency. The efficiency of the ET cover system will be a function of soil pore volume, pore size distribution and water holding capacity as well as the plants ability to remove excess water from the system (Hauser 2009). The temporal and spatial distributions of water within the cover system are important conditions that can be used to assess the proficiency of the system. In this context the timing of water availability with respect to plant water demand will be an extremely important in determining the effectiveness of the cover system in removing water from the soil reservoir.

#### 2.4.1.1 Seasonal Variation in Topsoil/PG Water Content

Spatial and temporal variations in liquid water content, air temperature, precipitation and topsoil/PG temperature for the 2011 and 2012 growing seasons are presented in Figures 2.9, 2.10 and 2.11 for the 15, 30 and 46 cm treatment plots, respectively. The topsoil material responded rapidly to snowmelt and rainfall precipitation events throughout the growing season. Snowmelt was estimated to have begun on 29 March, 2011 and 9 March, 2012 when the average air temperature exceeded 0 $^{o}$C for a period of 3 days. Infiltration began shortly after as shown by the immediate increases in soil water contents nearest the soil surface for all treatments (Figures 2.9-B ~ 2.11-B). Field observations had noted that all snow present on the various treatment plots had melted and infiltrated before 27 April, 2011. The 2012 snowmelt event was slightly different than that of the 2011 year as marked by a refreezing event that occurred between 19 March and 25 March, 2012 (Figures 2.9 ~ 2.11).

During the spring snowmelt in both years, the underlying PG material remained in a frozen state limiting the amount of water able to drain from the topsoil cap. As a result of this phenomenon the water content within the topsoil cap increased rapidly and approached near saturation for the 15 cm plot for 2011 and 2012. The same cannot be stated with regards to the 30 and 46 cm plots as a result of their increased storage capacity; however, significant increases in water content were observed due to the increase in the amount water that was available and

the retardation effects of the underlying frozen PG material (Figures 2.10 - 2.11). Restrictions in flow between the topsoil and the PG material can be attributed to the decrease in hydraulic conductivity between the topsoil and PG material; however, this is only the case at high matric potentials where the hydraulic conductivity of the topsoil is much higher relative to the PG (i.e. near saturated conditions). The more obvious explanation for restricted flow during early spring melt is the presence of ice filled pores within the PG material, which remained frozen or partially frozen until 21, 25 and 26 April, 2011 and 3, 19 and 21 April 2012 for the 15, 30 and 46 cm treatment plots, respectively. After these dates the overlying topsoil material began to drain and the water contents fell back down to residual levels; however, the drainage of the topsoil in 2012 was offset by early spring precipitation events that were otherwise not present during the 2011 spring snowmelt.

Following spring snowmelt and infiltration the water contents within the topsoil caps across all capping soil treatments were very responsive to rainfall events of magnitude > 20 mm (Figures 2.9 ~ 2.11). The fluctuation in water content at deeper depths within the topsoil cap became depressed as a result of the soils capacity to retard the movement of the infiltrating water long enough for potential plant utilization and/or redistribution. Following such periods of heavy rainfall the water content would gradually drop back down to residual water content levels (approximately 0.10 $cm^3$ $cm^{-3}$). This gradual decline in water content

would usually take place over a period of 14 to 17 days following precipitation events, given there were sustained periods following the rainfall event of minimal precipitation.

The observed water content at each interface of the three treatments was generally higher than the overlying topsoil cap, but lower than the underlying PG material. The interface is generally the boundary between differing materials which may disrupt vertical water movement as discussed in Dyck and Kachanoski (2009). The water content at the interface of the 15 cm plot treatment (Figure 2.9-C) was consistently higher than that of the 30 cm treatment (Figure 2.10-D) and 46 cm treatment (Figure 2.11-E), which could be due in part to greater evapotranspirational demand from the 30 and 46 cm plots as evident by their slightly more robust plant growth during the growing season (Turner 2013).

The variability among soil water contents between the various plot interfaces may also be explained by: 1) topographical variability of topsoil/PG gradients resulting in convergence or divergence of lateral flow; and 2) misrepresentative proportion of topsoil versus PG material within the sample volume of the horizontally installed TDR probes along the topsoil/PG interface resulting in measurements more reflective of PG than of topsoil. Generally, the interface between the two layers is characterized by the very transient and variable moisture regime of the topsoil cap and very steady moisture regime in the PG.

Water content distribution within the PG material was considerably different than the overlying topsoil, most notably with respect to seasonal stability; however, spring thaw and snowmelt infiltration did play a significant role in water content variability during the early spring when the vegetation was still dormant. During the spring snowmelt period, the water contents for the layer of PG directly underlying the topsoil/PG interfaces approached near saturation for all treatment plots due to the influx of infiltrating snowmelt water. The period after spring snowmelt infiltration was marked by a decrease in PG water content that was a product of drainage or evapotranspiration; however, given the limited ability of the plants at this early stage during the growing season it can be assumed that this redistribution of water is primarily a function of drainage.

Throughout the remaining growing season the average water content within the PG material was approximately 0.35 $cm^3$ $cm^{-3}$ across all treatment plots (Figures 2.9 ~ 2.11). The lack of fluctuation of water contents observed in the PG during the growing season is likely a result of the nature of the hydraulic properties between the soil and PG as well as the evapotranspirational demand of the active vegetation. However, increases in water content of the PG material at deeper depths (> 30cm below topsoil/PG interface) were observed for the 15, 30 and 46 cm treatment plots following high magnitude precipitation events (Figure 2.9-G, 2.10-H and 2.11-H), which could be attributed to preferential flow paths that could be present either on or off the plots. Utilization of pore water

from the PG material by the plants was thought to be minimal as a result of the limited number of roots within the PG material. Field observations yielded that the majority of root material was located within the topsoil cap and concentrated on the topsoil/PG interface (Turner 2013).

### 2.4.2 Snowmelt Infiltration, Percolation and Net Flux Estimates

Precipitation in the form of snow is a valuable source of fresh water throughout the prairie regions. The water that is released during snowmelt has been shown to contribute significantly to soil water, groundwater and surface runoff (Maulé and Gray 1994; Zebarth et al. 1989). One study estimated that snow-water contributed 27% to soil water and 44% to groundwater in the Edmonton area (Maulé et al. 1994), while another study found that snowmelt provided 40-70% of groundwater recharge (Earman et al. 2006).

In context of reclamation standards, the philosophy regarding infiltration versus runoff of surface water derived from snowmelt is split between the benefits and risks associated with each. On the one hand, snowmelt runoff can lead to flooding, erosion, drainage problems and potentially the transport of contaminants off site; however, snowmelt runoff has the advantage of removing excess water from the system that could otherwise infiltrate into an unstable and contaminated substrate. Conversely, infiltration of snowmelt into an appropriate cover system would provide the necessary water requirements for plant growth, reduce

the risk of erosion, drought stress, and ultimately facilitate the function of a closed biological cover system. In the Edmonton area snowfall accounts for approximately 26% of all annual precipitation, which in turn contributed close to 50% of groundwater recharge (Maulé et al. 1994); therefore, a clear understand of snowmelt infiltration is important in assessing the effectiveness of the cover system on limiting deep drainage.

To assess the effectiveness of the various capping depths, the cumulative infiltration into the topsoil material was quantified using the one-dimensional soil water continuity equation:

$$\frac{\partial \theta(z,t)}{\partial t} = -\frac{\partial q(z,t)}{\partial z} \quad [2.4]$$

Where θ is the total water content ($cm^3\ cm^{-3}$), t is time (days), q is the soil water flux ($cm^3\ cm^{-2}\ day^{-1}$) and z is depth (cm). Integrating both sides of Eq. 2.4 between two depths (z1 and z2) results in:

$$\frac{\partial}{\partial t}\int_{z1}^{z2} \theta(z,t)dz = -\int_{z1}^{z2} \frac{\partial q(z,t)}{\partial z} dz \quad [2.5a]$$

Which, expressed in terms of storage, is:

$$\frac{\partial W_{z1,z2}(t)}{\partial t} = q(z1,t) - q(z2,t) \quad [2.5b]$$

where, $W_{z1,z2}(t)$ is the soil water storage between depths z1 and z2 as a function of time, and *q(z1,t)* and *q(z2,t)* are the net vertical soil water fluxes at depth z1 and z2, respectively. Eq. 2.5b represents the change in storage between two depths over a period of time, which is equal to the net soil water flux between those two depths over the same period of time.

For discrete time intervals (∆t), Eq. 2.5b can be simplified to:

$$\Delta W_{z1,z2|\Delta t} = [q(z1) - q(z2)]\Delta t \quad [2.6]$$

This describes the change in soil water storage between two depths measured at two discrete times which is the result of the cumulative net vertical flux occurring in the soil volume bounded by the two depths. Positive changes in soil water storage indicate that the net cumulative flux entering into the soil volume (i.e. infiltration – evapotranspiration) is greater than the net cumulative flux exiting the soil volume (i.e. percolation and lateral flow), whereas negative changes in soil water storage would indicate the opposite.

Using the water balance equation to determine drainage and runoff over larger time scales will lend to a more general understanding of the hydrological environment. This method involves monitoring some key hydrological components of the water cycle. Water balance can be described as the changes in water storage during a specified time interval as equal to the difference in water inputs and outputs over the same time interval (Hillel 1998). The inputs include precipitation (P, mm) in the form of rain and snow (snow water equivalent, SWE, mm) and irrigation (I, mm). The outputs or losses include evapotranspiration (ET, mm), drainage (D, mm) and runoff (R, mm). For the purposes of this study the soil water balance can be expressed as:

$$\Delta W = P - ET - D - R \quad [2.7]$$

where, $\Delta W$ is the change in soil storage over a given time period (mm). Note the exclusion of irrigation from the Eq. 2.7 due to the absence of any irrigation treatment on site. During initial spring conditions when snowmelt is initiated and plant growth is dormant the evapotranspiration term can be reduced to zero. Essentially, Eqs. 2.6 and 2.7 are equivalent if one sets $q(z1)\Delta t$ equal to P-ET-R and $q(z2)\Delta t$ equal to D.

#### 2.4.2.1 Cumulative Net Fluxes in Topsoil Cap and PG Stack during Snowmelt and Growing Season

Estimates for cumulative infiltration into the topsoil caps were estimated using the measurements from the vertically installed TDR probes and percolation estimates for the PG material were calculated using the measurements from the horizontally installed probes at -7.5 and -15 cm for discrete time intervals during the snowmelt period of 2011 and 2012.

During the snowmelt period, ET is assumed to be very close to zero. Therefore, the snowmelt infiltration increases soil water storage and is equal to the snow water equivalent (SWE) in the snowpack prior to melt minus net runoff. Rainfall during snowmelt may also contribute to increased soil water storage. In terms of Eq. 2.6, for example, setting z1 at the soil surface, z2 at the topsoil/PG interface, and $\Delta t$ equal to the "snowmelt period" $q(z1)\Delta t$ = snowmelt infiltration + rainfall infiltration = SWE – $R_{\Delta t}$ + $P_{\Delta t}$, and $q(z2)\Delta t$ = D. The vertical TDR probes spanned the

entire depth of the topsoil cap. The vertical probes therefore, measured the average soil water content over the entire topsoil cap which can then be used to estimate soil water storage by multiplying by the length of the TDR probe.

In terms of coordinates, setting z = 0 cm at the topsoil/PG interface with z increasing upward (Table 2.1) results in z1 = depth of topsoil, z2 = 0 cm for the topsoil cap. For the PG, we are interested in the depths bounded by the topsoil/PG interface and the two TDR probes at 7.5 and 15 cm below the interface; i.e., z1 = 0 cm, z2 = -7.5 cm, z3 = -15 cm for the PG. For the horizontal probes in the PG, soil water storage is estimated by assuming each horizontal TDR probe represents the 3.75 cm of PG material above and below its location. Therefore, according to Eq. 2.6, by measuring the change in soil water storage between z1 and z2 ($\Delta W_{z1,z2|\Delta t}$) over the snowmelt period (and subsequent periods) in the topsoil cap and underlying PG, we can interpret the relative magnitude of surface and drainage fluxes over different time periods (i.e., snowmelt and post-snowmelt/growing season).

Time series of the vertical TDR probe measurements for the 2011 and 2012 snowmelt period and growing season are shown in Figure 2.12. Snowmelt began on 29 March, 2011 and 9 March, 2012 when the average air temperature exceeded 0 $^{o}$C (grey vertical line in Figure 2.12-A). The start of infiltration was noted by the initial increase in water content. Infiltration of snowmelt began 7, 5 and 2 April, 2011 and 28, 17 and 17

March, 2012 for the 15, 30 and 46 cm treatment plots, respectively (red vertical lines in Figure 2.12-B ~ D). Field observations noted that all snow had melted and infiltrated before 27 April, 2011 and 7 April, 2012.

During the spring snowmelt, the temperature of the underlying PG material remained below 0 $^{o}$C, with significant (although decreasing) amount of ice still present (Figs. 2.9 – 2.11), limiting the amount of water able to drain from the topsoil cap. As a result of this condition the topsoil within the 15 cm plot approached near saturation during the early spring (Figure 2.9-B), while the 30 and 46 cm plots did not as a result of their increased storage capacity (Figure 2.10-B & Figure 2.11-B). Restrictions in flow between the soil and PG material can be attributed to the hydraulic nature of the underlying PG material, which has a saturated hydraulic conductivity that is an order of magnitude lower than that of the capping soil; however, the hydraulic conductivity is further lowered by the presence of ice filled pore space within the PG material creating a capillary barrier.

This does not rule out the possibility of drainage from the topsoil cap into the PG. As seen in Figs. 2.9-2.11, the liquid water content of the PG increases during the snowmelt period. Heat transported with drainage water from the topsoil cap into the PG may have facilitated thawing of the PG. Nevertheless, water content in the topsoil caps began to decrease only when the underlying PG material had a temperature of > 0 $^{o}$C, indicating that the presence of ice was restricting percolation of water from the topsoil into the PG. On 20 April, 2011 and 13 April 2012 the 15 cm plot

started to drain; drainage of the topsoil commence on 29 April, 2011 and 28 April, 2012 for the 30 cm plot and 25 April, 2011 and 14 April, 2012 for the 46 cm plot (green vertical lines in Figure 2.12-B~ D). Before these dates the PG material directly underlying the capping soil had an average temperature < 0 $^{o}$C and can be assumed to have ice within the pore space restricting flow.

The period of snowmelt infiltration into the topsoil cap was estimated between the beginning of snowmelt (29 March, 2011 and 9 March, 2012) and the maximum observed water content within the topsoil cap, which corresponded to the beginning of the active growing season (23 April, 2011 and 14 April, 2012). It was also observed that all the snow had melted by the date of the observed maximum water content in 2011 and 2012. Between these dates the evapotranspiration is negligible due to the limited photosynthetic ability of the plants during this part of the year when the average air temperature was < 1 $^{o}$C for a period of time greater than 5 days (Hayashi et al. 2010) and because of the frozen condition of the underlying PG material, it was assumed that drainage below the topsoil cap was negligible during this period. Therefore, the net, cumulative, vertical flux (Eq. 2.6) in the topsoil cap during this period, is likely exclusively attributable to snowmelt infiltration.

The amount of infiltration into the topsoil cap as estimated by the vertical TDR probes follows a general linear relationship with capping depth (Table 2.3). The estimates for infiltration for the 15, 30 and 46 cm

treatment are 40, 79 and 126 mm for 2011 and 35, 49 and 63 mm for 2012, respectively; indicating that an increase in soil capping depth results in an increase in infiltration of spring melt water into the capping soil. Conversely, this would suggest that the potential for runoff and/or subsurface lateral flow is highest in treatments where the topsoil cap is relatively thin (i.e. < 15 cm), because of the insufficient storage capacity of the thinner topsoil cap and inhibited drainage into the frozen PG. The amount of water that infiltrated into each capping soil treatment, with respect to amount of water that was available (i.e. snow water equivalent (SWE) + additional rainfall precipitation) during the 2011 spring snowmelt period was 23, 45 and 71% for the 15, 30 and 46 cm treatment respectively, compared to 2012 which yielded 36, 51 and 66% for the 15, 30 and 46 cm treatment, respectively.

The proportion of water that infiltrated into the 30 and 46 cm treatment plots are comparable between 2011 and 2012; however, the 15 cm treatment plot during 2012 was approximately 1.5 times that of the previous year. This phenomenon could be due in part to the limited potential for runoff that was created by the following circumstances: 1) limited autumn rainfall events resulted in drier topsoil conditions that were more receptive to spring infiltration; 2) limited winter precipitation (i.e. snowfall) resulted in limited surpluses of water during the spring snowmelt; and (3) increased spring precipitation that was not present in 2011.

Using Eq. 2.6 to represent the water balance during these infiltration periods it was possible to infer that the potential drainage and/or runoff estimates for the 15, 30 and 46 cm treatment plots were 137, 98 and 51 mm for 2011 and 61, 47 and 33 mm for 2012; however, given that the PG material underlying the topsoil remained frozen until approximately 25 April, 2011 and 20 April, 2012 it can be assumed that the potential for drainage is low and that runoff is the primary mechanism. These estimates might be high as studies have indicated that sublimation may account for up to 50% of water loss from snowpack during the winter (Fassnacht 2004; Pomeroy and Essery 1999; Pomeroy and Li 2000); therefore, assuming 50% sublimation losses, the conservative estimates of potential runoff for the 2011 snowmelt period are 49, 10 and -37 mm and 13, 1 and -15 mm for the 2012 snowmelt period for the 15, 30 and 46 cm treatment plots, respectively. However, the negative value with respect to the runoff potential for the 46 cm treatment plot could be due to: 1) introduction of snowmelt runoff from the adjacent plots, and 2) subsurface convergence of the interface boundary.

It is assumed that percolation/drainage during the spring below the topsoil/PG interface did not commence until the PG temperature was $0^{o}C$ or above. Changes in storage in the 15 cm layer of PG below the topsoil/PG interface are a result of water draining from the overlying topsoil which would increase storage and drainage below the 15 cm thick PG layer. The change in storage in the 15 cm of PG directly below the

topsoil/PG interface was negative in both 2011 and 2012, indicating that the cumulative, net, vertical flux (Eq. 2.6) for this layer of soil is a result of net drainage/percolation. Therefore, we refer to the net cumulative, vertical flux during the snowmelt period for the PG as net percolation. Net percolation estimates for the 15 cm thick layer of PG directly below the topsoil/PG interface are summarized in Table 2.3. During the spring snowmelt period of 2011 the estimated snowmelt percolation was 17, 16 and 20 mm and 9, 5 and 1 mm for the 2012 spring snowmelt period for the 15, 30 and 46 cm treatment plots, respectively.

These estimates account for 10, 9 and 11% of water from the snowmelt period for 2011 and 9, 5 and 1% for the 2012 snowmelt period for the 15, 30 and 46 cm treatment plots, respectively. In terms of the amount of percolation as a proportion of infiltrating water the estimates are 43, 20 and 16% for 2011 and 26, 10 and 2% for 2012 for the 15, 30 and 46 cm treatments, respectively. This trend is primarily a function of the increased ability of the thicker capping soil to retain water once it has infiltrated; however, the fact that more water is able to enter into the thicker capping soils results in greater amounts of water that is able to accumulate on top of the PG material until it has completely thawed. For example, in 2012 the limited amount of water available to the environment resulted in minimal percolation of water into the PG material which favored the thicker capping soils ability to retain moisture; however, in 2011 water was overwhelmingly abundant, creating an environment whereby the

capping soil was unable to retain the added moisture, resulting in an increase in percolation into the PG material.

Growing season cumulative net flux estimates for the topsoil caps and the 15 cm thick layer of PG directly below the topsoil/PG interfaces are summarized in Table 2.4. Cumulative, net flux estimates for the topsoil caps for the 15, 30 and 46 cm treatment plots for the 2011 growing season were 13, 27 and 20 mm and 2, 10 and 10 mm for 2012, respectively, while the estimates for the 15 cm thick PG layer directly below the topsoil/PG interface were 9, 12 and 19 mm for 2011 and 1, 1 and -2 mm for 2012, respectively. For both topsoil and PG, the observed changes in storage were positive for both years with the exception of the PG underlying the 46 cm cap in 2012.

This indicates that the cumulative net flux across upper boundary of both materials (soil surface for the topsoil and topsoil/PG interface for the PG) was greater than the cumulative flux of the bottom boundary of both materials (topsoil/PG interface for the topsoil and 15 cm below the interface for the gypsum). In other words, for the topsoil, the sum of the snowmelt infiltration, growing season precipitation exceeded the sum of ET and drainage below the topsoil/PG interface. For the PG, the water draining below the topsoil/PG interface was greater than the water draining below the 15 cm layer of PG underlying the interface, except in the case of the 46 cm plot in 2012.

The magnitude of the cumulative fluxes across the individual boundaries of the topsoil cap and the PG (i.e., $q1(z1)\Delta t$ and $q2(z2)\Delta t$) during the growing season, however, cannot be estimated by Eq. 2.6. Because of special conditions during snowmelt (i.e. low ET and frozen PG), assumptions could be made about the fluxes across the boundaries of the topsoil (i.e., soil surface) and the PG (i.e., topsoil/PG interface). As a result, estimates of snowmelt infiltration and percolation/drainage through the PG could be made, but these estimates are still subject to uncertainty. For example, there was still liquid water in the PG even when its temperature was below freezing. This would suggest that percolation through the PG is possible even when subsurface temperatures are $<0^{o}C$.

During the growing season, there are many processes that result in upward and downward fluxes across the boundaries of the topsoil cap and the PG and it is difficult to separate them with simplifying assumptions. For example, a cumulative, net vertical flux of zero does not mean there was not water moving through the system, it just means that the flux across the top boundary (z1) is equal to the flux across the bottom boundary (z2). Therefore, the net cumulative fluxes for the 2011 and 2012 growing season do not give information about the magnitude and direction of fluxes across the topsoil/PG interface.

### 2.4.3 Daily Flux Estimates

Estimating the overall and/or instantaneous water fluxes within an ET cover system is critical in determining the potential for percolation of water into the PG material. The overarching purpose of a ET system is to minimize the potential for percolation of water from the topsoil cap into the waste material; therefore, estimating the apparent water fluxes across varying capping soil depth will facilitate our understanding of the efficiency of the ET cover system as well as lend in our understanding of the general energy flow within the system. While Eq. 2.6 may be used to estimate cumulative, net, vertical fluxes over a period of time, the in-situ measurements of soil water potential with the MPS-1 sensors at this site can be used to estimate hydraulic gradients which, when coupled with knowledge of the soil hydraulic conductivity, can produce estimates of soil water fluxes across and below the topsoil/PG interface.

Instantaneous flux estimates were computed using the Buckingham-Darcy Flux Law equation:

$$J_w = -K(h_m)\frac{\partial H}{\partial z} \qquad [2.8]$$

where, H (cm) is the total hydraulic head ($h_g + h_m$) within the unsaturated soil, z (cm) is depth and $K(h_m)$ (cm $day^{-1}$) is the unsaturated hydraulic conductivity. Given that daily matric potentials at +7.5, 0 and -7.5 cm from the topsoil/PG interface were measured, it is possible to compute the total hydraulic head over each depth increment. Furthermore, given the parameters for the moisture retention curve have been computed and

used to establish a unsaturated hydraulic conductivity curve for the topsoil and PG material (Figure 2.8), it is then possible to relate a midpoint matric potential reading with the depth boundary of z1, z2 and z3 to infer a unsaturated hydraulic conductivity. Thus, for each day three flux estimated can be produced for each depth boundary. These boundaries include; +7.5 cm to 0 cm (z1 – z2), 0 cm to -7.5 cm (z2 – z3) and +7.5 cm to -7.5 cm (z1 – z3). For vertical flux estimates across the topsoil/PG interface an effective hydraulic conductivity for 7.5 cm of topsoil and 7.5 cm of PG material was used (i.e., harmonic mean of the hydraulic conductivities of the two materials).

#### 2.4.3.1 Daily Vertical Flux Estimates

Individual daily flux estimates for each of the topsoil treatments across the topsoil/PG interface (i.e. z1 to z3) were assessed for the 2011 and 2012 snowmelt period and growing season and the results are shown in Figure 2.13. Negative flux estimates (indicating downward flux) during the spring snowmelt infiltration coincided with the with the beginning of snowmelt; 7, 5 and 2 April, 2011 and 28, 17 and 17 March, 2012 for the 15, 30 and 46 cm treatment plots, respectively.

Table 2.5 summarizes the magnitude and direction of cumulative fluxes in the topsoil (for the 7.5 cm layer above the interface), PG (for the 7.5 cm layer below the interface) and across the topsoil/PG interface (between 7.5 above and 7.5 cm below the interface). All treatment plots

exhibited negative vertical fluxes across the topsoil/PG interface as a result of snowmelt infiltration/ percolation; however, the magnitude of the spring snowmelt flux across the topsoil/PG interface is significantly greater in 2012 than what was present in 2011 due primarily to the increased amount of spring precipitation that was not present in 2011 (Figure 2.13; Table 2.5).

The increase in spring precipitation from 2011 to 2012 impacted the ET system profusely, resulting in not only an increase in downward flux estimates but also an increase the duration of downward flux. For example, during the 2011 spring snowmelt period an average of 38 consecutive days were associated with downward flux gradients across the topsoil/PG interfaces. During the 2012 spring snowmelt period an average of 60 consecutive days were associated with downward flux gradients across the topsoil/PG interfaces.

This increase in the amount of time devoted to downward flux ultimately diminishes the functionality and effectiveness of the ET cover system by limiting the plants affinity to remove water from discrete locations in the soil profile (i.e. topsoil/PG interface). During early spring, daily flux estimates were sensitive to rainfall events of minimal magnitude (i.e. $\leq$ 10 mm). As a result of these events the vertical flux would become depressed (Figure 2.13). These moments of depression or reversal can be used to illustrate the limited ability of the plants to transpire water in the early summer; however, after June those rainfall events do not impact the

daily flux gradients as abruptly. Large magnitude precipitation events (> 25 mm) that occur over discrete moments (< 1 day) and low magnitude precipitation events (< 25 mm) that occur over longer periods (> 3 days) do impact the direction and magnitude of the vertical flux within the reclaimed system. For example on 16 June, 2011, a 45 mm precipitation event occurred on site resulting in an immediate reversal of flux direction across the topsoil/PG interface of the 15, 30 and 46 cm treatment plots.

The negative flux estimates were sustained across all treatment due to low magnitude precipitation events that continued for several days (Figure 2.13-B~D). The 15 cm treatment plot however, was able to recover to a positive vertical flux within the topsoil cap due in part to the limited storage capacity of capping soil which meant the soil water reservoir was more easily drained by the biological system. As moisture is removed from the surface of the capping soil first it was observed that the deeper the capping soil treatment the greater the amount of time required for the effects of evapotranspiration to penetrate to the topsoil/PG interface (Figure 2.13).

During periods of minimal precipitation, evapotranspiration was the dominant factor impacting vertical flux estimates. For example, the 15 cm plot showcased positive vertical flux estimates from 12 April to 14 June, 2011 (Figure 2.13-B). During this period the total amount of precipitation that occurred on site was 29 mm. The limited amount of precipitation coupled with the limited amount of water that had infiltrated into the 15 cm

plot during spring snowmelt resulted in positive vertical flux estimates that reached a maximum magnitude of 1.30 cm $day^{-1}$ (Figure 2.13-B). Positive vertical flux estimates were also observed in the 30 and 46 cm treatment plots throughout the growing season during periods of minimal precipitation.

The cumulative fluxes across the topsoil/PG interface during the 2011 and 2012 growing season (23 April – 15 September) are 0.006, -41.0 and -24.9 cm and -7.5, -49.6 and -92.8 cm for the 15, 30 and 46 cm treatment plots (Table 2.5), respectively. While periods of upward flux account for more than 50% of the growing season, the cumulative flux is negative. In other words, while the forces that account for downward movement of water only contribute to < 50% of the growing season, the magnitude of the contribution dominates the general flux continuum across the topsoil/PG interface. In both snowmelt and growing seasons, the 15 cm plot exhibited the least amount of downward flow across the topsoil/PG interface indicating that the limited storage capacity of the 15 cm treatment plot was useful in reducing the amount of water (snowmelt or growing season precipitation) for percolation by limiting the amount of infiltration. This result can also be attributed to the higher concentration of root material present in the 15 cm plots as compared to the deeper capping treatments (Turner 3013).

### 2.4.4 Uncertainties in Soil Water, Infiltration, Percolation and Flux Estimates

The TDR-based estimates of snow water infiltration and percolation during snowmelt periods may be under estimated. Sources of errors in the snowmelt infiltration estimates can be traced back to the distribution of water content measurements that were used to compute storage. As a result of increasing depth computation in deriving storage terms the errors will linearly increase with increasing capping depth; however, variability between the various water content measurements during the steady state observations were very small (< 0.01 $cm^3$ $cm^{-3}$).

Other sources of error with regards to infiltration estimates include the possibility of steady state flow within the PG material during snowmelt periods. For example, the topsoil cap of the 15 cm treatment had a very high water content that remained stable during snowmelt infiltration. We assumed the lack of change in water content was due to the limited ability of the frozen PG material to transmit the water; however, under steady state flow dynamics water content distribution within the topsoil cap would not change. The result of this assumption would have been an underestimation of the amount of water infiltrating into the 15 cm plot. Furthermore, it was observed that there was liquid water in the PG material even when its temperature was below freezing. This would suggest that percolation through the PG is possible even during very low temperatures. In summary, there may have been drainage during periods

where there is no observable change in soil water storage in the topsoil cap, contrary to the assumption that zero was used for the percolation estimates using Eq. 2.6.

As mentioned above, TDR estimates of unfrozen water and ice content during periods when the soil is frozen are based on the assumption that the total water content within the sampling volume of the TDR probe does not change. Unfortunately, it is during times of snowmelt infiltration into frozen soils when this assumption is most likely to be violated. Because soil thawing and snowmelt infiltration both increase the liquid water content of the soil, there is some uncertainty associated with the unfrozen water and ice content estimates presented, especially in the more responsive topsoil cap. However, because of the very dry fall soil water conditions in the topsoil, these uncertainties are not expected to cause a misinterpretation of the processes occurring in the field. However, as mentioned above, changes in soil water storage in a volume of soil does not give enough information to estimate the cumulative fluxes across the boundaries of the soil volume in question.

The estimations for daily flux values based on Buckingham-Darcy Flux Law are likely grossly over-estimated. For example, the cumulative fluxes estimated by integrating the daily fluxes with time results in cumulative flux estimates greater than the amount of growing season precipitation and SWE. The daily fluxes are based on two parameters that govern the Buckingham-Darcy Flux Law, the total hydraulic gradient

($\Delta H/\Delta z$) and the unsaturated hydraulic conductivity (K(*hm*)). One source of error during the computation of flux estimates is a product of the unsaturated hydraulic conductivity, which is based on the moisture retention curves and independent estimates of saturated hydraulic conductivity for the topsoil and PG material. Both materials exhibited a narrow distribution with regards to their moisture retention dynamics, which results in large changes in matric potential given a small change in water content.

This discrepancy is most apparent within the narrow confines that define the loamy sand topsoil material. In this regard the predicted hydraulic conductivity of the topsoil was more responsive to small changes in water content. Because the saturated hydraulic conductivities of the topsoil and PG material were measured on repacked cores under warm, isothermal conditions in the lab, it is likely that the predicted hydraulic conductivities of the materials (Fig. 2.8) are much greater than they actually are in the field. This potential discrepancy is further exploited when combined with the second source of computational error, the hydraulic gradient. While the MPS-1 sensors are optimal when functioning across a wide range of unsaturated conditions, they are not as sensitive during near saturated conditions, which is when the largest fluxes occur in the field.

Another source of error associated with daily flux estimates is directly related to the application of the Buckingham-Darcy Flux Law under

these specific boundary conditions. Eq. 2.8 that was presented in section 2.4.3 applies to a cross section of soil where H and K(*hm*) are constant. While the equation was applied under the assumption that for each time increment (1 day) the matric potential and water content were constant across a finite soil volume (Jury et al. 1991), it is likely that both are temporally and spatially variable. However, the flux estimates from Eq. 2.8 are useful in determining the direction of flux and comparing the relative magnitude of the fluxes between the two years.

## 2.5 Conclusions

Significant amounts of water were available during snowmelt periods which contribute approximately 40% of total annual precipitation in 2011 and 19% of total annual precipitation in 2012. Specific conclusions include:

- Increases in capping soil thickness resulted in increased infiltration of snowmelt water due to the higher storage capacity of the thicker capping depths.
- Increases in capping soil thickness resulted in decreased potential of lateral snowmelt runoff.
- Increases in capping soil thickness resulted in greater percolation below the capping soil due to the combination of the increased amount of infiltration and the limited ability of the capping soil to retain water.

- The estimated hydraulic gradient across the topsoil/PG interface indicated that during the early spring and severe precipitation events (i.e. > 25 mm) drainage/percolation was occurring throughout all treatment depths.
- The daily flux across the topsoil/PG interface was highly sensitive to high intensity (> 25 mm) / short duration (< 1 day) precipitation events as well as low intensity (> 5 mm < 25 mm) / long duration (> 3 days) precipitation events, both of which resulted in downward flux into the PG material.
- Evapotranspiration contributed significantly to upward flux patterns across the topsoil/PG interface during the active growing season in terms of duration; however, with respect to magnitude the negative downward flux pattern dominated due to precipitation.
- Cumulative vertical flux estimates across the topsoil/PG interface throughout the 2011 and 2012 active growing season indicated that an increase in capping soil thickness resulted in greater flux across the interface in a downward (negative) direction.
- Percolation estimates for capping soil depths < 46 cm were < 3% of annual precipitation; however, the temporal variation in downward flux estimates suggest spring snowmelt is the dominant event contributing to percolation.

## 2.6 References


Abril, J.M., R. García-Tenorio and G. Manjón. 2009. Extensive radioactive characterization of a phosphogypsum stack in SW Spain: 226Ra, 238U, concentrations and 222Rn exhalation rate. Journal of Hazardous Materials 164:790-797.

Agriculture and Rural Development. 2011. Alberta soil information viewer. [Online] Available: http://www4.agric.gov.ab.ca/agrasidviewer/. [2011 Sept. 13].

Alberta Environment, 2008. Amending approval Environmental Protection and Enhancement Act R.S.A. 2000, c.E-12. Approval No. 210-02-00. Approval holder: Agrium Products Inc., Redwater AB. Effective date April 4, 2008. 41 pp.

Averitt, D.W. and J.E. Gliksman. 1990. Free water in phosphsphogypsum. Fertilizer Research. 24:57-62.

Bayrock, L.A. and Hughes, G.M. 1962. Surficial geology of the Edmonton district, Alberta. Research Council of Alberta. Earth Sciences Report 196-06. 43pp.

Campbell Scientific (Canada) Corp. 2007. Products: sensors and supporting hardware [Online] Available: http://www.campbellsci.ca/Products_Sensors.html. [2011 Sept. 12].

Dalton, F.N., Harkelrath, W.N., Rawlins, D.S., and Rhoades, J.D. 1984. Time-domain reflectometry: Simultaneous measurements of soil water content and electrical conductivity with single probe. Science 224:898-990.

Dalton, F.N. and van Genuchten, M.TH. 1986. The time-domain reflectometry method for measuring soil water content and salinity. Geoderma 38:237-250.

Dasberg, S. and Dalton, F.N. 1985. Field measurement of soil water content and bulk electrical conductivity with time-domain reflectometry. Soil Science Society of America Journal 49:293-297.

Dyck, M.F. and Kachanoski, R.G. 2009. Measurement of transient soil water flux across a soil horizon interface. Soil Science Society of America Journal 73:1604-1613.

Earman, S., Campbell, A.R., Phillips, F.M., and Newman, B.D. 2006. Isotopic exchange between snow and atmospheric water vapor: Estimation of snowmelt component of ground water recharge in the southwestern United States. Journal of Geophysical Research 111:1-18.

Environment Canada. 2012. National climate data and information archive. [Online] Available:

http://www.climate.weatheroffice.gc.ca/advanceSearch/searchHistoricDataStations_e.html?searchType=stnName&timeframe=1&txtStationName=fort+saskatchewan&searchMethod=contains&optLimit=yearRange&StartYear=1840&EndYear=2012&Month=9&Day=21&Year=2012&selRowPerPage=25&cmdStnSubmit=Search. [2012 Mar. 20].

Environment Canada. 2013. Canadian climate normals 1971-2000. [Online] Avaiable: http://www.climate.weatheroffice.gc.ca/climate_normals/results_e.html?stnID=1886&prov=&lang=e&dCode=4&dispBack=1&StationName=fort_saskatchewan&SearchType=Contains&province=ALL&provBut=&month1=0&month2=12.[2013, Mar. 11].

Fassnacht, S.R. 2004. Estimating alter-shield gauge snowfall undercatch, snowpack sublimation, and blowing snow transport at six sites in the conterminous United States. Hydrological Processes 15:3481-3492.

Hallin, I.L. 2009. Evaluation of a substrate and vegetation cover system for reclaimed phosphogypsum stacks at Fort Saskatchewan, Alberta. MSc Thesis. University of Alberta, Edmonton, AB. 107 pp.

Hauser, V.L. 2009. Evapotranspiration landfill covers. Pages 35-49 *in* Evapotranspiration covers for landfills and waste sites. CRC Press, Boca Raton, FL. USA.

Hayashi, M., Jackson, J.F, and Xu, L. 2010. Application of the versatile soil moisture budget model to estimate evaporation from prairie grassland. Canadian Water Resource Journal 35:187-208.

He, H. and Dyck, M. F. 2012. Application of multiphase dielectric mixing models for understanding the effective dielectric permittivity of frozen soils. Vadose Zone Journal. doi: 10.2136/vzj2012.0060.

Hillel, D. 1998. Water balance and energy balance in the field. Pages 589-615 *in* Environmental soil physics. Academic Press, San Diego, CA. USA.

Jackson, E. M. 2009. Assessment of soil capping for phosphogypsum stack reclamation at Fort Saskatchewan, Alberta. MSc Thesis. University of Alberta, Edmonton, AB. 162 pp.

Jones, S.B. and Friedman, S.P. 2000. Particle shape effect on the effective permittivity of anisotropic or isotropic media consisting of aligned or randomly oriented ellipsoidal particles. Water Resources Research 36:2821-2833.

Jury, W.A., Gardner, W.R., and Gardner, W.H. 1991. Water movement in soil. Pages 73-121 *in* Soil physics, fifth edition. John Wiley and Sons Inc. New York, NY. USA.

Luther S.M., M.J. Dudas and P.M. Rutherford. 1993. Radioactivity and chemical characteristics of Alberta phosphogypsum. Water, Air, and Soil Pollution 69:227-290.

Maulé, C.P. and Gray, D.M. 1994. Estimated snowmelt infiltration and runoff for the prairie provinces. Canadian Water Resource Journal 19:253-265.

Maulé, C.P., Chanasyk, D.S., and Muehlenbachs, K. 1994. Isotopic determination of snow-water contribution to soil water and groundwater. Journal of Hydrology 155:73-91.

Natural Regions Committee. 2006. Natural regions and subregions of Alberta. Compiled by D.J. Downing and W.W. Pettapiece. Government of Alberta. Publication. No. T/852. Edmonton, AB. 264 pp.

Nichol, C.K. 2009. In: Jackson, E. M. 2009. Assessment of soil capping for phosphogypsum stack reclamation at Fort Saskatchewan, Alberta. M.Sc. Thesis. University of Alberta, Edmonton, AB. 162 pp.

Pomeroy, J.W. and Essery, R.L.H. 1999. Turbulent fluxes during blowing snow: field tests of model sublimation predictions. Hydrological Processes 13:2963-2975.

Pomeroy, J.W. and Li, L. 2000. Prairie and Arctic areal snow cover mass balance using a blowing snow model. Journal of Geophysical Research 105:26619-26634.

Rutherford, P.M., M.J. Dudas, and R.A. Samek. 1994. Environmental impacts of phosphogypsum. The Science of the Total Environment 149:1-38.

Rutherford, P.M., Dudas, M.J. and Arocena, J.M. 1995. Trace elements and fluoride in phosphogypsum leachates. Environmental Technology 16:343-354.

Rydzynski, R. 1990. Pollution loads from a large chemical plant and phosphogypsum stack. In: Proceedings of the Third International Symposium on Phosphogypsum. Orlando, FL. FIPR Publication No. 01-060-083. pp. 64-73.

SENES. 1987. An analysis of the major environmental and health concerns of phosphogypsum tailings in Canada and methods for their reduction. Prepared by: SENES Consultants Limited. Willowdale, Ontario. 560 pp.

Sihvola, A.H. and Lindell, I.V. 1990. Polarizability and effective permittivity of layered and continuously inhomogeneous dielectric ellipsoids. Journal of Electromagnetic Waves and Applications. 3:1-26.

Strydom, C.A. and J.H. Potgieter. 1999. Dehydration behavior of a natural gypsum and a phosphogypsum during milling. Thermochimica Acta 332:89-96.

Svarich, D. 1999. The Fort Saskatchewan nitrogen operations: facilities fact book. Agrium Incorporated. Fort Saskatchewan, AB.

Thorne, W.E.R. 1990. Reclamation of a phosphogypsum tailings pond: an examination of the relevant issues. MEDes Thesis. University of Calgary. Calgary, AB. 330 pp.

Topp, G.C., Davis, J.L., and Annan, A.P. 1980. Electromagnetic determination of soil water content: Measurements in coaxial transmission lines. Water Resources Research 16:574–582.

Turner, L. 2013. Influence of soil cap depth and vegetation on reclamation of phosphogypsum stacks in Fort Saskatchewan, Alberta. M.Sc. Thesis. University of Alberta, Edmonton, AB. 172 pp.

van Genuchten, M. Th. 1980. A closed-form equation for predicting the hydraulic conductivity of unsaturated soils. Soil Science Society of America Journal 44:892-898.

Wissa, A.E.Z. 2002. Phosphogypsum disposal and the environment. In: J.J. Schultz and D.R. Waggoner (eds.). Proceedings of international workshop on current environmental issues of fertilizer production. June 7-9, 1999. Prague, Czech Republic. IFDC. Muscle Shoals, AL. Pp. 195-205.

Zebarth, B.J., De Jong, E., and Henry, J.L. 1989. Water flow in a hummocky landscape in central Saskatchewan, Canada, II. Saturated flow and groundwater recharge. Journal of Hydrology 110:181-198.

Table 2.1 Soil sensors and placement depth below soil surface

| Soil Treatment | Sensor | Depth[y] |
|---|---|---|
| 15 cm | TDR Probe | 7.5, 0[z], -7.5, -15, -30, -45 cm, and 15 cm vertical |
| | Temp. Probe | 7.5, 0[z], -7.5, -15, -30 and -45 cm |
| | MPS-1 Probe | 7.5, 0[z], and -7.5 cm |
| 30 cm | TDR Probe | 15, 7.5, 0[z], -7.5, -15, -30, -45 cm, and 30 cm vertical |
| | Temp. Probe | 15, 7.5, 0[z], -7.5, -15, -30, and -45 cm |
| | MPS-1 Probe | 7.5, 0[z], and -7.5 cm |
| 46 cm | TDR Probe | 30, 15, 7.5, 0[z], -7.5, -15, -30 cm, and 46 cm vertical |
| | Temp. Probe | 30, 15, 7.5, 0[z], -7.5, -15, and -30 cm |
| | MPS-1 Probe | 7.5, 0[z], and -7.5 cm |

z PG/Soil interface.

y positive and negative values indicate above and below topsoil/PG interface.

Table 2.2 Physical Properties of Topsoil and Phosphogypsum

| Properties | Topsoil | PG[z] |
|---|---|---|
| % Sand | 84 (2.7) | 33 (2.0) |
| % Silt | 11 (1.6) | 61 (2.8) |
| % Clay | 5 (2.2) | 6 (2.7) |
| Texture | Loamy Sand | Silt Loam |
| Bulk Density (Mg $m^{-3}$) | 1.54 (0.19) | 1.28 (0.24) |
| Water Holding Capacity ($cm^3$ $cm^{-3}$) | 0.27 (0.03) | 0.29 (0.03) |
| Saturated Hydraulic Conductivity (cm $s^{-1}$) | 7.4 X $10^{-3}$ (8.0 X $10^{-5}$) | 3.7 X $10^{-4}$ (6.6 X $10^{-6}$) |

z Phosphogypsum (PG)
Mean values present, SD in parentheses

Table 2.3 Estimates of cumulative spring infiltration into the topsoil and cumulative spring percolation into the PG material

| Plot | Year | $H_2O$ (SWE[z] + Precip.[y]) (mm) | Estimated Spring[x] Infiltration – Topsoil (mm) | Estimated Spring[x] Percolation – PG[t] (mm) | Runoff[v] Estimate (mm) |
|---|---|---|---|---|---|
| 15 | 2011 | 177 (89)[u] | 40 | 17 | 137 (49)[u] |
| 30 | 2011 | 177 (89)[u] | 79 | 16 | 98 (10)[u] |
| 46 | 2011 | 177 (89)[u] | 126 | 20 | 51 (-37)[u] |
| 15 | 2012 | 96 (48)[u] | 35 | 9 | 61 (13)[u] |
| 30 | 2012 | 96 (48)[u] | 49 | 5 | 47 (1)[u] |
| 46 | 2012 | 96 (48)[u] | 63 | 1 | 33 (-15)[u] |

z Snow Water Equivalent (SWE).
y Cumulative precipitation on site from November 1, 2010 & 2011 to April 23, 2011 & April 14, 2012.
x 29 March, 2011 to 23 April, 2011 & 9 March, 2012 to 14 April, 2012.
v Estimated Runoff = Water available to the system ($H_2O$) – Cumulative Spring Infiltration.
u Parentheses = estimation for 50% loss of water to sublimation.
t Phosphogypsum (PG)

Table 2.4 Estimates of net, cumulative vertical flux within the topsoil and PG material during the growing season

| TMT | Year | Annual Precipitation (mm)[w] | Net Flux[w] - Topsoil | | Net Flux[w] - PG[y] | |
|---|---|---|---|---|---|---|
| | | | (mm) | (% Annual Precip.) | (mm) | (% Annual Precip.) |
| 15 | 2011 | 427.3 | 13.3 | 3.1 | 9.2 | 2.2 |
| 30 | 2011 | 427.3 | 26.5 | 6.2 | 11.5 | 2.7 |
| 46 | 2011 | 427.3 | 19.8 | 4.6 | 18.9 | 4.4 |
| 15 | 2012 | 506.4 | 2.3 | 0.5 | 0.7 | 0.1 |
| 30 | 2012 | 506.4 | 9.7 | 1.9 | 0.5 | 0.1 |
| 46 | 2012 | 506.4 | 9.5 | 1.9 | -1.8 | -0.4 |

w 1 March, 2011 & 2012 to 1 October, 2011 & 2012.
y Phosphogypsum

Table 2.5 Average flux estimates within and across the substrate materials during the active growing season and spring snowmelt period (estimated with Eq. 2.8)

| | | Spring Snowmelt[z] | | | Active Growing Season[y] | | |
|---|---|---|---|---|---|---|---|
| TMT | Year | Topsoil[x] Flux (cm day$^{-1}$) | PG[xv] Flux (cm day$^{-1}$) | Soil/PG[wv] (cm) | Topsoil[x] Flux (cm day$^{-1}$) | PG[xv] Flux (cm day$^{-1}$) | Soil/PG[wv] (cm) |
| 15 | 2011 | 0.15 | -4.62 | -16.1 | 0.17 | -1.85 | 0.006 |
| 30 | 2011 | -0.45 | -8.86 | -74.4 | -0.19 | -2.08 | -41.0 |
| 46 | 2011 | -0.87 | -5.48 | -60.7 | -0.37 | 5.74 | -24.9 |
| 15 | 2012 | -0.53 | -10.77 | -121.7 | 0.08 | -3.70 | -7.5 |
| 30 | 2012 | -0.73 | -10.63 | -205.6 | -0.21 | -0.87 | -49.6 |
| 46 | 2012 | -0.49 | -10.89 | -128.6 | -0.36 | 0.24 | -92.8 |

z 29 March, 2011 – 23 April, 2011 & 9 March, 2012 – 14 April, 2012
y 23 April, 2011 – 15 September, 2011 & 14 April – 15 September, 2012.
x 7.5 cm thick layer
w Cumulative Flux Estimate - 15 cm thick layer across soil/PG interface
v Phosphogypsum (PG)

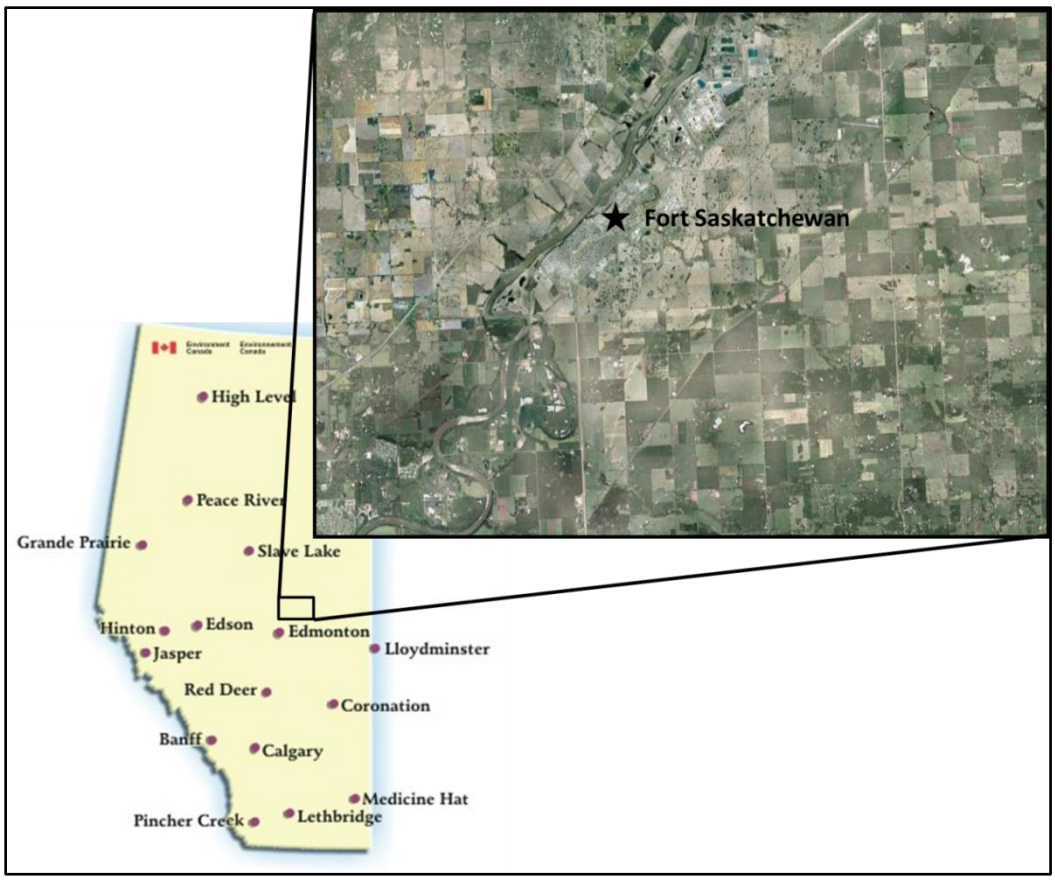

Figure 2.1: Location of Agrium Nitrogen Operations facility in Fort Saskatchewan, Alberta, Canada.

Figure 2.2: Aerial map of Agrium Nitrogen Operations facility detailing the various phosphogypsum stack locations (Blue) and the property boundaries. Areas shaded red indicate Sherrit Inc. property.

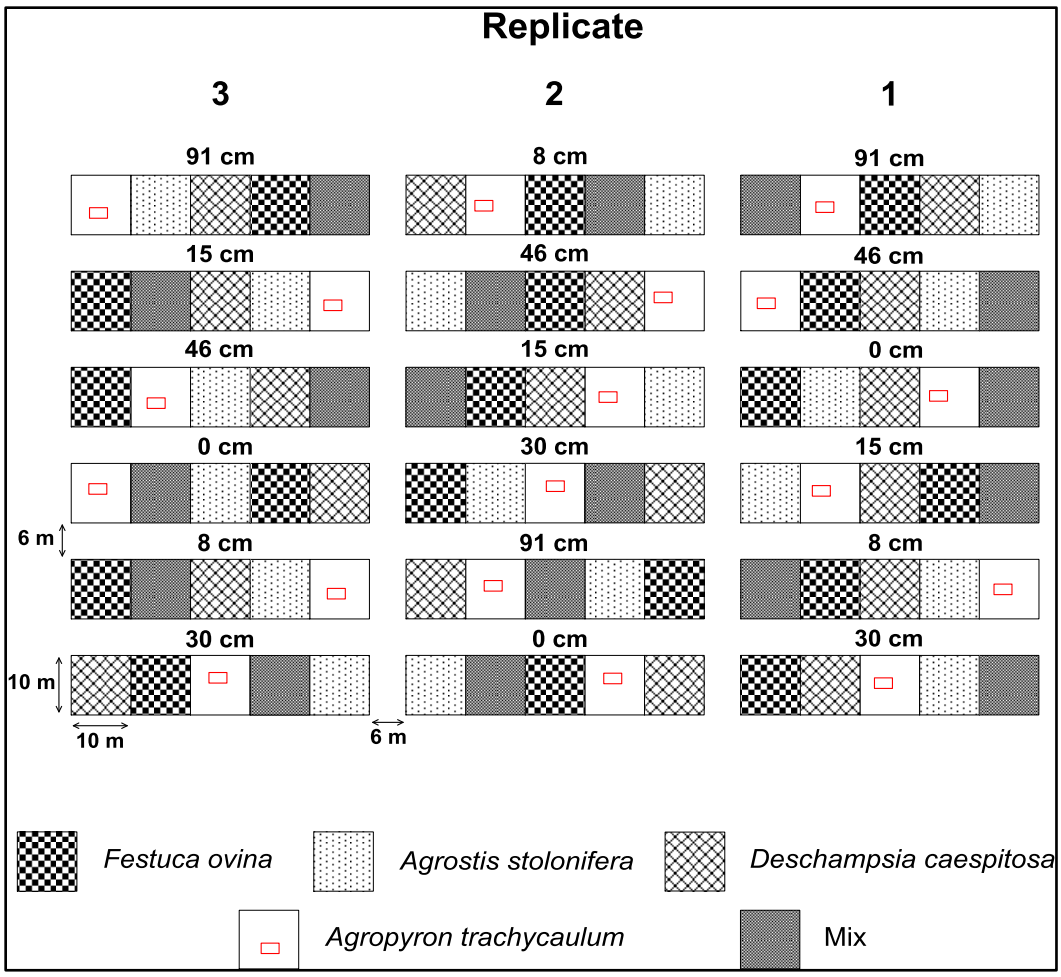


Figure 2.3: Experimental research plots located onsite at Agrium Nitrogen Operations, Fort Saskatchewan, Alberta.

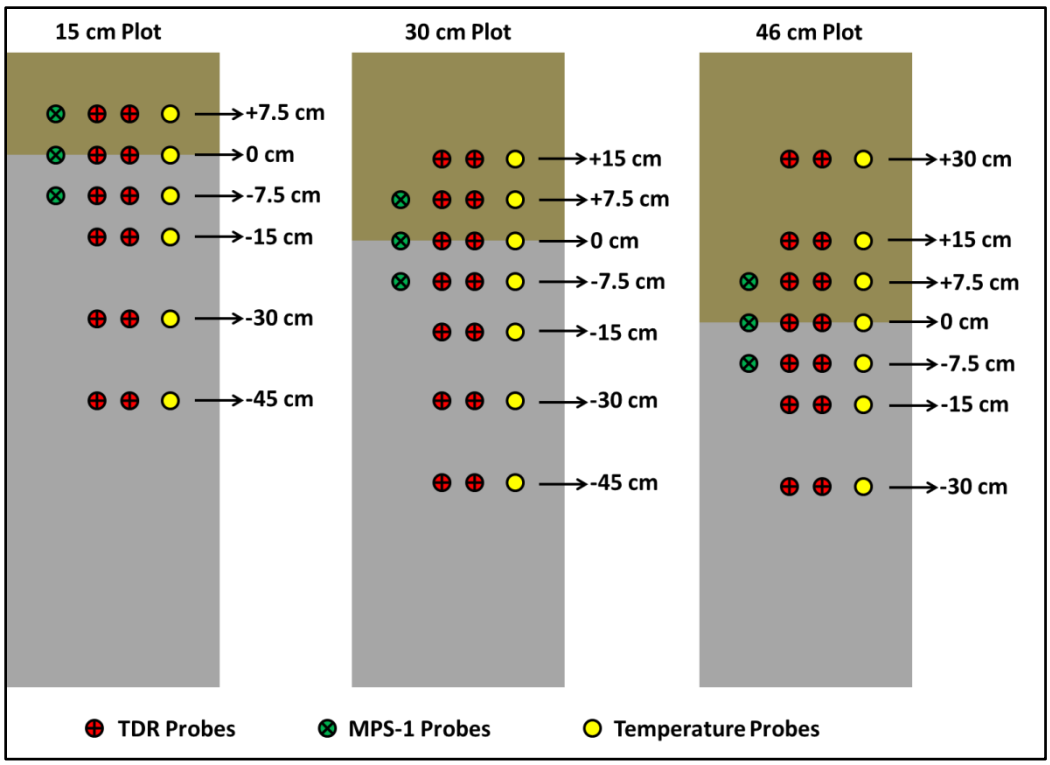

Figure 2.4: TDR, MPS-1 and temperature probe locations in the 15, 30 and 46 cm treatment plot profile.

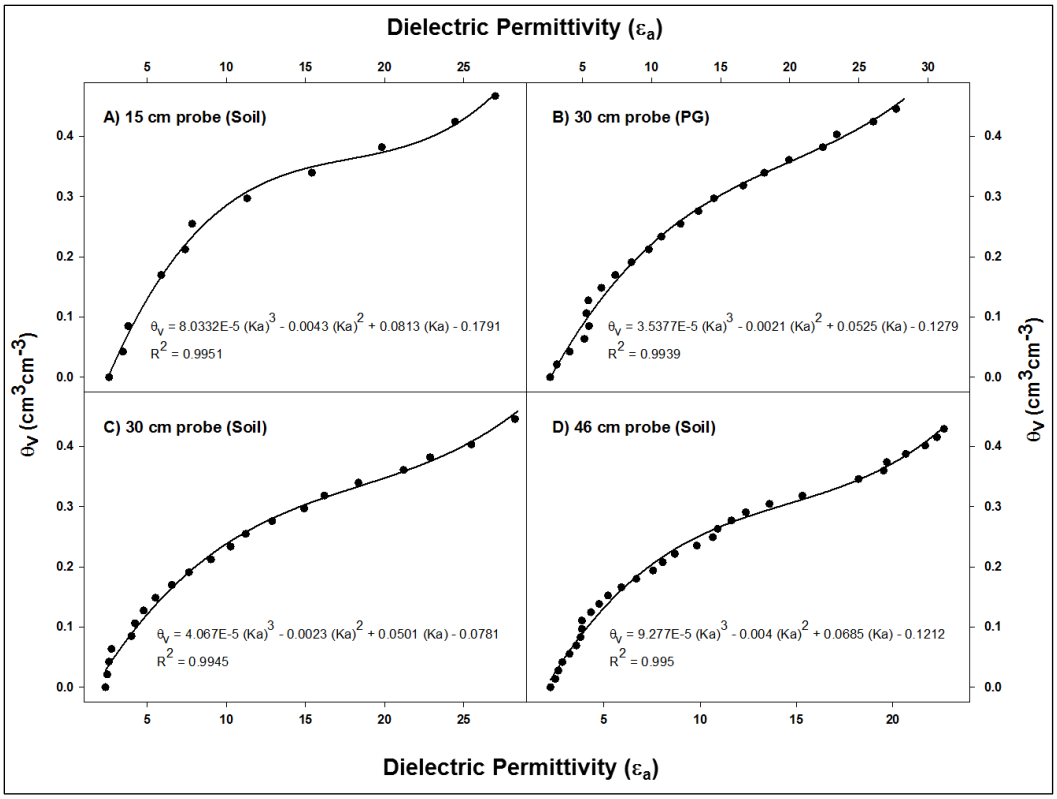


Figure 2.5: Calibration curves pertaining to the 15 cm (A), 30 cm (C) and 46 cm (D) probes lengths for the topsoil material as well as the 30 cm (B) probe length for the PG material.

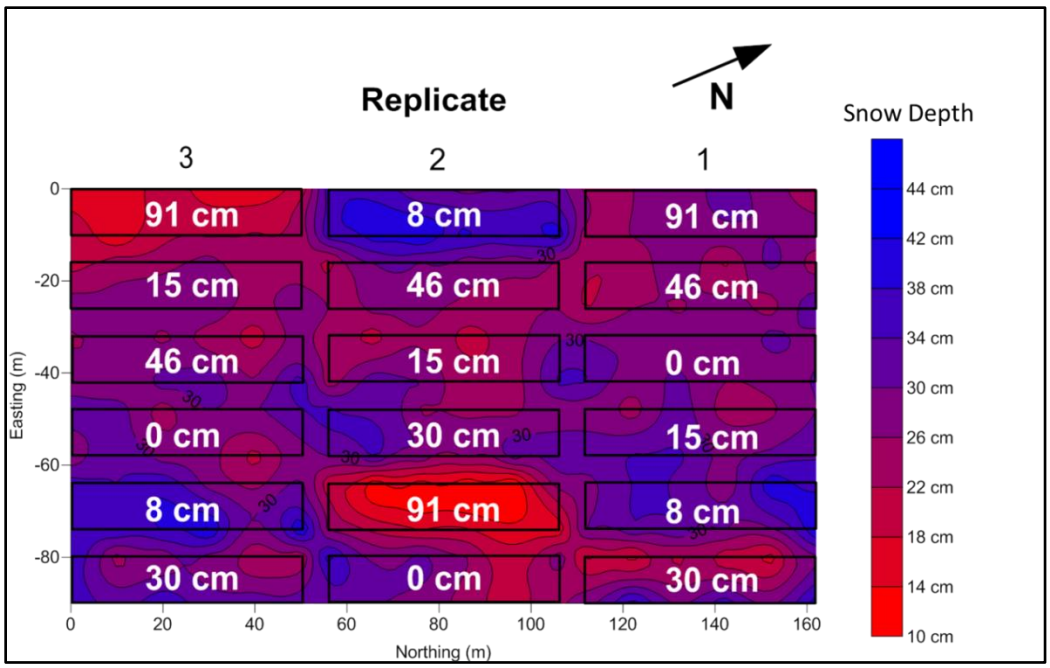


Figure 2.6: Snow depth contour plot of 216 discrete snow depth measurements taken on 26 February, 2011.

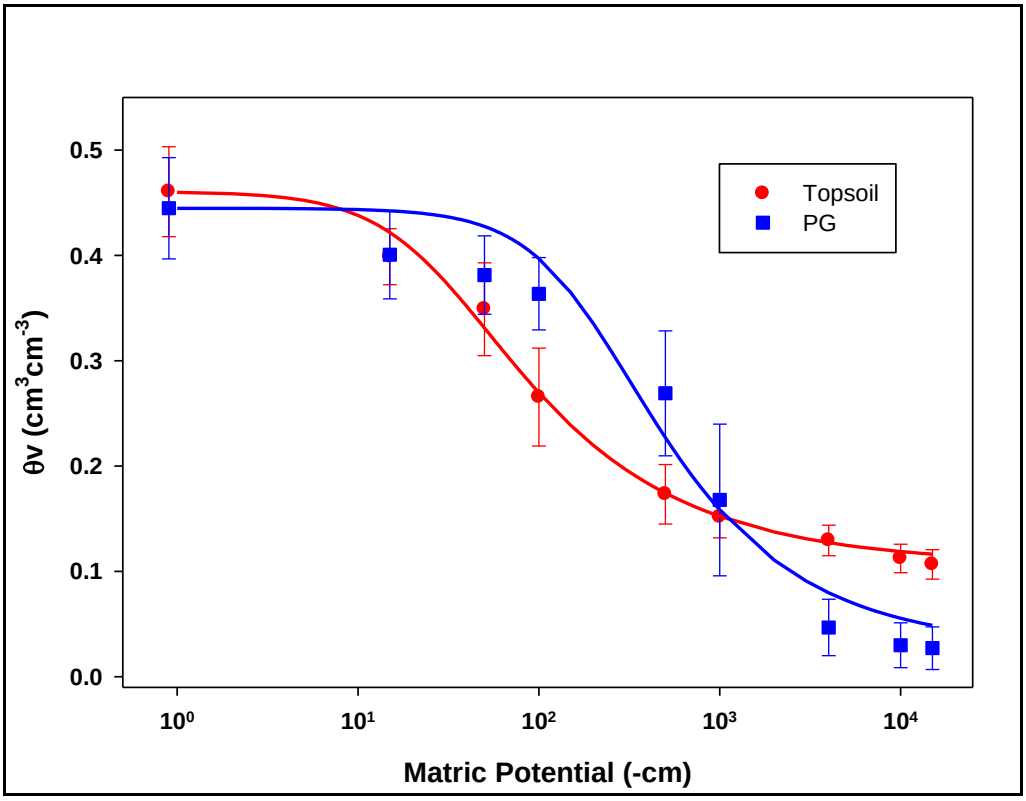


Figure 2.7: van Genuchten model fitted to the moisture retention curves for the topsoil (red) and PG (blue) substrates with standard deviation represented with error bars (1980).

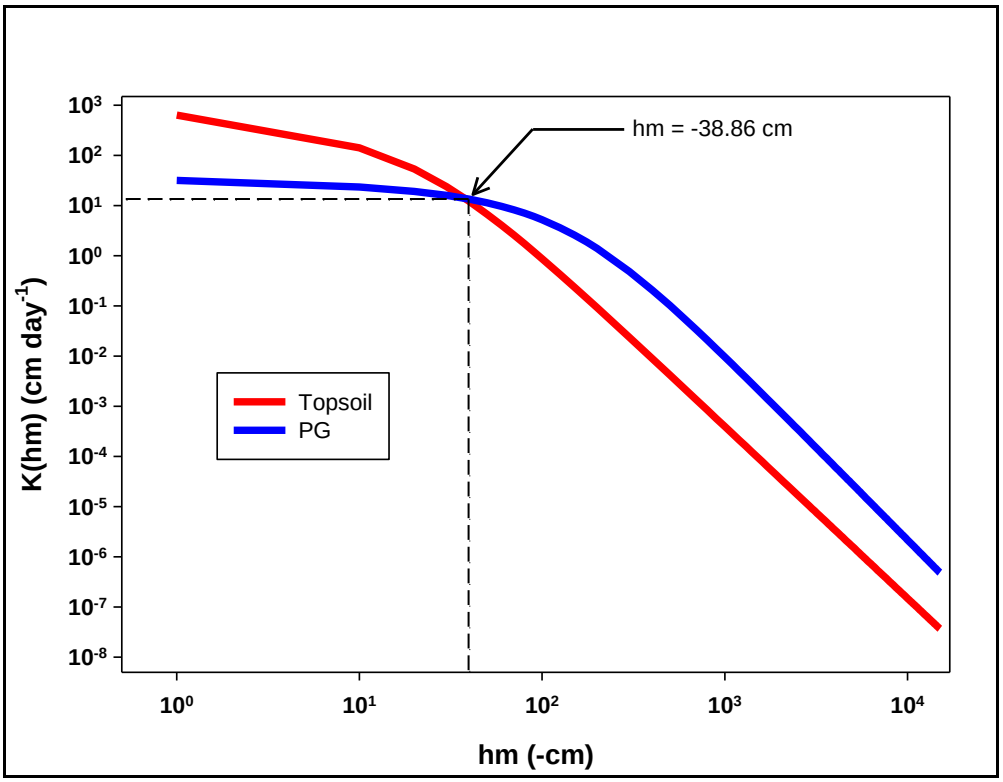

Figure 2.8: Hydraulic conductivity curves for PG and Topsoil as predicted using the van Genuchten-Mualem model (1980).

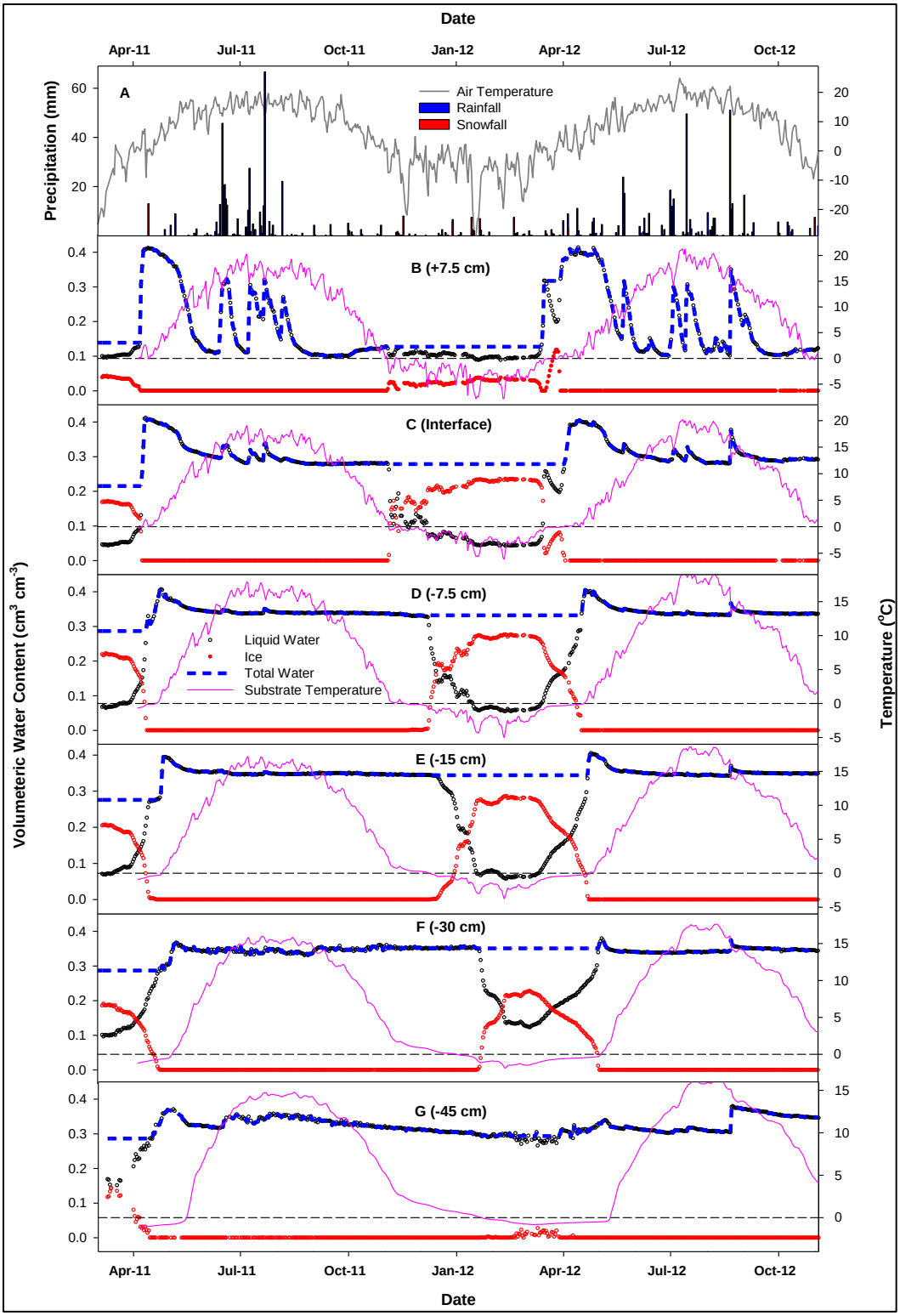


Figure 2.9: Time series of daily mean air temperature and precipitation (A), and liquid water, ice, total water content (liquid water + ice) and daily mean substrate temperature (B – G) of each depth below ground surface for the 15 cm treatment plot during March 2011 to November 2012. Black dashed line indicates 0 $^{o}$C reference.

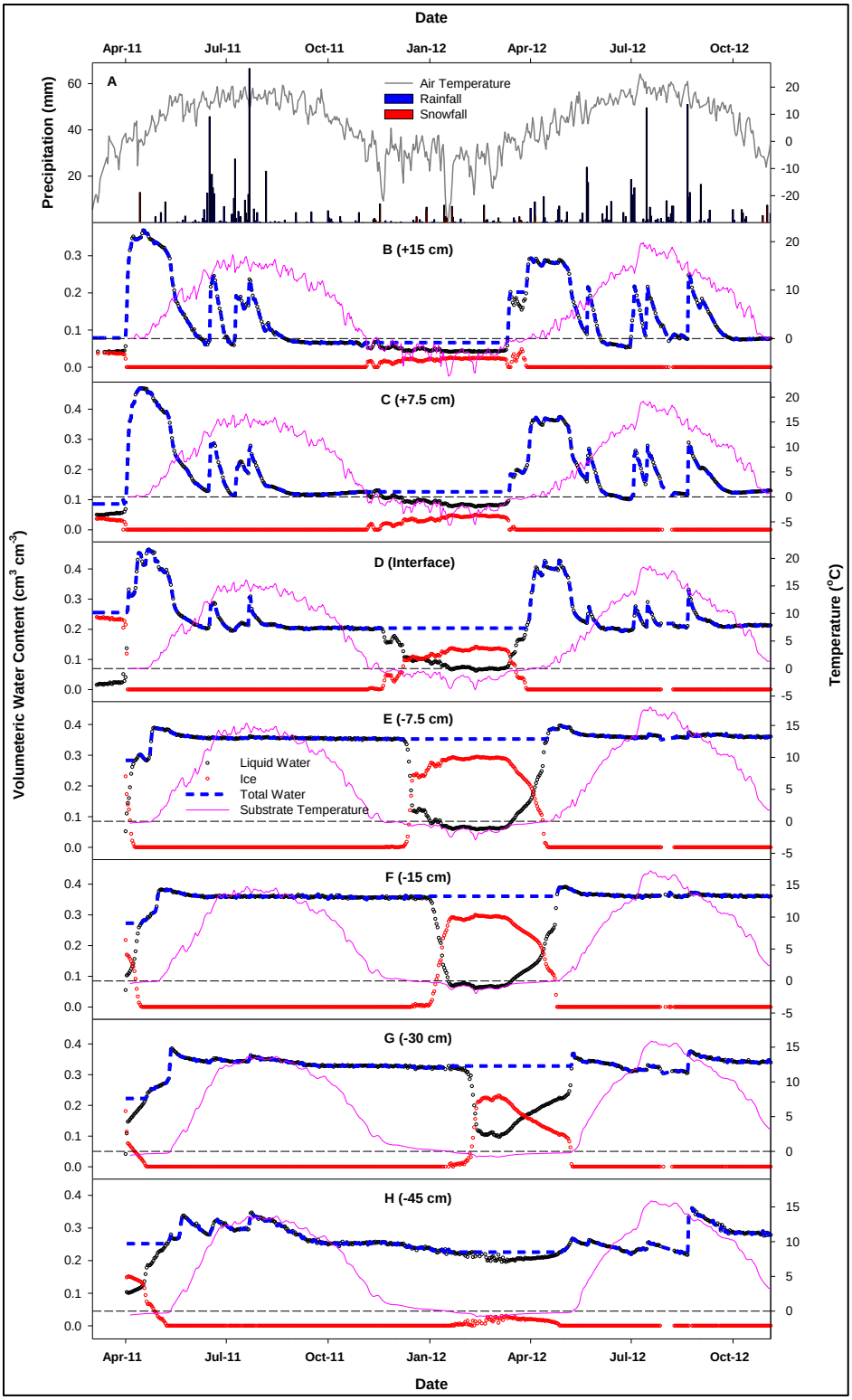


Figure 2.10: Time series of daily mean air temperature and precipitation (A), and liquid water, ice, total water content (liquid water + ice) and daily mean substrate temperature (B – H) of each depth below ground surface for the 30 cm treatment plot during March 2011 to November 2012. Black dashed line indicates 0 $^{o}$C reference.

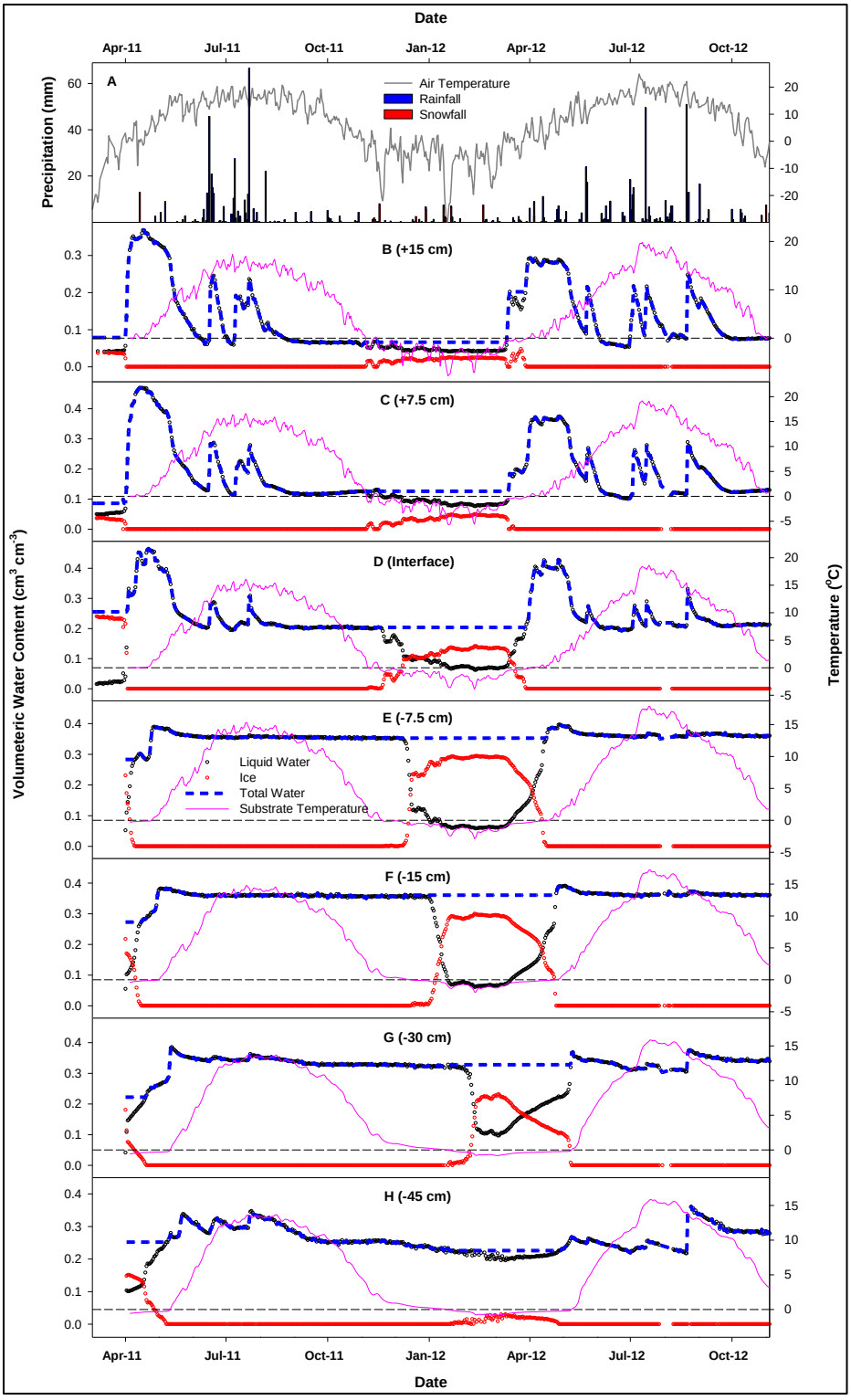


Figure 2.11: Time series of daily mean air temperature and precipitation (A), and liquid water, ice, total water content (liquid water + ice) and daily mean substrate temperature (B – H) of each depth below ground surface for the 46 cm treatment plot during March 2011 to November 2012. Black dashed line indicates 0 $^{o}$C reference.

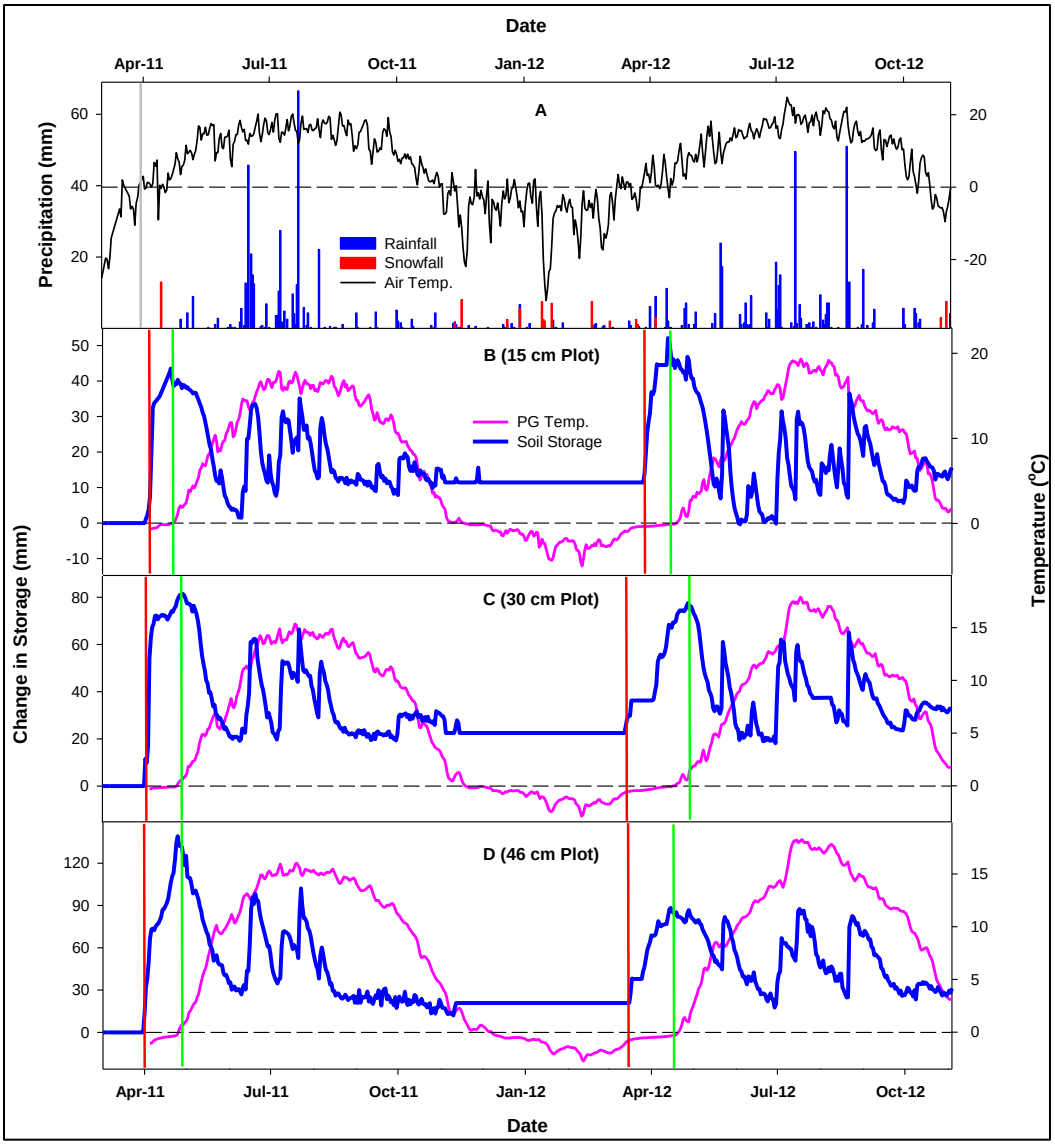


Figure 2.12: Time series of daily mean air temperature and precipitation (A), and change in storage within the topsoil cap and daily mean PG temperature directly below the soil/PG interface for each treatment plot (B-D) during March 2011 to November 2012. Grey, red and green vertical lines indicated the start of spring melt, start of infiltration and peak infiltration / start of drainage, respectively. Black dashed line indicates 0 $^{o}$C reference.

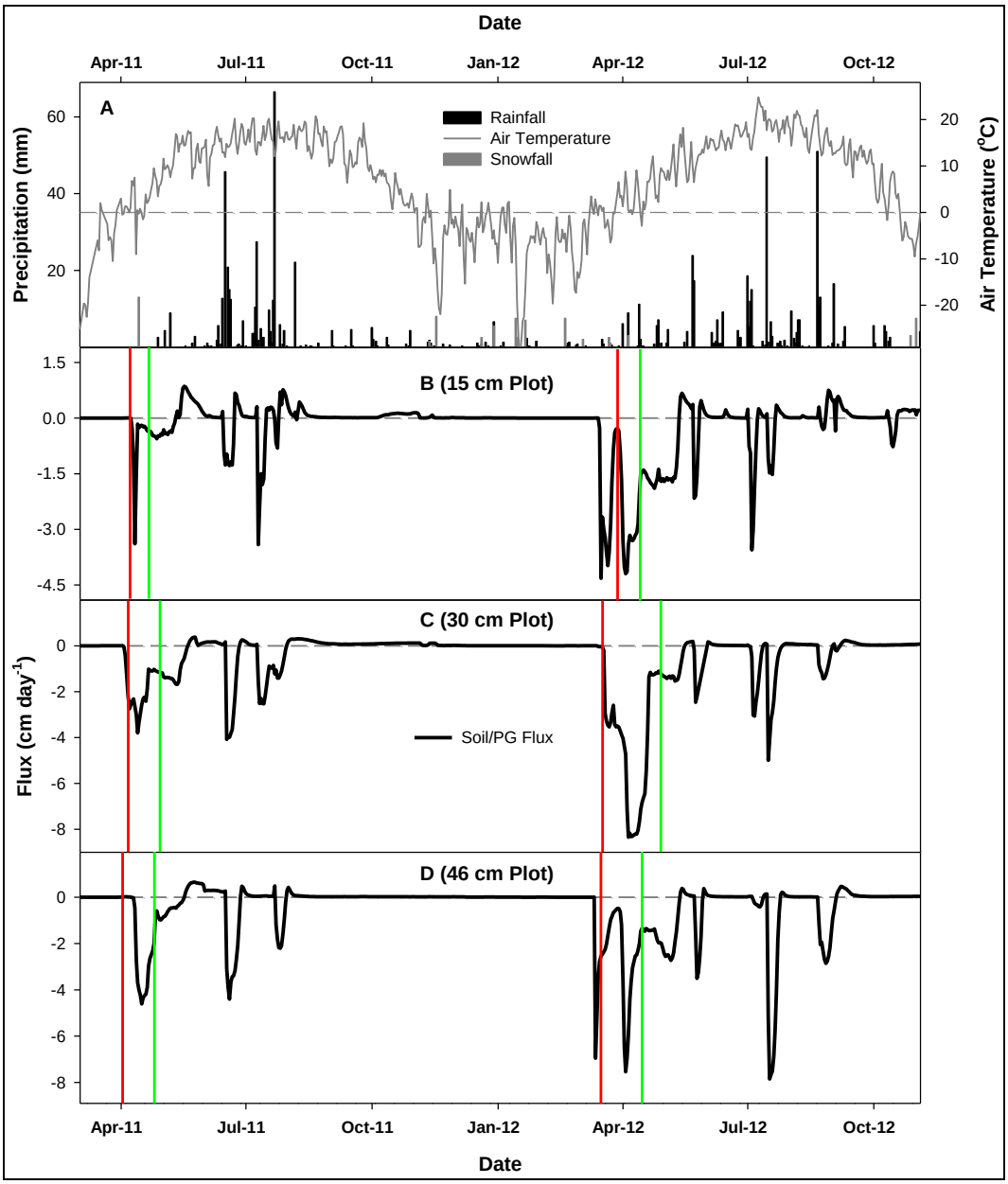


Figure 2.13: Time series of daily mean air temperature and precipitation (A), and instantaneous flux estimates (Eq. 2.8) across soil/PG interface for the various plot treatments (B-D) during March 2011 to November 2012. Red and green vertical lines indicated the start of infiltration and peak infiltration / start of drainage, respectively. Positive and negative flux indicates upward and downwards movement of water in the vertical direction.

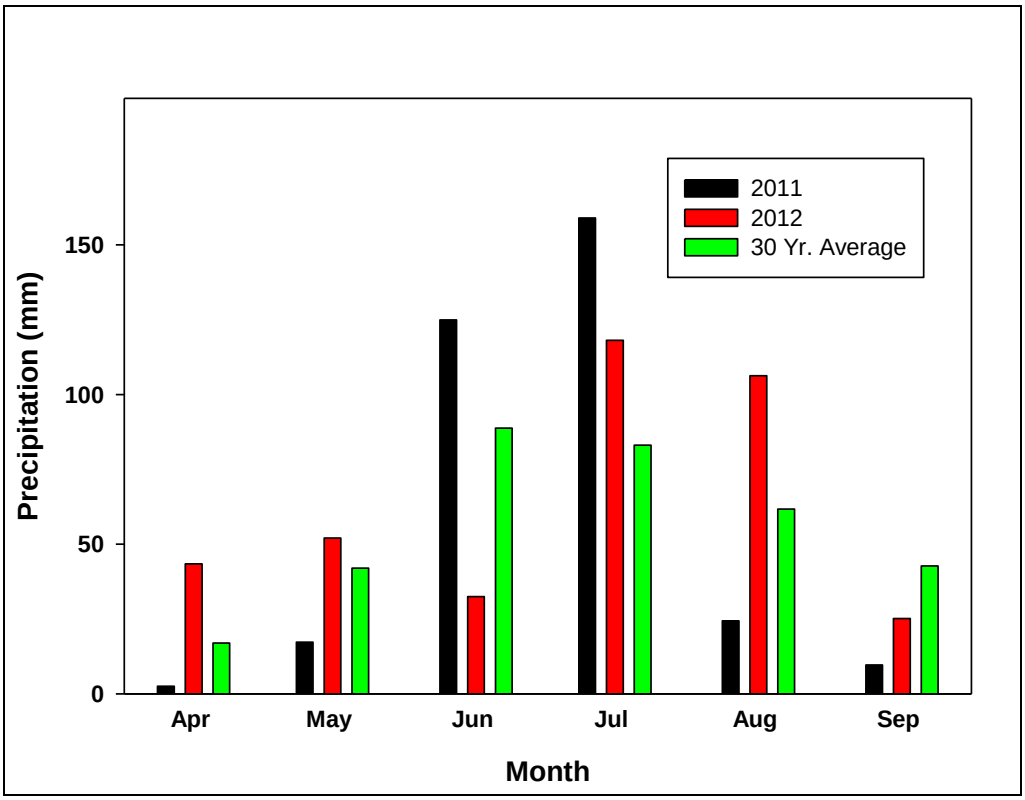

Figure 2.14: Cumulative monthly rainfall precipitation for the 2011 (Black), 2012 (Red), and the 30 year average (Green) for the Fort Saskatchewan area (Environment Canada 2013).

# 3.0 INFLUENCE OF CAPPING SOIL DEPTH ON SOLUTE TRANSPORT IN PHOSPHOGYPSUM STACK RECLAMTION

## 3.1 Deep Drainage and Solute Transport in Anthropogenic Altered Environments

Movement and translocation of aqueous solutions through the unsaturated zone is a fundamental process that can be used to help estimate deep drainage and groundwater recharge rates. Understanding the physical parameters that define deep drainage is critical for assessing the risks associated with anthropogenic activities, including applications of herbicides, fertilizers, and uncontrolled releases of industrial fluids. Deep drainage has often been discussed as a function of climatic and geomorphic variability (Gee et al. 2005; Vaccaro 1992). Regions of relatively high precipitation have been routinely assessed and methods of determining deep drainage in humid climates are well developed (Delin and Risser 2007; Gee and Hillel 1988).

Humid regions can have deep drainage rates in the order of > 100 mm $yr^{-1}$, where semi-arid regions typically have deep drainage rates of approximately < 10 mm $yr^{-1}$ (Delin and Risser 2007; Dyck 2001). Water transport in the unsaturated zone, and subsequent groundwater recharge, has often been estimated on a site-by-site basis to determine deep drainage rates or fluxes (Dyck et al. 2003; Woods et al. 2006). To quantify these fluxes, the use of environmental tracers is preferred (Allison and Forth 1982; Hayashi et al. 1998; Joshi 1997; Woods et al. 2006).

Numerous types of conservative tracers have been used in the evaluation of deep drainage such as chlorine ($^{36}Cl$), nitrogen ($^{15}N$), oxygen ($^{18}O$), tritium ($^{3}H$), carbon ($^{13}C$) and chloride ($Cl^-$) (Dyck 2001). The presence of these tracers in the vadose zone indicates vertical movement of soil water with time.

Practical applications of the theories governing deep drainage can also include waste leachate predictions and measurements from landfills, preferential flow paths in municipal solid waste facilities and mined waste rock, and landfill cover system assessment for percolation (Bendz et al. 1997; Eriksson et al. 1997; Rosqvist and Destouni 2000; Varank et al. 2011; Zhang et al. 2012). Percolation, sometimes referred to as leakage, is a topic of great importance with regards to waste cover systems effectiveness.

Investigating the amount of percolation is vital to understand the boundary conditions that will ultimately be applied to the reclaimed system. In a study by Breshears et al. (2005), the researchers investigated percolation below a 0.2 m thick evapotranspiration (ET) cover system and found that the average percolation rate was 15 mm $yr^{-1}$ or 3% of annual precipitation. In another study by Albright et al. (2004), the researchers found that percolation rates were as high as 157 mm $yr^{-1}$ or 20% of annual precipitation through a 1.8 m cover soil. In Nyhan et al. (1990), the researchers concluded that percolation rates were 35 mm $yr^{-1}$ or 6% of annual precipitation through a 0.2 m thick cover soil. It is not clear that

more or less cover soil will positively or negatively impact percolation estimates; however, it is clear that site-specific parameters and characteristics are of great importance in building our understanding of this issue.

## 3.2 Solute Transport Theory and Application

Transport of water and solute through the unsaturated zone can be separated into two individual processes. The first is movement of water and solute into and through the root zone. The water fluxes associated with inter-root zone transport are transient and include infiltration and evapotranspiration, both of which result in concentration and hydraulic gradients. The second process involves the movement of water and solute below the root zone, inevitably resulting in groundwater recharge (Dyck 2001; Gee and Hillel 1988). To investigate deep drainage rates and soil water flux the application of solute transport can be used.

Solute transport through porous media involves the application of the conservation of mass law which includes the original solute mass entering a known volume, solute mass exiting the known volume, solute mass stored in the known volume, and loss of solute mass within the known volume by chemical or biological means. In mathematical terms (Jury et al. 1991):

$$\frac{\partial J_s[x,y,z,t]}{\partial z} = \frac{\partial C_T[x,y,z,t]}{\partial t} - r_s(z,t) \qquad [3.1]$$

where, $J_S$ (kg $m^{-2}$ $s^{-1}$) is the total solute flux in the z direction, $C_T$ (kg $m^{-3}$) is the total solute concentration, z, y and x (m) are spatial coordinates, t (s) is time and $r_S$ (kg $m^{-3}$ $s^{-1}$) is the reaction rate per volume, or more commonly referred to as the source/sink term.

Conventionally, solute flux is the sum of a number of transport processes including convection, diffusion, and/or hydrodynamic dispersion (Jury et al. 1991). The convective solute flux ($J_C$ (g $cm^{-2}$ $s^{-1}$)), or the convective movement of a solute mass through a porous media, is governed by the advective movement of water flow within the system and is describes as:

$$J_c = J_w C_R \qquad [3.2]$$

where, $J_W$ is the volumetric water flux ($m^3$ $m^{-2}$ $s^{-1}$), and $C_R$ is the resident concentration of the dissolved solute (kg $m^{-3}$). The diffusion component of solute flux results from the movement of dissolved constituents along concentration gradients described as:

$$J_d = -D_S \frac{\partial C_l}{\partial z} \qquad \text{where } D_S = -\xi(\theta) D_w \qquad [3.3]$$

where, $J_d$ is the liquid diffusion flux (kg $m^{-2}$ $s^{-1}$), $D_S$ is the soil liquid diffusion coefficient ($m^2$ $s^{-1}$), $\xi(\theta)$ is the liquid tortuosity factor, $\partial C_l/\partial z$ is the concentration gradient (kg $m^{-3}$ $m^{-1}$), and $D_W$ is the binary diffusion coefficient of the solute in water (Jury et al. 1991).

The final component of solute flux is hydrodynamic dispersion, which is caused by variation in pore water velocity resulting in erratic and tortuous movement of solute within the porous media and is described as:

$$J_h = -D_h \frac{\partial C_l}{\partial z} \qquad \text{where } D_h = \lambda V \qquad [3.4]$$

where, $J_h$ is the solute hydrodynamic dispersion flux (kg $m^{-2}$ $s^{-1}$), $\partial C_l/\partial z$ is the concentration gradient (kg $m^{-3}$ $m^{-1}$), $D_h$ is the hydrodynamic dispersion coefficient ($m^2$ $s^{-1}$) which can be computed from the dispersivity ($\lambda$ (m)) and the pore water velocity (V(m $s^{-1}$)) (Jury et al. 1991).

The total solute flux therefore, is the summation of solute flux, diffusive flux, and hydrodynamic dispersive flux and is commonly written as:

$$J_s = -D_e \frac{\partial C_l}{\partial z} + J_w C_l \qquad [3.5]$$

where, $D_e$ is the effective diffusion-dispersion coefficient ($m^2$ $s^{-1}$).

### 3.2.1 Convective Dispersive Transport Model

The general use of tracer application to estimate deep drainage can be achieved by measuring the distribution of the applied solute within the soil profile. The transport of said solute is governed by convection and hydrodynamic dispersion which effectively mixes the solute as it is transported through the porous media, resulting in a unique solute profile distribution. Substitution of Eq. 3.5 into Eq. 3.1 and subsequent division by volumetric water content and setting $r_s(z,t)$ to zero (which is legitimate for a conservative solute) results in the convective dispersive equation (Jury et al. 1991):

$$\frac{\partial C_l}{\partial t} = D \frac{\partial^2 C_l}{\partial z^2} - V \frac{\partial C_l}{\partial z} \qquad [3.6]$$

where, $D\ \frac{\partial^2 C_l}{\partial z^2}$ describes the diffusive/dispersive solute transport and $V\frac{\partial C_l}{\partial z}$ describes the advective solute transport.

When the convective dispersive equation is applied to an experimental circumstance whereby a single pulse of solute is administered to the soil surface the solution to Eq. 3.6 is (Kreft and Zuber 1978):

$$C_{IFR}(x,t) = \frac{A}{nS}\left\{\frac{2}{\sqrt{4\pi Dt}}exp\left[-\frac{(x-Vt)^2}{4Dt}\right] - \frac{V}{2D}\ \exp\left(\frac{Vx}{D}\right)erfc\left(\frac{x+Vt}{\sqrt{4Dt}}\right)\right\} \quad [3.7]$$

where, $C_{IFR(x,t)}$ is the predicted concentration at a static distance *(x (*m*))* away from source at an instantaneous time *(t (*s*)),* given the tracer was injected in flux stream and detected within the resident fluid*. A (k*g/m$^3$*)* is the amount of tracer injected, S (m$^2$) is the cross sectional area of flow, n (m$^3$ m$^{-3}$) is the effective porosity, *D* (m$^2$ s$^{-1}$) is the dispersion coefficient, and *V (*m/s*)* is the average pore water velocity, which can be calculated from the water flux and volumetric water content (Kreft and Zuber 1978).

Eq. 3.7 can be used to describe solute distribution in the soil profile to define the mean travel depth and variability of the solute distribution. In this context the mean travel depth of a conservative tracer is analogous with the advective water flow within the system since the solute does not react or adsorb to the soil surface, thus giving the observer insight into the average water movement within the soil system. The limitation however of this deterministic theory is that it is mechanistic in nature and is often limited by boundary conditions and parameters pertaining to the soil system which need to be defined (Hillel 1998). Furthermore, the nature of

the transport model defines the system as steady state; however, under real world conditions the soil system is more appropriately defined as transient.

### 3.2.2 Convective Stochastic Transport Model

The alternative to the deterministic approach to solute transport modeling can be found through the use of the transfer function model (TFM) as described by Jury (1982). The rationale governing this method is based on an observational continuum whereby the transport of solute within the soil is reflective of the probability distribution function (PDF) of the solute travel times and not the parameters that define the system itself. In this regard the transfer function is free of assumptions pertaining to the mechanisms governing solute transport (Hillel 1998).

According to the TFM, the movement of a solute within an unsaturated soil system is ultimately governed by the travel-time PDF, $f_L(t)$, such that the solute entering the system at time zero and Z=0, will reach Z=L within the time interval $t$, to $t + dt$ (Jury and Sposito 1985). The average field scale solute flux concentration at Z=L, after $t + dt$, is described as (Jury 1982):

$$C(L,t) = \int_0^\infty C_{IN}(t - t')f_L(t')dt' \qquad [3.8]$$

Assuming under steady state flow conditions that convective solute transport dominates in the vertical direction over lateral solute mixing, the

travel time PDF, $f_z(t)$, at depth $Z$ can be referenced to that of the observed depth $L$ as described by (Jury 1982):

$$f_z(t) = \frac{L}{Z} f_L(t\frac{L}{Z}) \quad [3.9]$$

Using a two-parameter lognormal function, which shape reflects field average solute concentration data, to describe $f_L$ and $f_Z$ yields (Jury et al. 1982):

$$f_L(t) = \frac{1}{t\sigma\sqrt{2\pi}} \exp\left(\frac{-(ln(t)-\mu)^2}{2\sigma^2}\right) \quad [3.10]$$

where, $\mu$ and $\sigma$ are parameters that define the shape of the PDF, respectively. Based on these statistical parameters mean travel time, variance and dispersivity can be computed. Eq. 3.10 is suitable for experiments where solution concentrations at a fixed depth are monitored with time (i.e., breakthrough curves).

In the field, a common practice is to take soil core to measure concentration as a function of depth at one point in time (i.e., concentration profile). Therefore, we can define a travel depth PDF as:

$$f_t(z) = \frac{1}{z\sigma\sqrt{2\pi}} \exp\left(\frac{-(ln(z)-\mu)^2}{2\sigma^2}\right) \quad [3.11]$$

where, $\mu$ and $\sigma$ are parameters that define the shape of the PDF and are used to compute the median travel depth ($Med_t(z)$), the mean travel depth ($E_t(z)$), variance ($Var_t(z)$) and dispersivity ($Disp_t(z)$) as described as (Jury and Sposito 1985):

$$Med_t[z] = Z \; when \int_0^Z f_t(z) \cdot dz = 0.5 \quad [3.12]$$

$$E_t(z) = \int_0^z f_t(z) \cdot z \cdot dz \quad [3.13]$$

$$Var_t(z) = \int_0^z f_t(z) \cdot (z - E_t(z))^2 \cdot dz \quad [3.14]$$

$$Disp_t(z) = \frac{Var_t(z)}{E_t(z)^2} \quad [3.15]$$

## 3.3 Research Objectives

The overall objective of this research is to contribute to a reclamation plan for PG stack closure by identify the optimal amount of topsoil needed to provide the necessary requirement for plant establishment and growth, while minimizing the potential translocation and percolation of water into and through the PG material. Specific objectives include:

- Characterization of seasonal redistribution of applied conservative tracer within the ET cover system.
- Quantify the rate of water movement in soil and its relationship to capping soil thickness.
- Evaluation of deep drainage estimates within reclaimed systems.

## 3.4 Materials and Methods

### 3.4.1 Site Description, Experimental Design and Measurements

The experimental site description and methods have been previously described in Section 2.3 of the previous chapter. Briefly, however, the research site is located atop a decommissioned PG stack located at the Agrium Nitrogen Operations Facility, near Fort Saskatchewan, Alberta, Canada. The climate in the region is defined as semi-arid to humid, with 459.5 mm of annual precipitation (Environment

Canada 2012). Soils of the area are dominated by Orthic Black Chernozems of the Mundare series with a minor component (20%) falling within the Eluviated Eutric Brunisol of the Primula series (Agriculture and Rural Development 2011).

Eighteen (50 m x 10 m) plots were constructed atop the decommissioned PG stack in a complete randomized design during the fall of 2006 (Jackson 2009). The plots were arranged into three replicates each containing six topsoil capping depth treatments including 8, 15, 30, 46, and 91 cm, as well as a 0 cm control (Figure 3.3). Each topsoil depth treatment was further subdivided into 5 subplots (10 m x 10 m) that contained five different plant species treatments including *Agropyron trachycaulum* (Link) Malte ex H.F. Lewis (slender wheatgrass), *Agrostis stolonifera* L. (redtop), *Deschampsia caespitosa* (L.) P. Beauv. (tufted hairgrass), *Festuca ovina* L. (sheep fescue) and a mixture of 54% redtop, 2% slender wheatgrass, 28% tufted hairgrass, 8% sheep fescue and 8% Alsike clover (Jackson 2009).

Meteorological parameters that were measured on site include precipitation, solar radiation, wind speed and direction, air temperature and relative humidity. Snowfall data was collected from the Fort Saskatchewan meteorological station, located 1.79 km south of the field site (Environment Canada 2012). A snow survey was also conducted on 26 February, 2011 which was used to compute snow water equivalent (SWE).

### 3.4.2 Conservative Tracer Selection and Application

The use of conservative tracers in soil-water investigations has been used in a variety of applications including agricultural and industrial chemical release risk assessment (Böhlke 2002; Hamilton et al. 2007), deep drainage and groundwater recharge investigations (Hayashi et al. 1998; Joshi 1997; Murphy et al. 1996) and waste water irrigation systems (Gainer 2012). In arid and semi-arid regions, the rates associated with deep drainage are small and difficult to assess using conventional methods (Dyck et al. 2003). Water and solute flux below the root zone in arid and semi-arid environments are typically in the order of < 10 mm $yr^{-1}$ (Gee et al. 1994; Keller et al. 1988).

To quantify these small fluxes, the employment of environmental tracers is preferred (Allison and Forth 1982; Hayashi et al. 1998; Joshi 1997; Woods et al. 2006). Numerous types of conservative tracers have been used in the evaluation of deep drainage such as $^{36}Cl$, $^{15}N$, $^{18}O$, $^{3}H$, $^{13}C$ and $Cl^-$ (Dyck 2001). $^{3}H$ and $^{36}Cl$, for example, are distinct environmental tracers that were deposited on the land surface during the above ground nuclear tests of the 1950s and 1960s (Tyler and Walker 1994). The presence of these tracers in the vadose zone indicates vertical movement of soil water with time.

Bromide ($Br^-$) is another conservative tracer that has been used to investigate soil-water dynamics (Frey et al. 2012; Segal et al. 2009). The application of any given dissolved tracer is subject to the investigation to

determine whether or not the cation component will have an impact on the environment. Calcium bromide ($CaBr_2$) was selected as the salt tracer for two main reasons. Firstly, calcium was present already in the soil environment in the form of calcium sulfate ($CaSO_4$) and therefore would not have much impact in greater quantities. Secondly, bromide is a conservative tracer that was not present in the soil environment before application, therefore resulting in a zero background concentration. The use of other tracers such as potassium chloride (KCl) or calcium chloride ($CaCl_2$) were not considered because of the pre-established presence of chloride within the soil environment (Table 3.1) (Jackson 2009).

The *Agropyron trachycaulum* subplots were selected for the conservative tracer experimentation to establish a controlled plant community that would be representative of the final reclamation goals as suggested by previous research (Hallin 2009; Jackson 2009). Within the *Agropyron trachycaulum* subplots a 2 m by 3 m area was established as the location for the conservative tracer application. The calcium bromide salt was dissolved in tap water (Table 3.1) to give a final application concentration of 6.25 g $L^{-1}$. The application area was divided into 3 - 1 m by 2 m sections where 4 L of 6.25 g $L^{-1}$ $CaBr_2$ solution was administered. The total amount of solution applied to each 6 $m^2$ area was 12 L or approximately 75 g of $CaBr_2$ to give a $Br^-$ application rate of 10 g $m^{-2}$. The $Br^-$ application was administered on 6 January, 2011.

### 3.4.3 Soil Sampling and Bromide Extraction

On 7 October, 2011, 274 days after tracer application, 18 undisturbed cores, one from each *Agropyron trachycaulum* subplot, were gathered within the 2 m by 3 m application area using a 7730 DT Geoprobe® (Geoprobe 2013). The duration of tracer migration (i.e. 274 days) encompassed both the spring snowmelt and the entire active growing season for 2011. Each soil core was sampled to a depth of 1 m using a 4.2 cm (1-5/8") inside diameter Giddings® soil sampling core to minimize compaction (Giddings Machine Company Inc. 2013). Each core was subsequently section into 5 cm increments, as delineated from the topsoil/PG interface, and immediately placed in polyethylene sampling bags. Each sample was weighed and dried to obtain field water content measurements. Samples were dried at 55$^{o}$C for 48 hours to minimize molecular water loss from within the crystalline structure of the PG material (Averitt and Gliksman 1990; Strydom and Potgieter 1999). After dry weights were recorded, samples were ground and sieved through a 2 mm mesh and stored in a cool dark location until further analysis.

$Br^-$ concentrations were measured using Ion Chromatography method. To obtain the necessary extraction, 15 g of substrate material was mixed with 30 ml of distilled water and shaken for 30 minutes. Upon completion the samples were centrifuged at 8000 rpm for 15 minutes to facilitate the sedimentation of the substrate material. The remaining fluid was syphoned off and filtered through a 0.45 μm membrane. The filtered

extractions were analyzed with a Dionex Ion Chromatograph and responses were compared to known calibration standards to determine sample concentrations (Tabatabai and Frankenberger 1996).

### 3.4.4 Mean Travel Depth, Median Travel Depth, Variance, Dispersivity, Soil Water Velocity and Residence Time

Median travel depth, mean travel depth, dispersivty and variance estimates were computed using the method of moments as outlined in Butters and Jury (1989), Jury and Sposito (1985), and Jury et al. (1991). These parameters were calculated for all replicates of all treatments except for replicate 1 of the 0 cm treatment, replicate 1 of 8 cm treatment, replicate 2 of the 15 cm treatment and replicate 2 of the 91 cm treatment.

The analytical results from these replicates of the 8, 15 and 91 cm treatments yielded no detectable amount of $Br^-$ and therefore were not included in the results. Replicate 1 of the 0 cm treatment had a highly skewed concentration profile which resulted in unrealistic estimates of mean travel depth, variance, and dispersivity. Only the median travel depth was calculated for replicate 1 of the 0 cm treatment. The $Br^-$ concentration profiles were used to fit a lognormal PDF according to Jury and Sposito (1985):

$$C(t,z) = \frac{Mo}{z\sigma\sqrt{2\pi}} \exp\left(\frac{-(ln(z)-\mu)^2}{2\sigma^2}\right) \qquad [3.16]$$

where, *C(t,z)* is the predicted $Br^-$ concentration at depth *z*(m) , *Mo* is the mass recovery (g $m^{-2}$), and finally $\mu$ and $\sigma$ are parameters that define the

shape of the PDF, respectively. Substitution of Eq. 3.16 into Eqs. 3.12, 3.13, 3.14 and 3.15 results in expressions which describe the median travel depth ($Med_t(z)$ the mean travel depth *($E_t(z)$)*, the variance *($Var_t(z)$)* as well as the dispersivity *($Disp_t(z)$)* of the DBTC's (Jury et al. 1991):

$$Med_t(z) = exp(\mu) \quad [3.17]$$

$$E_t(z) = exp\left(\mu + \frac{\sigma}{2}\right) \quad [3.18]$$

$$Var_t(z) = exp(2\mu + \sigma) \cdot [exp(\sigma) - 1] \quad [3.19]$$

$$Disp_t(z) = exp(\sigma) - 1 \quad [3.20]$$

Soil water velocity for the various capping soil treatment were calculated using the following equation:

$$V = \frac{\Delta E_t(z)}{\Delta t} \quad [3.21]$$

Where *t* is the time (yr) to which the tracer had traveled and $E_t(z)$ is the mean travel depth (cm). The travel time to 100 cm was computed using the soil water velocity whereby the distance was divided by the observed tracer velocity. The 100 cm distance was selected as a benchmark representative distance to which it can be confidently assumed that all water movement past that point will be in the negative direction based on the fact minimal root material had been observable past the topsoil/PG interface within capping treatments 0, 8, 15, 30 and 46 cm, and no root accumulation was observed at or near the topsoil/PG interface of the 91 cm treatment (Turner 2013).

## 3.5 Results and Discussion

### 3.5.1 Mean Travel Depth of Bromide Tracer

Spatial distributions in $Br^-$ concentration profiles are presented in Figure 3.5. The average $Med_t(z)$ and $E_t(z)$ for each capping soil treatment are summarized in Table 3.2. The concentration profiles show detectable $Br^-$ in the first two depths for treatments with capping thicknesses greater than 8 cm. This shallow $Br^-$ is likely a result of plant uptake and re-deposition from dead leaves as was confirmed with tissue samples of plant material collected near the application areas (Turner 2013). The general trend suggests that an increase in capping soil thickness results in deeper penetration of the conservative tracer with respect to the soil surface (Figure 3.6 and 3.7) just as there was greater spring infiltration associated with deeper soil caps (see Section 2).

The $E_t(z)$ up to this point has been reference with respect to the soil surface; however, to better understand the movement of water in relation to the PG material it might be more effective to describe the $E_t(z)$ as a function of the topsoil/PG interface, which will be referred to as $E_t(z)$' here after. Figures 3.6 and 3.7 illustrate the relationship between both the $E_t(z)$ / $Med_t(z)$ and capping soil treatment and $E_t(z)$' and capping soil treatment, respectively. Nonlinear regression was used to describe the relationship between $E_t(z)$ and capping soil treatment. The relationship follows an exponential rise to an asymptote function where the $E_t(z)$ and $Med_t(z)$ do

not appear to change significantly at capping soil depths > 15 cm (Figure 3.6). This result would suggest that an increase in capping soil depth > 15 cm does not significantly impact vertical water movement over the course of a single growing season; however, with reference to the topsoil/PG interface ($E_t(z)$') it was shown to be not significantly different for capping soil treatment 0 to 46 cm (Figure 3.7).

The relationship between the $E_t(z)$' and capping soil treatment follows a non-linear trajectory whereby an increase in capping soil depth was positively correlated with an increase in the observed location of the $Br^-$ tracer in the positive vertical direction from the topsoil/PG interface (Figure 3.7). Furthermore, the 0, 8, 15 and 30 cm treatments all showed net water movement into the PG material and only the 46 and 91 cm treatment showed an absence of water movement into the PG material; however, given the number of observation the 46 cm treatment was not shown to have a significant difference in $E_t(z)$' with respect to the 0, 8, 15 and 30 cm treatments (Figure 3.7).

### 3.5.2 Dispersivity and Variance Estimates

$Br^-$ variance and dispersivity estimates are presented in Table 3.3 and Figure 3.8. The variance which applies to the $Br^-$ solute transport was shown to decrease with increasing capping soil depth according to an exponential function. The results, suggest that the greater the distance traveled in the vertical direction, the spread or variance of the

concentration profiles decreased. This observation is contradictory to convective dispersive and convective stochastic solute transport theories for homogeneous soils. Convective dispersive transport theory predicts a linear increase in variance with increased travel depth (i.e., constant dispersivity) and convective stochastic theory predicts that variance increases quadratically with increasing travel depth (i.e., linear increase in dispersivity as a function of depth; Dullien 1979; Hillel 1998; Jury et al. 1991).

Like the variance estimates, the dispersivity estimates are inversely exponentially related to the capping soil depth. The dispersivity and variance decrease with increasing capping soil depth because the influence of the PG material becomes less dominant as more loamy sand topsoil is added. The tortuous nature of material is the dominant factor in defining the dispersivity and permeability of the soil (Bear 1972; Childs and Collis-George 1950; Costa 2006; Dullien 1979; Perfect et al. 2002; Saar and Manga 1999). In this regard the specific pore geometry of the PG material is extremely irregular in comparison to the capping soil (Figure 3.9). According to the Kozeny-Carmen equation, the permeability (k) of soil is inversely related to the specific surface area (a) that is exposed to the fluid (Dullien 1979; Hillel 1998):

$$k = \frac{f^3}{ca^2(1-f)^2} \qquad [3.22]$$

where, *f* is the porosity and *c* is a particle-shape factor. The increased surface area of the PG material results in greater turbulence with respect

to water flow within the porous media and therefore greater tortuosity and dispersion. Furthermore, the greater proportion of finer pores within the PG material (see moisture retention curves in Section 2, Fig. 2.7) results in greater tortuosity and dispersion within the system.

### 3.5.3 Snowpack SWE and Snowmelt Infiltration

The comparison of SWE with respect to $E_t(z)$ was not found to correlate significantly across all treatment plots (Figure 3.10). The likely reason for this lack of correlation is because it is spring infiltration that would result in greater transport of the applied solute and not the amount of water available to the system during infiltration. In the Section 2, it was shown that not all of water in the snowpack infiltrated into the topsoil caps and the amount of water that did infiltrate was a function of the capping depth. More water was observed to infiltrate during spring snowmelt in deeper topsoil caps. Therefore, the increasing mean travel depth with increasing capping depths is consistent with observations of soil water dynamics presented in Section 2.

Because of equipment constraints, TDR-based estimates of spring infiltration could not be derived for all replicates of all treatments. The estimates of spring infiltration in Section 2 are only for 1 replicate of the 15, 30 and 46 cm treatments. Despite the limited data, the spring infiltration for the 0, 8 and 91 cm capping depth treatments can be extrapolated from the 15, 30 and 46 cm estimates. Figure 3.11 shows a

highly significant relationship between capping depth and spring infiltration estimates from Section 2. This relationship was used to extrapolate additional spring infiltration amounts in the 0, 8 and 91 cm capping treatments which were then compared to the average mean travel depths calculated from the concentration profiles (Fig. 3.5 and Table 3.2); the results of this comparison are shown in Fig. 3.12. Like the $E_t(z)$ versus capping treatment depth, the $E_t(z)$ versus estimated and extrapolated spring infiltration is a nonlinear, exponential rise to a maximum. The predicted spring infiltration for the 91 cm cap was constrained to 177mm, 100% of the water that was available during spring infiltration in 2011, because the relationship in Fig. 3.11 predicts an unrealistically high infiltration rate. This suggests that the observed relationship between $E_t(z)$ measured after one year of transport and capping depth treatment is likely dominated by the influence of capping depth on spring infiltration.

### 3.5.4 Soil Water Velocity and Travel Time to 100 cm Depth

Soil water velocity and travel times to 100 cm are presented in Table 3.4 and Figure 3.13. The lowest average soil water velocity was observed in the 8 cm treatment (14.8 cm $yr^{-1}$), whereas the highest average soil water velocity was observed in the 91 cm treatment (69.8 cm $yr^{-1}$) (Table 3.3). Soil water velocity was exponentially related to the capping soil depth; however, the velocity did not significantly change at capping soil depths > 15 cm (Figure 3.13). Conceptually this would

suggest that an increase in capping soil depth results in an increase in the average velocity. Like the mean travel depth, the observed velocities are a function of the influence of the topsoil cap thickness on spring infiltration, growing season water dynamics and the increased intrinsic permeability of the topsoil material coupled with the decreased intrinsic permeability of the PG material. For example, when the capping soil is limited (< 15 cm), the amount was spring infiltration is limited, and the overall intrinsic permeability of the topsoil-PG system is dominated by the material with the least permeability (i.e. the PG material); however, when the capping soil is not limited (> 15 cm) the overall intrinsic permeability is governed by the topsoil material. In this regard the average solute velocity (i.e., water velocity) at which the water is able to travel is directly related to the amount of water entering the soil system at the soil surface and the intrinsic permeability of the overall porous material, which is ultimately controlled by the pore geometry (Childs and Collis-George 1950; Millington and Quirk 1959).

The expected travel time to 100 cm was computed by using the average pore water velocity. Like the mean travel depth, these travel times for the various capping soil treatments were non-linearly correlated with capping depth (Figure 3.13). The predicted residence times for the 0 and 8 cm capping soil treatments are 4.9 and 8.9 years, respectively. The predicted residence times for the 15, 30, 46 and 91 cm capping soil treatments ranged from 2.1 to 1.4 years and were found to be not

significantly different from one another. This trend is a direct result of the average velocity which is dictated by the influence of the varying capping depth treatments. For example, the 0 and 8 cm treatments are strongly influenced by the presence of the PG layer and reduced spring infiltration and therefore have slower average pore water velocities, which would result in longer residence times. Conversely, capping depth treatments that exceed 15 cm are more strongly influenced by the highly permeable loamy sand topsoil and greater amounts of spring infiltration and therefore have faster velocities and shorter residence times.

These results, however, are misleading because they do not take into account the instantaneous increases in velocity that are associated with snowmelt infiltration. In this regard the movement of water within the system is not equally spread throughout the growing season, but rather focused on periods when the amount of water that was available to the system exceeded the evapotranspiration demands of the plant community. Furthermore, these results suggest that the velocities remain constant during the times predicted; however, as the water is transported through the topsoil cap into the PG material the velocities will most likely diminishes in much the same way long-term deep drainage rates do in the natural environment.

For example, in a study by Dyck (2001), the researcher observed that the mean travel depth a conservative tracer was 0.62, 0.72, 0.79, 1.34, 1.79, 1.68 m for 1, 2, 3, 4, 28 and 34 years after initial application.

The results indicated that the movement of the solute, while rapid during initial infiltration events, became retarded over time due soil water extraction by plant roots. Thus the initially high velocities following solute application decrease while the solute moves through the root zone and eventually reach the velocity dictated by the average annual deep drainage flux.

## 3.6 Conclusions

Water movement within the ET cover system during the active growing season was evaluated using the distribution of a conservative tracer 274 days after a single pulse application. The results were consistent with the water dynamics presented Section 2: increased capping soil depth is associated with an increase in the mean travel depth of the bromide tracer. Significant amounts of bromide were observed in the underlying PG material of the 0, 8, 15 and 30 cm treatment plots, but the net vertical movement of the bromide quantified by *Et(z)* was much greater in the 46 and 91 cm treatment plots.

The relationship between observed and predicted spring infiltration as a function of capping depth and average mean travel depth suggests that the solute transport is dominated by the influence of the capping depth on spring infiltration as described in Section 2. Soil water velocity was found to exponentially increase with increasing capping soil depth due to the greater influence of the highly permeable loamy sand topsoil

material. Residence times were non-linearly correlated with capping soil depth, whereby an increase in capping depth resulted in a decrease in the predicted travel time to 100 cm. Because of the greater soil water fluxes across the topsoil/PG interface observed under the thicker topsoil caps in Section 2, it is expected that in the long term, the bromide flux across and below the topsoil/PG interface under the thicker topsoil caps (30, 46, 91 cm) will exceed the 0, 8 and 15 cm topsoil caps.

## 3.7 References


Agriculture and Rural Development. 2011. Alberta soil information viewer. [Online] Available: http://www4.agric.gov.ab.ca/agrasidviewer/ [2011 Sept. 13].

Albright, W.H., C.H., Benson, and G.W. Gee. 2004. Field water balance of landfill covers. Journal of Environmental Quality 33:2317-2332.

Allison, G.B., and J.R. Forth. 1982. Estimation of historical groundwater recharge rate. Australian Journal of Soil Research. 20:255-259.

Averitt, D.W. and J.E. Gliksman. 1990. Free water in phosphsphogypsum. Fertilizer Research 24:57-62.

Bear, J. 1972. Dynamics of fluids in porous media. Elsevier, New York. 764 pp.

Bendz, D., V.P. Singh and M. Åkesson. 1997. Accumulation of water and generation of leachate in a young landfill. Journal of Hydrology 203:1-10.

Böhlke, J.-K. 2002. Groundwater recharge and agricultural contamination. Hydrogeology Journal 10:153-179.

Breshears, D.D., J.W. Nyhan, and D.W. Davenport. 2005. Ecohydrology monitoring and excavation of semiarid landfill covers a decade after installation. Vadose Zone Journal 4:798-810.

Butters, G.L., W.A. Jury, and F.F. Ernst. 1989. Field scale transport of bromide in an unsaturated soil: 1. Experimental methodology and results. Water Resources Research 25(7):1575-1581.

Butters, G.L. and W.A. Jury. 1989. Field scale transport of bromide in an unsaturated soil: 2. Dispersion modeling. Water Resources Research 25(7):1583-1589.

Childs, E.C. and N. Collis-George. 1950. The permeability of porous materials. Proceedings of the Royal Society A: Mathematical, Physical and Engineering Sciences 201(1066):392-405.

Costa, A. 2006. Permeability-porosity relationship: A reexamination of the Kozeny-Carman equation based on a fractal pre=space geometry assumption. Geophysical Research Letters 33:1-5.

Delin, G.N., and D.W. Risser. 2007. Ground-water recharge in humid areas of the United States-A summary of ground-water resources program studies, 2003-06. USGS Fact Sheet.

Dullien, F.A.L. 1979. Porous Media: Fluid transport and pore structure. Academic Press, Inc., New York. 396 pp.

Dyck, M.F. 2001. Long-term solute transport under transient, semi-arid conditions. M.Sc. Thesis. University of Saskatchewan, Saskatoon, Canada. 200 pp.

Dyck, M.F., R.G. Kachanoski, and E. de Jong. 2003. Long-term movement of a chloride tracer under transient, semi-arid conditions. Soil Science Society of America Journal 67:471-477.

Environment Canada. 2012. National climate data and information archive. [Online] Available: http://www.climate.weatheroffice.gc.ca/advanceSearch/searchHistoricDataStations_e.html?searchType=stnName&timeframe=1&txtStationName=fort+saskatchewan&searchMethod=contains&optLimit=yearRange&StartYear=1840&EndYear=2012&Month=9&Day=21&Year=2012&selRowPerPage=25&cmdStnSubmit=Search. [2012 Mar. 20].

Eriksson, N., A. Gupta, and G. Destouni. 1997. Comparative analysis of laboratory and field tracer tests for investigating preferential flow and transport in mining waste rock. Journal of Hydrology 194:143-163.

Frey, S.K., D.L. Rudolph, and B. Conant Jr. 2012. Bromide and chloride tracer movement in macroporous tile-drained agricultural soil during an annual climatic cycle. Journal of Hydrology 460-461:77-89.

Gainer, A.E. 2012. Quantification of deep drainage flux and drainage water quality characterization below the root zone of a short rotation coppice of willow and poplar receiving municipal treated wastewater irrigation in the lower foothills natural subregion of Alberta. M.Sc. Thesis. University of Alberta, Edmonton, AB. 116 pp.

Gee, G.W., and D. Hillel. 1988. Groundwater recharge in arid regions: Review and critique of estimation methods. Journal of Hydrology 2:255-266.

Gee, G.W., J.M. Keller, and A.L. Ward. 2005. Measurement and prediction of deep drainage from bare sediments at a semiarid site. Vadose Zone Journal 4:32-40.

Geoprobe. 2013. 7730 DT Geoprobe Systems. [Online] Available: http://geoprobe.com/7822dt. [2012 Oct. 7].

Giddings Machine Company Inc. 2013. Tooling Catalog. [Online] Available: http://www.soilsample.com /catalog/tooling.pdf. [2012, Oct. 7].

Hamilton, A.J., F. Stagnitti, X. Xiong, S.L. Kreidel, K.K. Benke, and P. Maher. 2007. Wastewater irrigation: The state of play. Vadose Zone Journal 6: 823-840.

Hayashi, M., G. van der Kamp, and D.L Rudolph. 1998. Water and solute transfer between a prairie wetland and adjacent uplands: II. Chloride cycle. Journal of Hydrology 207:56-67.

Hillel, D. 1998. Water balance and energy balance in the field. Pages 589-615 *in* Environmental soil physics. Academic Press, San Diego, CA. USA.

Jackson, E. M. 2009. Assessment of soil capping for phosphogypsum stack reclamation at Fort Saskatchewan, Alberta. M.Sc. Thesis. University of Alberta, Edmonton, AB. 162 pp.

Joshi, B. 1997. Estimation of diffuse vadose zone water flux in a semi-arid region. Ph.D. Thesis. University of Saskatchewan, Saskatoon, Canada. 319 pp.

Jury, W.A. 1982. Simulation of solute transport using a transfer function model. Water Resources Research 18:363-369.

Jury, W.A., L.H. Stolzy, and P. Shouse. 1982. A field test of the transfer function model for predicting solute transport. Water Resources Research 18:369-375.

Jury, W.A., and G. Sposito. 1985. Field calibration and validation of solute transport models for the unsaturated zone. Soil Science Society of America Journal 49:1331-1341.

Jury, W.A., W.R. Gardner, and W.H. Gardner. 1991. Soil Physics, Fifth Edition. John Wiley and Sons Inc., Canada. 328 pp.

Keller, C.K., G. van der Kamp, and J.A. Cherry. 1988. Hydrologeology of two Saskatchewan tills: I. Fractures, bulk permeability, and spatial variability of downward flow. Journal of Hydrology 101:97-122.

Kreft, A. and A. Zuber. On the physical meaning of the dispersion equation and its solutions for different initial and boundary conditions. Chemical Engineering Science 33:1471-1480.

Millington, R.J. and J.P. Quirk. 1959. Permeability of porous media. Nature 183:387-388.

Murphy, E.M., T.R. Ginn, and J.L. Phillips. 1996. Geochemical estimates of paleorecharge in Pasco basin: Evaluation of the chloride mass balance technique. Water Resources Research 32:2853-2868.

Nichol, C.K. 2009. In: Jackson, E. M. 2009. Assessment of soil capping for phosphogypsum stack reclamation at Fort Saskatchewan, Alberta. M.Sc. Thesis. University of Alberta, Edmonton, AB. 162 pp.

Nyhan, J.W., T.E. Hakonson, and B.J. Drennon. 1990. A water balance study of two landfill cover designs for semiarid regions. Journal of Environmental Quality 19:281-288.

Perfect, E., M.C. Sukop, and G.R. Haszler. 2002. Prediction of dispersivity for undisturbed soil columns from water retention parameters. Soil Science Society of America Journal 66:696-701.

Rosqvist, H. and G. Destouni. 2000. Solute transport through preferential pathways in municipal solid waste. Journal of Contaminant Hydrology 46:39-60.

Saar, M.O. and M. Manga. 1999. Permeability-porosity relationship in vesicular basalts. Geophysical Research Letters 26(1):111-114.

Segal, E., P. Shouse, and S.A. Bradford. 2009. Deterministic analysis and upscaling of bromide transport in a heterogeneous vadose zone. Vadose Zone Journal 8(3):601-610.

Strydom, C.A. and J.H. Potgieter. 1999. Dehydration behavior of a natural gypsum and a phosphogypsum during milling. Thermochimica Acta 332:89-96.

Ta, W. 2007. Study of the energy abrasion rates of five soil types subject to oblique impacts. Geoderma 140:97-105.

Tabatabai, M.A. and W.T., Frankenberger. 1996. Ion Chromatography. Methods of Soil Analysis, Part 3-Chemical Methods. Ed. D.L. Sparks. American Society of Agronomy, Inc., Soil Science Society of America, Inc. Madison, Wisconsin, US.

Turner, L. 2013. Influence of soil cap depth and vegetation on reclamation of phosphogypsum stacks in Fort Saskatchewan, Alberta. M.Sc. Thesis. University of Alberta, Edmonton, AB. 172 pp.

Tyler, S.W., and G.R. Walker. 1994. Root-zone effects on tracer migration in arid zones. Soil Science Society of America Journal 58:25-31.

Vaccaro, J.J. 1992. Sensitivity of groundwater recharge estimates to climate variability and change, Columbia Plateau, Washington. Journal of Geophysical Research 97:2821-2833.

Varank, G., A. Demir, S. Top, E. Sekman, E. Akkaya, K. Yetilezsoy, and M.S. Bilgili. 2011. Migration behavior of landfill leachate contaminants through alternative composite liners. Science of the Total Environment 409:3183-3196.

Woods, S.A., R.G. Kachanoski, and M.F. Dyck. 2006. Long-term solute transport under semi-arid conditions pedon to field scale. Vadose Zone Journal 5:365-376.

Zhang, H.J., D.S. Jeng, D.A. Barry, B.R. Seymour, and L. Li. 2012. Solute transport in nearly saturated porous media under landfill clay liners: A finite deformation approach. Journal of Hydrology 479:189-199.

Table 3.1: Chemical properties for substrate material found at research plots at Agrium, Fort Saskatchewan, AB.

| | Topsoil | PG[w] | Tap water |
|---|---|---|---|
| Calcium (mg $L^{-1}$) | 3812.0 (19)[z] | N/A | Not reported |
| Chloride (mg $L^{-1}$) | N/A | 103.3 (97.7)[z] | 8[x] |
| Bromide ($\mu g\ L^{-1}$) | < 0.4[y] | <0.4[y] | 56[x] |

z Adapted from Jackson 2009.
y Sampled in August 2010.
x Epcor water quality report February 2011.
w Phosphogypsum (PG)

Table 3.2: Average (standard deviation in parenthesis) bromide mean travel depth with 2010-2011 snow survey results.

| Capping Treatment | Interface depth below topsoil surface (cm) | $Med_t(z)$, (cm below soil surface) | $E_t(z)$ (cm below soil surface) | $E_t(z)$'(interface depth – $E_t(z)$, cm below soil surface) | SWE[z] (mm) | Mass Recovery (%) |
|---|---|---|---|---|---|---|
| 0 | 0.0 (0.0) | 10.1 (3.2) | 17.4 (8.9)[x] | -17.4 (8.9)[x] | 62.5 (5.1) | 34.0 (9.6) |
| 8 | 9.5 (1.5) | 10.8 (7.33) | 11.1 (7.6)[y] | -1.6 (5.5)[y] | 81.0 (10.7) | 48.0 (10.8)[y] |
| 15 | 17.0 (1.0) | 41.7 (22.8) | 42.0 (22.4)[y] | -25.0 (21.0)[y] | 66.0 (19.6) | 81.3 (42.9)[y] |
| 30 | 29.0 (1.6) | 38.9 (7.9) | 39.1 (8.0) | -10.1 (9.1)[y] | 76.0 (7.6) | 47.4 (19.3) |
| 46 | 46.7 (2.1) | 46.5 (9.6) | 46.6 (9.6) | -3.9 (10.5)[y] | 67.5 (2.4) | 53.6 (12.7) |
| 91 | 92.5 (4.5) | 52.4 (8.4) | 52.4 (8.4)[y] | -40.1 (2.0)[y] | 61.5 (13.2) | 58.3 (20.1)[y] |

z Snow Water Equivalent

y n= 2 due to limited $Br^-$ mass recovery

x $E_t(z)$, $Var_t(z)$, $E_t(z)$' and dispersivity estimate from the first rep not included in average and standard deviation because of a highly skewed distribution

Table 3.3: Average (standard deviation in parenthesis), variance and dispersion estimates for the various capping soil treatments

| Capping Treatment | Interface Depth (cm) | Variance ($cm^2$) | Dispersivity (cm) |
|---|---|---|---|
| 0 | 0.0 (0.0) | 322.2 (390.7)[y] | 0.72 (0.49)[y] |
| 8 | -9.5 (1.5) | 9.8 (12.4)[z] | 0.050 (.025)[z] |
| 15 | -17.0 (1.0) | 21.1 (16.0)[z] | 0.025 (0.031)[z] |
| 30 | -29.0 (1.6) | 9.6 (11.5) | 0.0048 (0.0050) |
| 46 | -42.7 (2.1) | 4.9 (1.8) | 0.0022 (0.00019) |
| 91 | -92.5 (4.5) | 0.3 (0.2)[z] | 0.00012 (0.00010)[z] |

z n=2 due to limited Br- mass recovery

y $E_t(z)$, $Var_t(z)$, $E_t(z)$' and dispersivity estimate from the first rep not included in average and standard deviation because of a highly skewed distribution

Table 3.4: Average (standard deviation in parenthesis) soil water velocity and residence times for the various capping soil treatments

| Capping Treatment | Interface depth below topsoil surface (cm) | Soil Water Velocity (cm $yr^{-1}$) | Travel Time to 100 cm (Years) |
|---|---|---|---|
| 0 | 0.0 (0.0) | 23.2 (11.8)[y] | 4.9 (2.5)[y] |
| 8 | 9.5 (1.5) | 14.7 (10.2)[z] | 8.9 (6.2)[z] |
| 15 | 17.0 (1.0) | 56.0 (29.9)[z] | 2.1 (1.1)[z] |
| 30 | 29.0 (1.6) | 52.0 (10.7) | 2.0 (0.4) |
| 46 | 42.7 (2.1) | 62.0 (12.8) | 1.7 (0.4) |
| 91 | 92.5 (4.5) | 69.8 (11.2)[z] | 1.5 (0.2)[z] |

z n=2 due to limited $Br^-$ mass recovery

y $E_t(z)$, $Var_t(z)$, $E_t(z)'$ and dispersivity estimate from the first rep not included in average and standard deviation because of a highly skewed distribution

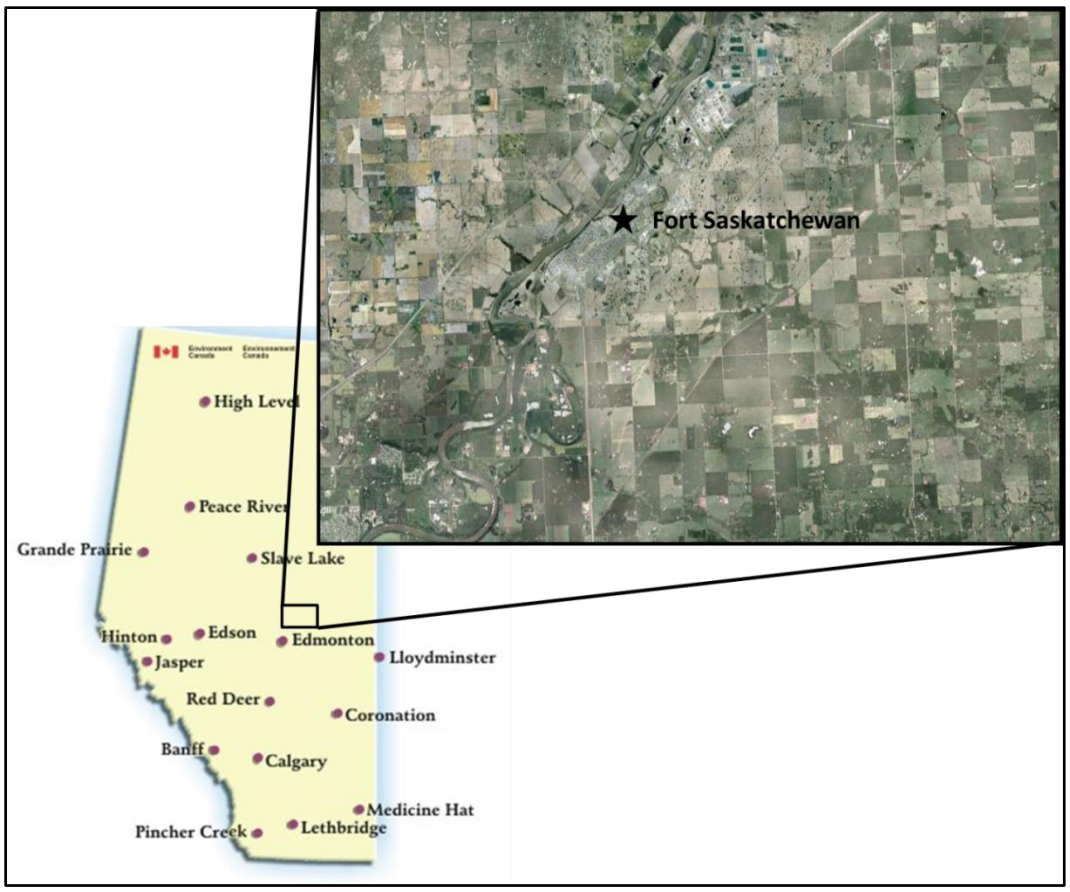

Figure 3.1: Location of Agrium Nitrogen Operations facility in Fort Saskatchewan, Alberta, Canada.

Figure 3.2: Aerial map of Agrium Nitrogen Operations facility detailing the various phosphogypsum stack locations (Blue) and the property boundaries. Areas shaded red indicate Sherrit Inc. property.

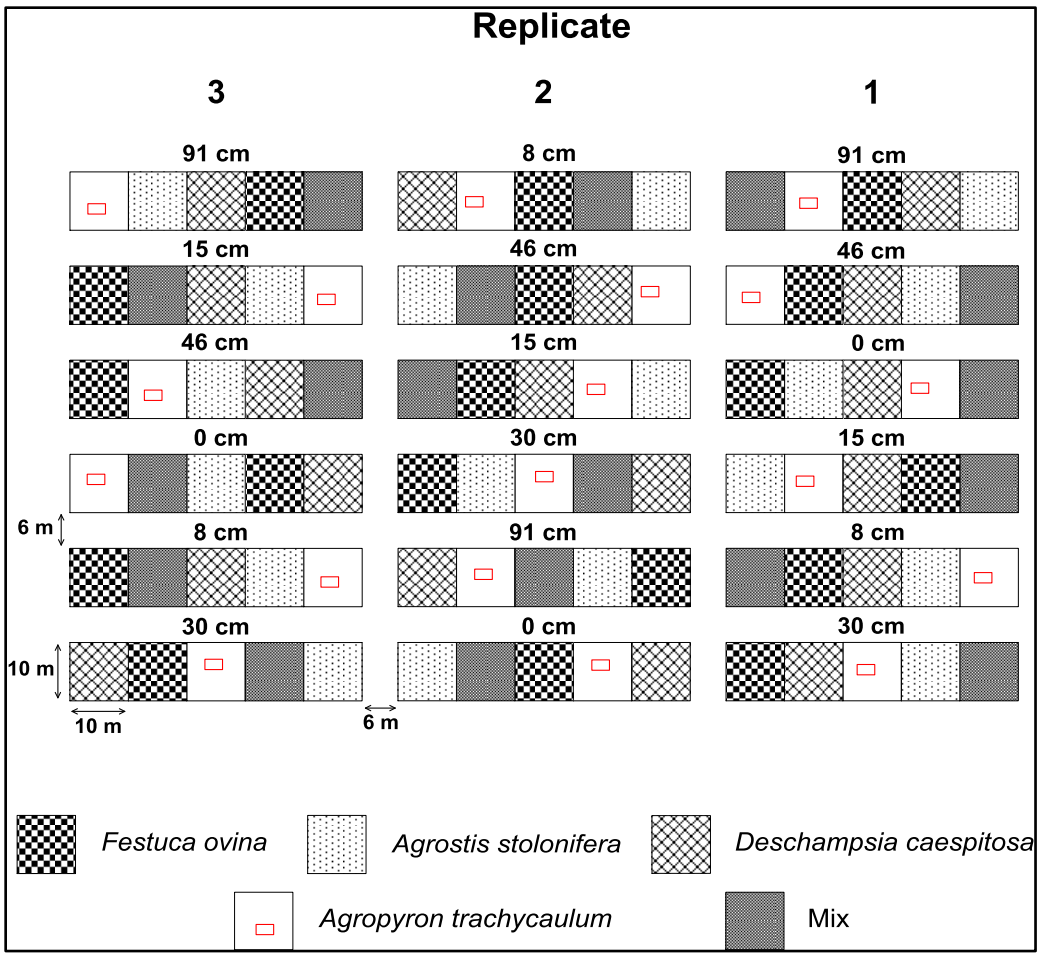


Figure 3.3: Experimental research plots located onsite at Agrium Nitrogen Operations, Fort Saskatchewan, Alberta. Red rectangles indicate the locations of $Br^-$ tracer application area.

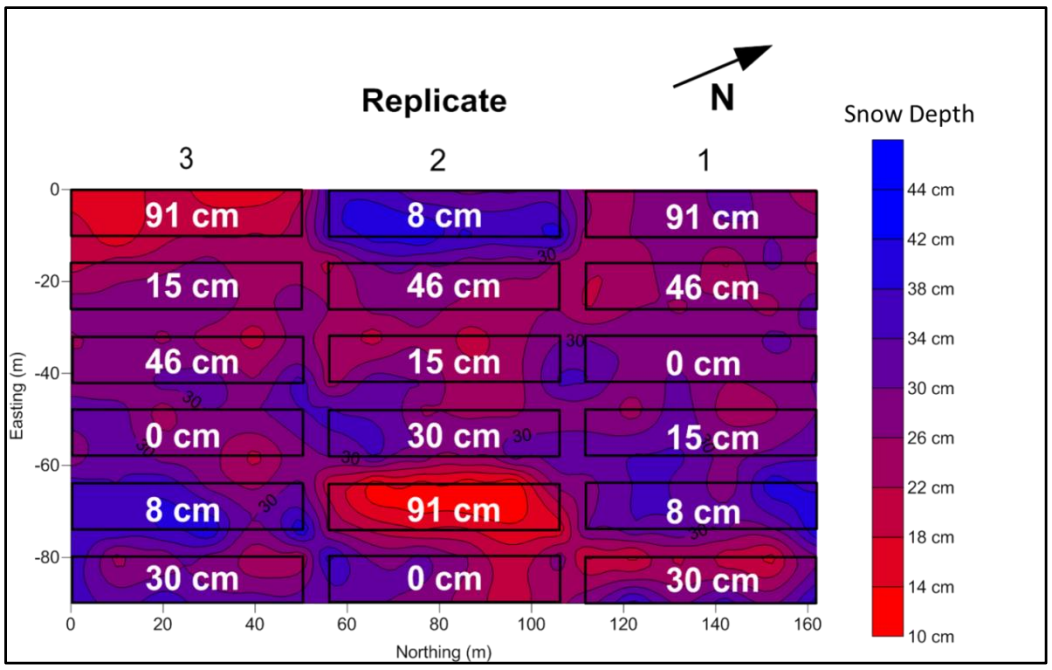

Figure 3.4: Snow depth contour plot of 216 discrete snow depth measurements taken on 26 February, 2011.

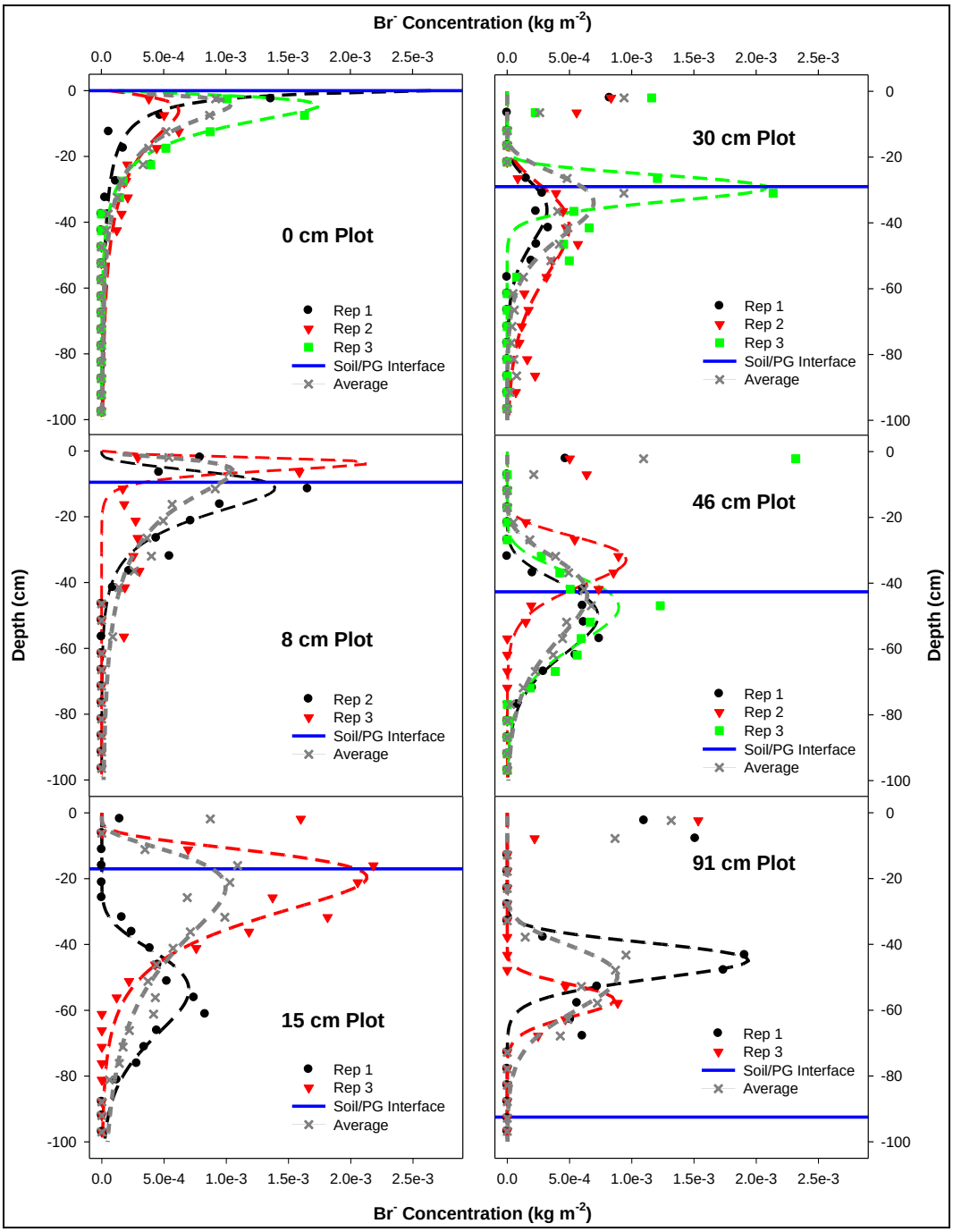


Figure 3.5: Bromide distribution with fitted probability density function for the various capping topsoil treatment plots.

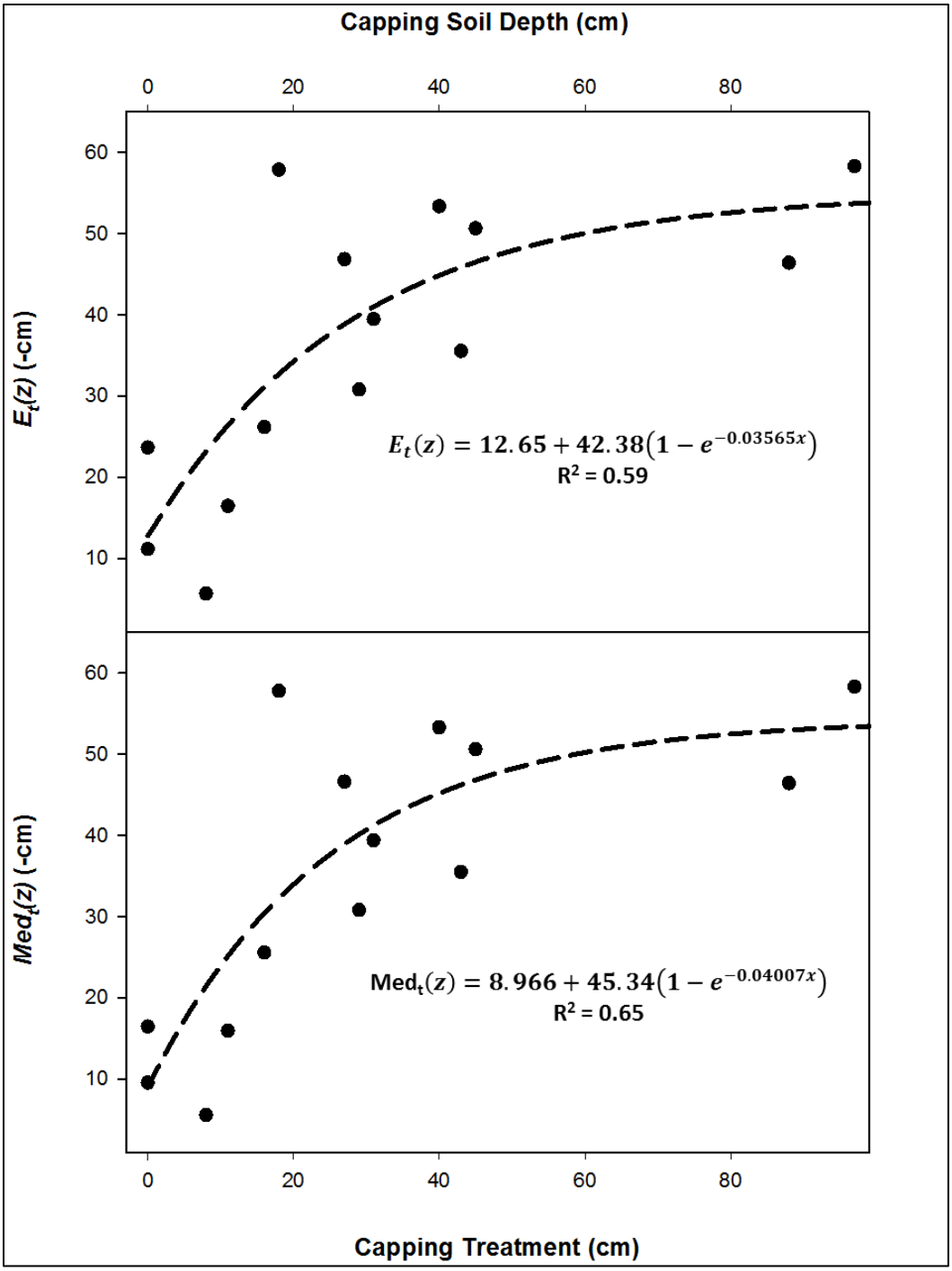


Figure 3.6: Top: Mean travel depth ($E_t(z)$) for the various capping soil treatment with an exponential curve fit to data. Bottom: Median travel depth ($Med_t(z)$) for the various capping soil treatment with an exponential curve fit to data.

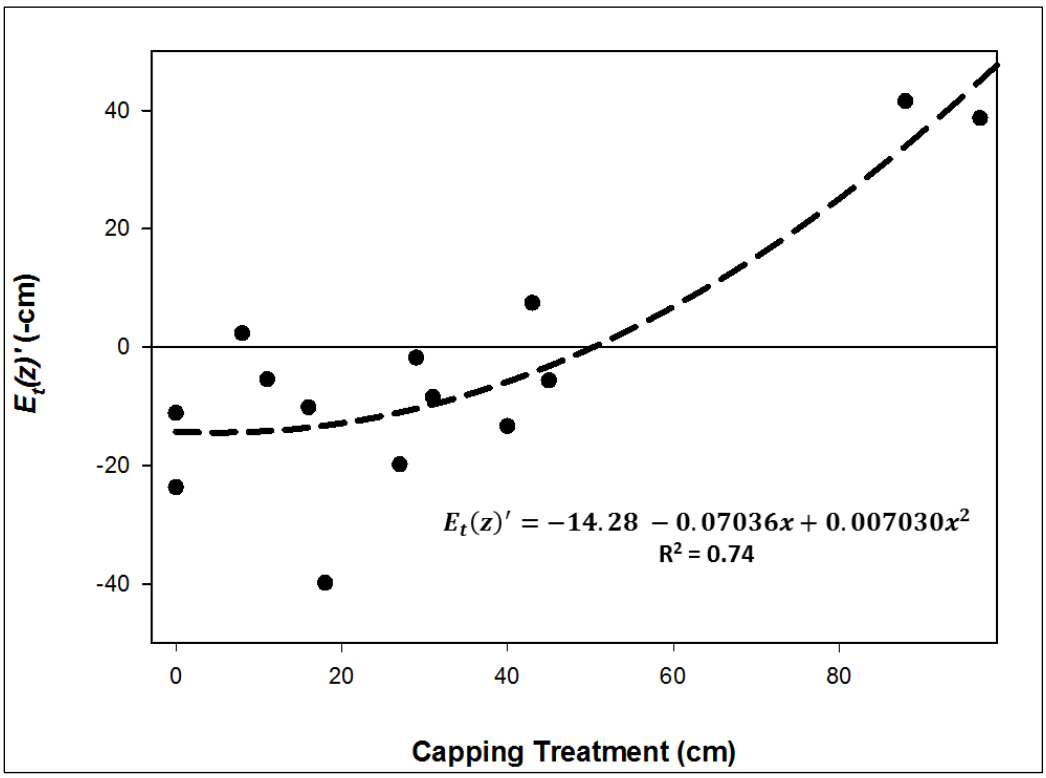

Figure 3.7: Mean travel depth with respect to the topsoil/PG interface ($E_t(z)'$) for the various capping soil treatment fit with a polynomial model.

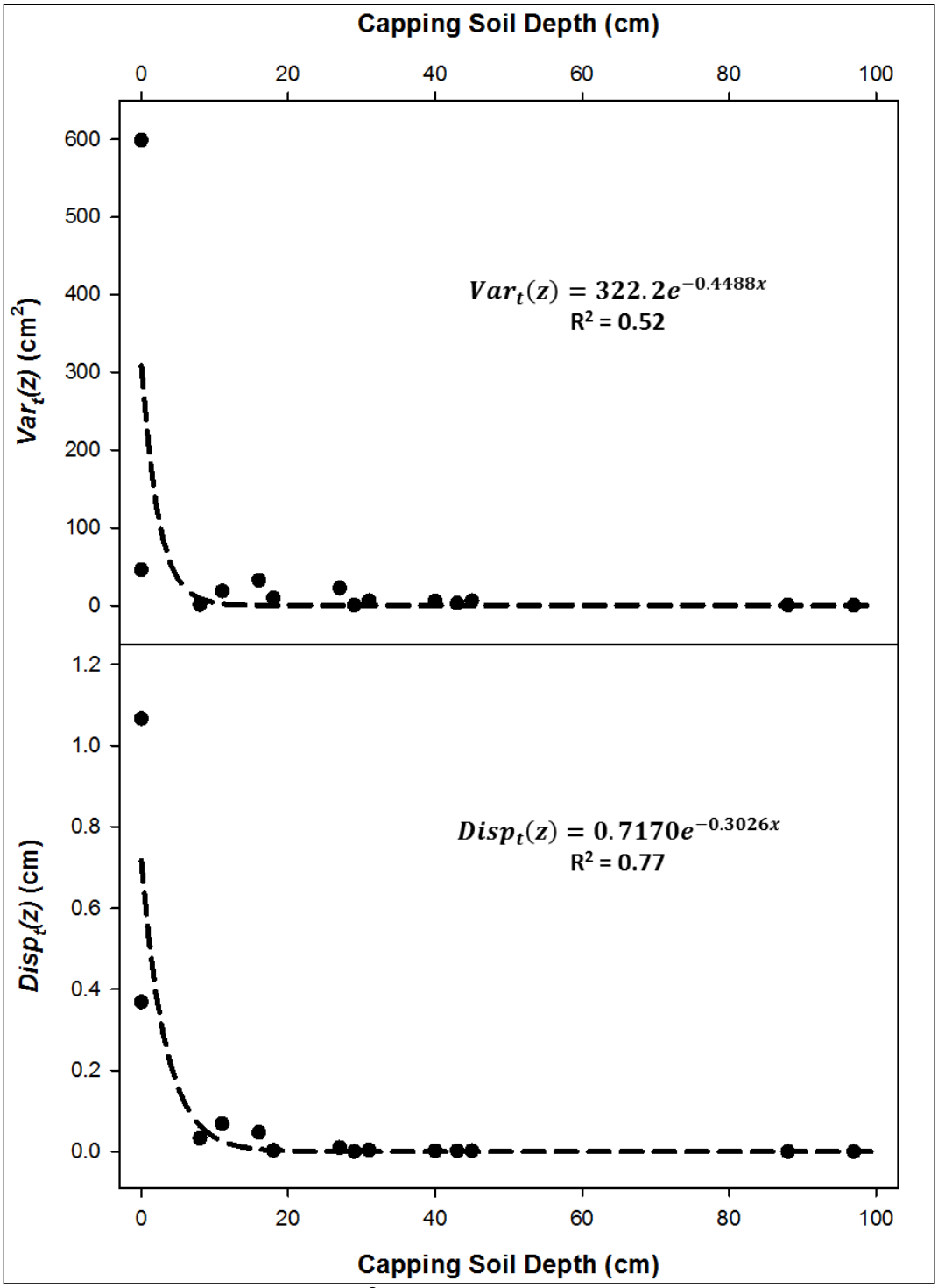


Figure 3.8: BTC variance (cm$^2$) as a function of capping soil depth (top) and BTC dispersivity (cm) as a function of capping soil depth (bottom).

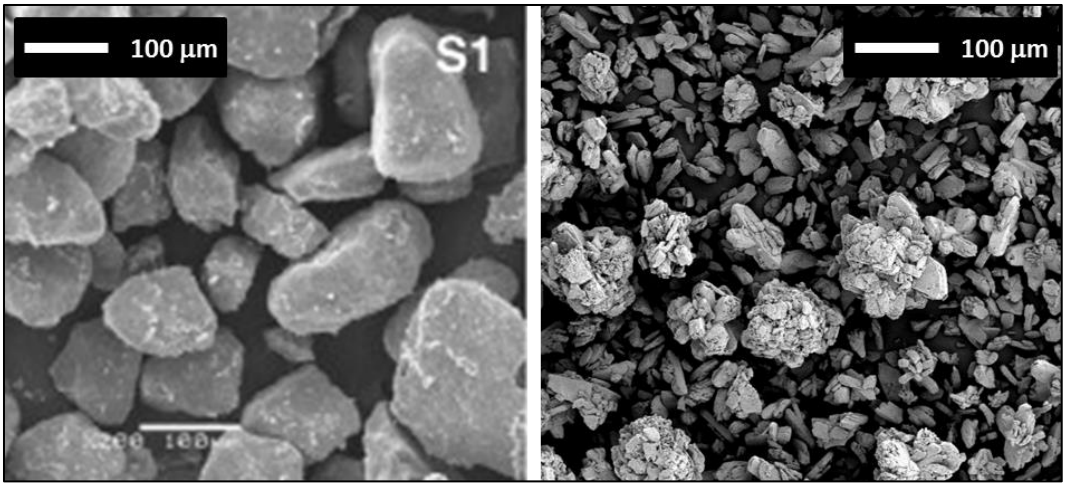

Figure 3.9: Scanning electron microscope images of sandy loam soil (Ta 2007) (left) and PG from Fort Saskatchewan, AB (Nichol 2009) (right).

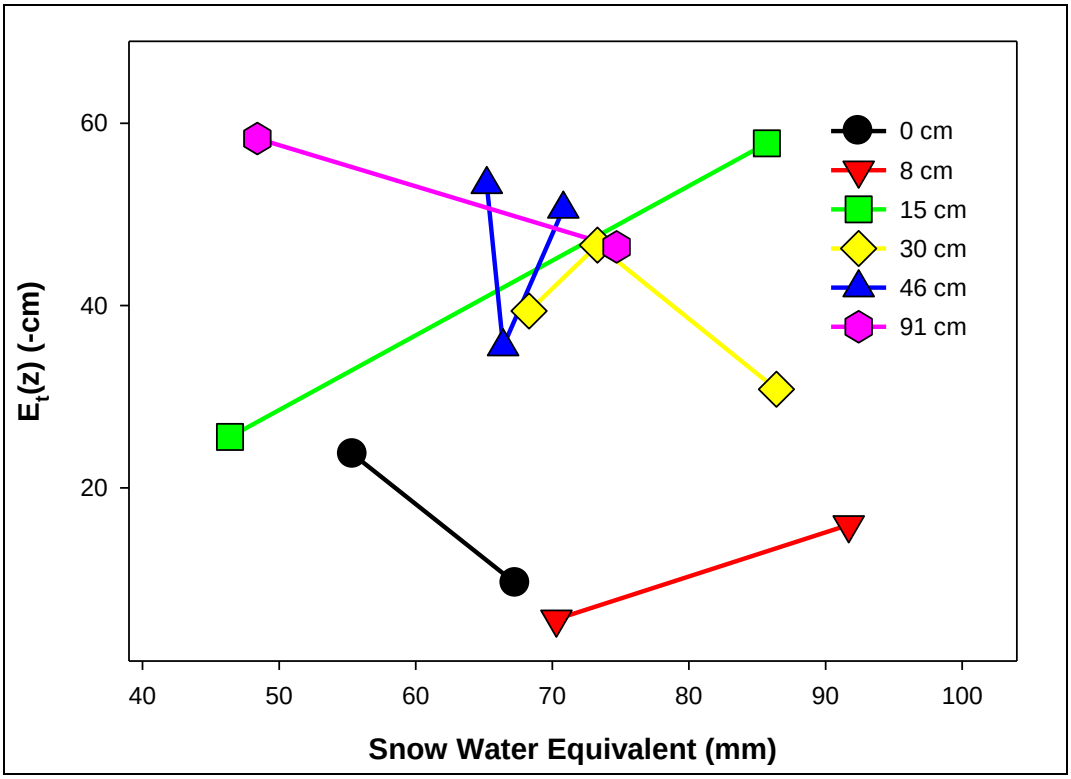

Figure 3.10: Mean travel depth interaction with SWE.

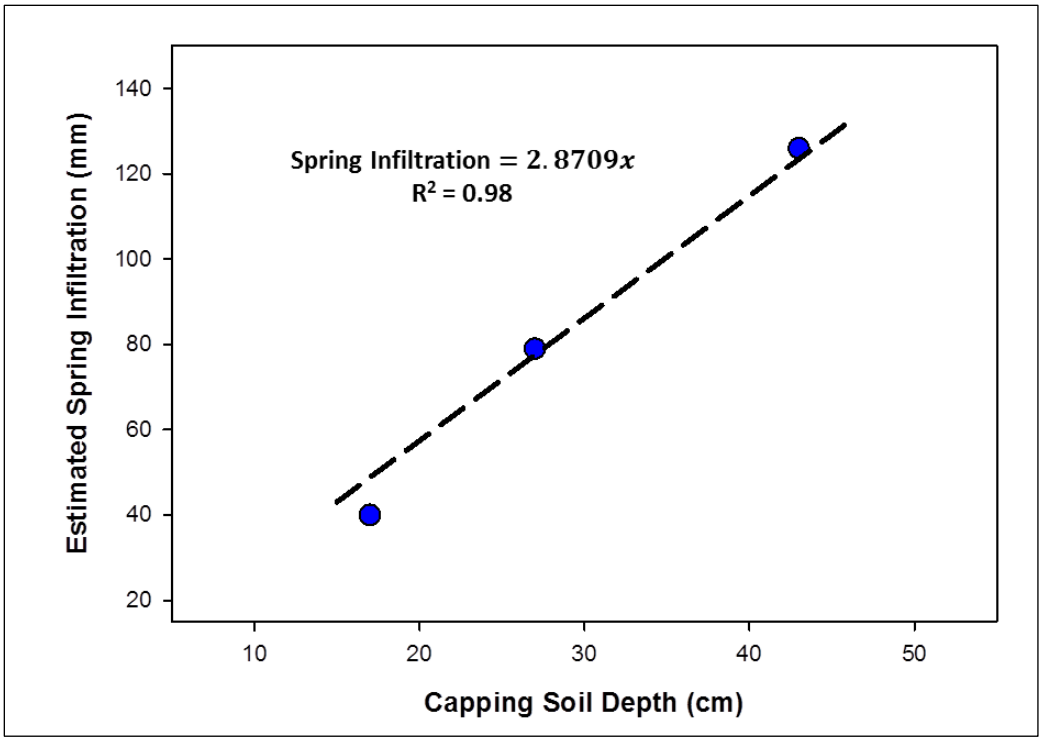


Figure 3.11: Estimated spring infiltration as a function of capping soil depth from Section 2 for 2011.

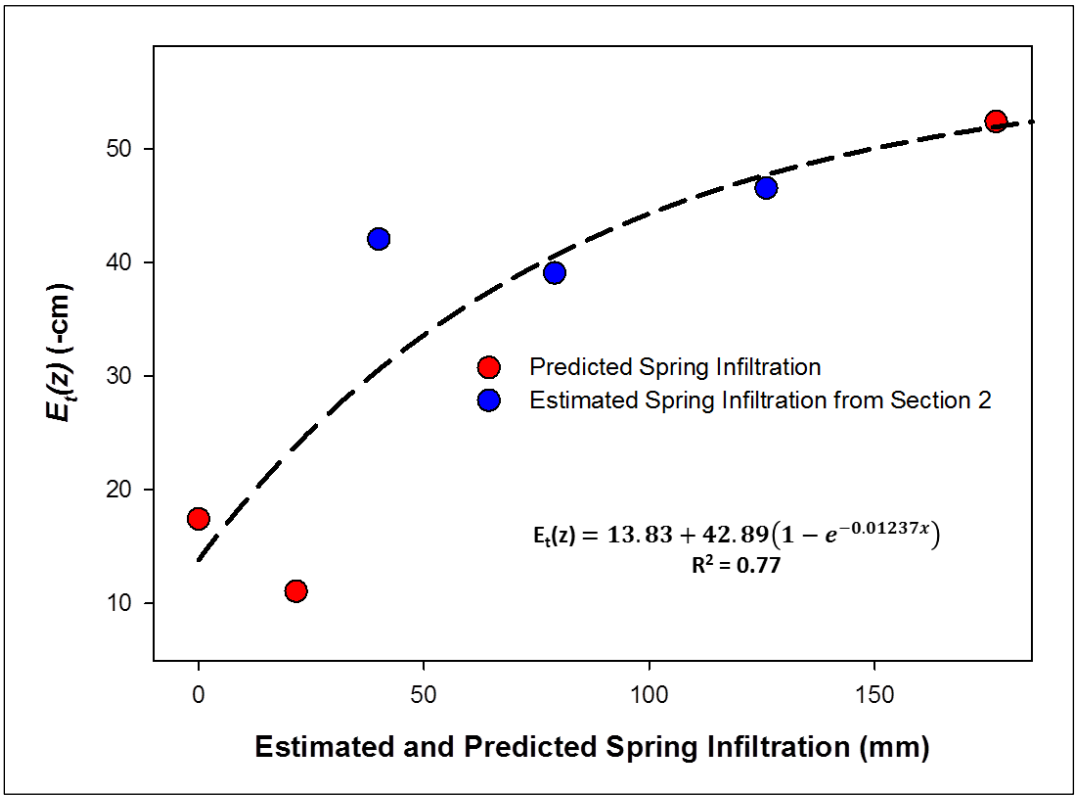


Figure 3.12: Mean travel depth (*Et(z)*) as a function of the predicted and estimated spring infiltration for 2011.

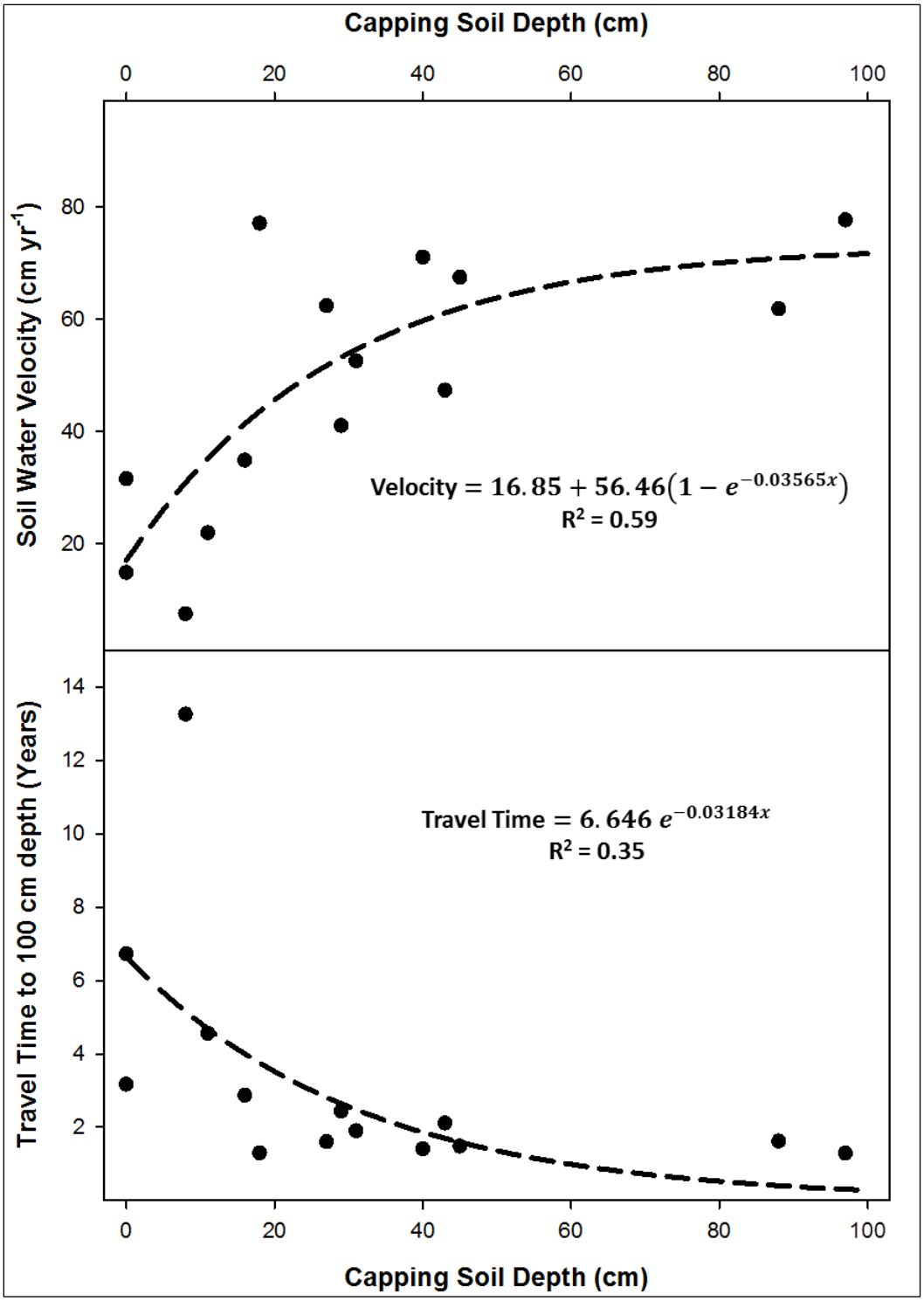


Figure 3.13: Soil water velocity (cm $yr^{-1}$) as a function of capping soil depth (top) and travel time to 100 cm depth (years) as a function of capping soil depth (bottom).

# 4.0 SUMMARY, SYNTHESIS AND FUTURE RESEARCH

## 4.1 Summary

The evaluation of a conventional or innovative cover system is a necessary component in waste isolation and containment to assess the effectiveness of the cover system at meeting the reclamation objectives. The three main objectives pertaining to landfill/waste containment include: (1) minimizing infiltrating water into the waste material and percolation from waste to groundwater; (2) isolation of waste material from the various receptors and control the potential redistribution by wind and water; and (3) control gas release (Hauser 2009).

These objectives, under the context of phosphogypsum (PG) stack reclamation can be reformulated to include: (1) prevention of contaminated water from entering the environment by means of surface or groundwater flow; (2) sustain structural integrity of PG stack; (3) minimize radionuclide emissions from PG stack; and (4) minimize interaction between precipitation and PG material (Alberta Environment 2008; FDEP 2006). The overall objective of this study was to evaluate the hydrological balance within of the evapotranspiration (ET) cover system and the interaction between the capping soil and the PG material.

Estimates for water distribution and movement within the ET cover system were determined using continuous water content measurements coupled with matric potential measurements. Increases in capping soil depth contributed to increases in spring infiltration due to the increased

internal capacity of the topsoil; however, the limited ability of the loamy sand material at retaining water resulted in higher percolation estimates with increasing capping depth. Net flux estimates for 2011 indicated that an increase in capping soil thickness resulted in an increase in net vertical flux within the topsoil and underlying PG material. These results were not confirmed in 2012 due primarily to the limited amount of water available to the system during spring snowmelt. The daily flux across the topsoil/PG interface was highly sensitive to high intensity (>25 mm) / short duration (< 1 day) precipitation events as well as low intensity (< 25 mm) / long duration (> 3 days) precipitation events, both of which resulted in downward flux into the PG material. Evapotranspiration contributed significantly to upward flux patterns across the topsoil/PG interface during the active growing season in terms of duration, as observed by the hydraulic gradient; however, with respect to magnitude the negative downward flux pattern dominated.

Estimates for advective water movement and velocity were determined by observing the distribution of a conservative tracer 274 days after a single pulse application. The results indicated that an increase in capping soil depth contributed to an increase in the depth to which the advective water movement was able to penetrate. The infiltrating water during the spring snowmelt and active growing season, on average, was able to penetrate into the PG material of 0, 8, 15 and 30 cm capping soil treatments, as well as the 46 cm capping depth in some instances. There

was no correlation between the amount of water that was available from snowmelt and the advective water movement, most likely due to surface redistribution, the ability of the PG material to retard to the movement of water and the influence of capping depth on spring infiltration which ultimately governed the advective movement of water within the reclaimed system. Soil water velocity was found to exponentially increase with increasing capping soil depth due to the greater proportional influence of the highly permeable loamy sand topsoil material in comparison to the PG material.

In general, the conclusions presented in Sections 2 and 3 suggest that an increase in capping soil depth contributed to greater infiltration of spring snowmelt water resulting in deeper penetration of the advective water front into the reclaimed system, which ultimately resulted in greater water percolation in treatments with > 15 cm capping soil. However, it must be explicitly mentioned that the results presented are specific to the boundary conditions applied including total precipitation, landscape topography and temporal variability with respect to evapotranspiration, as well as the physical properties pertaining to the topsoil and PG material. Further evaluation of shallow capping soil covers should be carried out with the use of simulation models.

## 4.2 Considerations

In order to meet all the reclamation objectives pertaining to water movement in the ET cover system the proponents will need to consider three critical aspects pertaining to the capping soil including: 1) the capping soil texture; 2) the sequence of textural stratification; and 3) capping soil thickness as a function of topographical variability and water redistribution. The first point is directed at the limited water retention capabilities and the elevated permeability of the coarse textured loamy sand topsoil that was investigated, and its role in expediting water movement during spring snowmelt and the precipitation events accounted for during the active growing season.

Secondly, the sequence of stratification to which the ET cover system is applied is further exacerbating the negative aspects of the hydraulic properties of the capping soil. The finer texture of the PG material will ultimately result in downward flux gradients due to the higher unsaturated hydraulic conductivity of the PG material at field capacity compared to the topsoil material due to the greater proportion of finer pores.

Finally, the topographical variability should be investigated and its role on water redistribution on the anthropogenic landscape. The research presented is solely focused on capping soil depth and the response of water movement; however, the plots that were used during the research were constructed on a topographically level area, which limits the

discussion of the results to the specific environmental constraints which were dictated by atmospheric distribution of water and not topographical redistribution of water.

## 4.3 Application

The application of the data presented can be further used in the context of risk management in order to fulfill the obligations pursuant to section 5.2.3 (c) of the Approval issued to Agrium Products Inc. by Alberta Environment (2008). Specifically, capping depth, physical properties of cover soil and PG material (i.e. texture, water retention characteristics, hydraulic conductivity and porosity), and atmospheric boundary conditions (i.e. air temperature, humidity, daily precipitation and substrate temperature) can be used to model water dynamics within the context of PG stack reclamation. Furthermore, the water content distribution and observed mean travel depth of the applied tracer data can be used to calibrate the model to refine the accuracy and reduce errors within the context of the model.

## 4.4 Future Research

In natural environments landscape topography contributes significantly to various soil-forming processes including the leaching of pedogenic salts to greater depths. The presence, or absence, of these pedogenic salts is an indication of the contribution of water distribution on

the landscape (Bedard-Haughn and Pennock 2002; Pennock et al. 2011; Woods et al., 2013). The significance of water redistribution on natural landscapes is fundamental in determining the overall hydrological balance; therefore, future research in the field of PG stack reclamation should focus on spatial variability with respect to snow and water redistribution on the anthropogenic landscape.

The understanding of the hydrological balances apparent on site is not localized at the scale of observation that was presented in the preceding chapters and theses; therefore, more knowledge is required at the landscape scale to determine the potential risks associated with long term water redistribution. Furthermore, the ideology regarding a single capping soil depth prescription for PG stack reclamation, or any reclamation, is outdated. Conceptually, reclamation could have the same fundamental relationship to the proponents as does precision agriculture to farmers. In this regard a successful ET cover system should be designed to account for the topographical and hydrological variability within the anthropogenic landscape.

PG stack reclamation in general is a short term solution to the problem of utilization; therefore, another avenue of future research could be to focus on potential value driven reuse options for PG. To date significant research has focused on agricultural, environmental restoration and construction (Degirmenci et al. 2007; Dippel 2004; Kazman et al. 1983; Rechcigl et al. 1993; Rutherford et al. 1994); however, little attention

is given to the value of residual phosphorus content couple with the sulphur content and the potential uses of each in biodiesel production. Field observation noted that significant algae blooms were present in isolated pools of water following precipitation events as well as discharge water located around the parameter of the PG stack #4. It is clear that the nutrient requirements for algae production are adequately being met under unsupervised conditions (Baliga and Powers 2010; Rodolfi et al. 2008), the research question then becomes, can a viable solution be created to use the PG material and other manufacturing wastes ($CO_2$, heat, $CaCO_3$, nitrogen based waste, etc.) to manufacture biodiesel from active algae cultures.

## 4.5 References


Alberta Environment. 2008. Construction, operation and reclamation of the Redwater fertilizer manufacturing plant. Approval No. 210-02-00. Edmonton, AB. 42 pp.

Baliga, R. and S.E. Powers. 2010. Sustainable algae biodiesel production in cold climates. International Journal of Chemical Engineering. 2010:1-13.

Bedard-Haughn, A.K. and D.J. Pennock. 2002. Terrain controls on depressional soil distribution in a hummocky morainal landscape. Geoderma. 110:169-190.

Degirmenci, N., A. Okucu and A. Turabi. 2007. Application of phosphogypsum in soil stabilization. Building and Environment 42:3393-3398.

Dippel, S.K. 2004. Mineralogical and geochemical characteristics of phosphogypsum waste material and its potential for use as a backfill at WMC fertilizers'' mine site, Phosphate Hill, N-W Queensland. M.Sc. Thesis. James Cook University. Douglas, QL. 336pp.

Florida Department of Environmental Protection. 2006. Chapter 62-673 phosphogypsum management.

http://www.floridadep.org/legal/rules/shared/62-673.pdf. Effective date: July 19, 2006. 15 pp. Last accessed November 29, 2008.

Hauser, V.L. 2009. Evapotranspiration landfill covers. Pages 35-49 *in* Evapotranspiration covers for landfills and waste sites. CRC Press, Boca Raton, FL. USA.

Kateb, H.E., H. Zhang, P. Zhang and R. Mosandl. 2013. Soil erosion and surface runoff on different vegetation covers and slope gradients: A field experiment in Southern Shaanxi Province, China. Catena. 105:1-10.

Kazman, Z., I. Shainberg, and M. Gal. 1983. Effects of low levels of exchangeable sodium and applied phosphogypsum on the infiltration rate of various soils. Journal of Soil Science. 135: 184-192.

Larney, F.J. and D.A. Angers. 2012. The role of organic amendments in soil reclamation: A review. Canadian Journal of Soil Science. 92:19-38.

Loch, R.J. 2000. Effects of vegetation cover on runoff and erosion under simulated rain and overland flow on a rehabilitated site in the Meandu Mine, Tarong, Queensland. Australian Journal of Soil Research. 38:299-312.

Pennock, D., A. Bedard-Haughn and V. Viaud. Chernozemic soils of Canada: Genesis, distribution, and classification. Canadian Journal of Soil Science. 91:719-747.

Rechcigl, J.E., P. Mislevy and A.K. Alva. 1993. Influence of limestone and phosphogypsum on Bahia grass growth and development. Soil Science Society of America Journal. 57: 96-102.

Rodolfi, L., G.C. Zittelli, N. Bassi, G. Padovani, N. Biondi, G. Bonini and M.R. Tredici. 2008. Microalgae for oil: Strain selection, induction of lipid synthesis and outdoor mass cultivation in a low-cost photobioreactor. Biotechnology and Bioengineering. 102(1):100-112.

Rutherford, P.M., M.J. Dudas, and R.A. Samek. 1994. Environmental impacts of phosphogypsum. The Science of the Total Environment. 149:1-38.

Woods, S. A., M. Dyck and R. G. Kachanoski. 2013. Spatial and temporal variability of soil properties and long-term solute transport under semi-arid conditions. Canadian Journal of Soil Science. 93:173-191.

# Appendix A

## In situ measurement of snowmelt infiltration under various topsoil cap thicknesses on a reclaimed site

Andre F. Christensen[1], Hailong He[1], Miles F. Dyck[1,3], Lenore Turner[1], David S. Chanasyk[1], M. Anne Naeth[1], and Connie Nichol[2]

*[1]Department of Renewable Resources, 751 General Service Building, University of Alberta, Edmonton, Alberta, Canada T6G 2H1; and [2]Agrium, Inc., 1751 River Rd, Fort Saskatchewan, Alberta, Canada T8L 4J1.*
*Received 1 May 2012, accepted 27 May 2013.*

Christensen, A. F., He, H., Dyck, M. F., Turner, L., Chanasyk, D. S., Naeth, M. A. and Nichol, C. 2013. **In situ measurement of snowmelt infiltration under various topsoil cap thicknesses on a reclaimed site**. Can. J. Soil Sci. **93**: xxx–xxx. Understanding the soil and climatic conditions affecting the partitioning of snowmelt to runoff and infiltration during spring snow ablation is a requisite for water resources management and environmental risk assessment in cold semi-arid regions. Soil freezing and thawing processes, snowmelt runoff or infiltration into seasonally frozen soils have been documented for natural, agricultural or forested systems but rarely studied in severely disturbed systems such as reclaimed lands. The objective of this study was to quantify the snowmelt infiltration/runoff on phosphogypsum (PG) tailings piles capped with varying thicknesses of topsoil (0.15, 0.3, and 0.46 m) at a phosphate fertilizer production facility in Alberta. There are currently no environmental regulations specifying topsoil capping thickness or characteristics for these types of tailings piles. Generally, the function of the topsoil cap is to facilitate plant growth and minimize the amount of drainage into the underlying PG. Experimental plots were established in 2006 to better understand the vegetation and water dynamics in this reconstructed soil. In 2011, time domain reflectometry (TDR) probes and temperature sensors were installed at various depths for continuous, simultaneous, and automated measurement of composite dielectric permittivity ($\varepsilon_{eff}$) and soil temperature, respectively. An on-site meteorological station was used to record routine weather data. Liquid water and ice content were calculated with TDR-measured $\varepsilon_{eff}$ permittivity and a composite dielectric mixing model. Spatial and temporal change of total water content (ice and liquid) revealed that snowmelt infiltration into the topsoil cap increased with increasing topsoil depth and net soil water flux from the topsoil cap into the PG material was positive during the snowmelt period in the spring of 2011. Given the objective of the capping soil is to reduce drainage of water into the PG material it is recognized that a capping soil with a higher water-holding capacity could reduce the amount of meteoric water entering the tailings.

**Key words:** Seasonally frozen soils, ground thermal regime, water and heat dynamics, phosphogypsum tailing, Fort Saskatchewan, snowmelt infiltration

Christensen, A. F., He, H., Dyck, M. F., Turner, L., Chanasyk, D. S., Naeth, M. A. et Nichol, C. 2013. **Quantification in situ des infiltrations de l'eau de fonte sous diverses épaisseurs de sol dans un site restauré**. Can. J. Soil Sci. **93**: xxx–xxx. Comprendre les conditions du sol et du climat qui influent sur le partage de l'eau entre le ruissellement et l'infiltration à la fonte des neiges printanière est indispensable à la gestion des ressources hydriques et à l'évaluation des risques environnementaux dans les régions froides semi-arides. Les mécanismes du gel et du dégel du sol ainsi que le ruissellement des eaux de fonte ou leur infiltration dans le sol gelé de façon saisonnière sont bien documentés pour les systèmes naturels, agricoles et forestiers, mais on les a rarement étudiés dans les systèmes très perturbés comme les terres restaurées. L'étude que voici devait quantifier l'infiltration/le ruissellement de l'eau de fonte dans les tas de résidus de phosphogypse surmontés d'une couche variable de sol de surface (capuchon de 0,15, 0,3 et 0,46 m d'épaisseur), à une usine de fabrication d'engrais phosphatés de l'Alberta. À l'heure actuelle, aucun règlement sur l'environnement ne régit l'épaisseur du capuchon de sol ni les caractéristiques des tas de résidus de cette nature. En général, le capuchon de sol a pour but de faciliter la croissance des plantes et de minimiser le drainage vers la couche de phosphogypse sous-jacente. En 2006, on a aménagé des parcelles expérimentales pour mieux comprendre la dynamique de la végétation et de l'eau sur un sol ainsi reconstitué. Cinq ans plus tard, on a installé des réflectomètres temporels et des thermomètres à diverses profondeurs afin de mesurer de façon continue, simultanée et automatique la permittivité diélectrique des matériaux composites ($\varepsilon_{eff}$) et la température du sol, respectivement. Une station météorologique a été installée sur les lieux pour enregistrer les conditions climatiques. La quantité d'eau à l'état liquide et de glace a été calculée à partir de la permittivité $\varepsilon_{eff}$ mesurée avec le réflectomètre et d'un modèle de mélange des fluides servant à déterminer les caractéristiques diélectriques des composites. La variation de la concentration totale d'eau (états liquide et solide) dans l'espace et le temps indique que l'infiltration de l'eau de fonte dans le capuchon de sol augmente avec l'épaisseur de la couche superficielle et que le flux net d'eau venant de

*[3]Corresponding author (e-mail: miles.dyck@ualberta.ca).*

**Abbreviations:** **PG**, phosphogypsum; **TDR**, time domain reflectometry

la surface et atteignant le phosphogypse avait été positif durant la fonte, au printemps 2011. Puisque le capuchon de sol a pour but de réduire le drainage de l'eau dans le phosphogypse, on convient qu'une couche retenant mieux l'eau pourrait réduire la quantité d'eau entraînant la météorisation qui pénètre dans la strate de résidus.

**Mots clés:** Sols gelés saisonnièrement, régime thermique du sol, dynamique de l'eau et de la chaleur, résidus de phosphogypse, Fort Saskatchewan, infiltration de l'eau de fonte

Snowmelt in cold, semi-arid areas may contribute to the recharge of soil water reservoirs and groundwater because of low evapotranspirational demand during spring snow ablation. Snowmelt; however, may become runoff if soil infiltration capacity is inhibited by ice lenses, ice-filled pores or basal ice layer built up on the soil surface at the base of the snowpack (Cary et al. 1978; Kane 1980; Miller 1980). Snowmelt runoff can lead to an increased probability of erosion of fertile surface soils, migration of pesticides and other agricultural chemicals, and the potential for spring flooding (Janowicz et al. 2002; Hall et al. 2012). Partitioning of the snowmelt into soil water and runoff has important implications for water resource management strategies and the development of mitigation strategies to reduce environmental risks associated with dissolved or suspended contaminants.

Prediction of infiltration into seasonally frozen soils is much more complicated than that of infiltration into unfrozen soils since (1) water flow is strongly coupled with heat transport, hence both hydraulic and thermal properties of the soil affect the spatial and temporal variability of the processes; (2) phase changes between ice and infiltration water may occur; and (3) hydraulic properties are considerably influenced by the amount of ice and its spatial and temporal distribution. The infiltration capacity of partially frozen soils is governed by many factors such as soil-atmosphere energy exchange, soil thermal regime, quantity and rate of snow water release from the snowpack, heat content of the infiltrating water, thermal and hydraulic properties of the soil, soil structure, total soil water content prior to ground freezing or ice content at the time of snow melt, the number of freeze–thaw cycles that change total water and ice content during the winter time, and their complex interactions (Kane 1980; Stein and Kane 1983a; Granger et al. 1984).

Methods developed for unfrozen soils are commonly applied to frozen soils for measurement of infiltration rate into frozen soils. These methods include time domain reflectometry (TDR) (Stein and Kane 1983a; Iwata et al. 2008), double/single-ring infiltrometers (Kane and Stein 1983), neutron scattering (Granger et al. 1984), lysimeter (Kane 1978; Stähli and Lundin 1999), and dye tracing methods (Stähli et al. 2004). Total and liquid soil water content, soil temperature, matric potential, snow pack characteristics (i.e., snow depth and snow water equivalent), depth to groundwater table, and meteorological data (i.e., air temperature, precipitation, and albedo) are usually monitored concurrently to quantify snowmelt infiltration. Empirical expressions consisting of snow water equivalent and soil water content at melt time (Granger et al. 1984; Zhao and Gray 1997) and numerical models (Gray and Granger 1985; Stadler et al. 1997; Stähli and Lundin 1999; Gray et al. 2001; Zhao et al. 2002) have been developed to predict snow infiltration into frozen soils.

Of these above-mentioned methods, TDR can be easily multiplexed and automated making it widely used for both field and laboratory measurement of soil water content (Spaans and Baker 1995). The TDR technique is based on the measurement of the travel time of an electromagnetic wave pulse generated by a TDR cable tester through a wave guide (also called probe) inserted into a porous medium such as soil, unfrozen or frozen. The travel time of the wave through the probe is a function of the effective dielectric permittivity of soil, $\varepsilon_{eff}$, which in turn, is a function of permittivity of the individual constituents in the soil (air, water, solids and ice), their volumetric fractions, and geometric arrangements. Recent research (He and Dyck 2013) showed composite dielectric mixing models can be used to estimate unfrozen water content and ice content in frozen soils. The ability to monitor unfrozen water and ice content in the field may contribute to improving our understanding of snowmelt infiltration into partially frozen soils.

Extensive investigations of snowmelt infiltration behavior of frozen agricultural land (Zhao et al. 2002; Iwata et al. 2008), forested land (Stein and Kane 1983b; Stadler et al. 1997), prairie (Granger et al. 1984; Gray and Granger 1985), or alpine soil in the field as well as in cold chambers (Stadler et al. 2000) have been reported. No study was found by the authors for markedly disturbed systems such as reclaimed sites. Therefore the purpose of this research is to investigate snowmelt infiltration on reclaimed systems, and specifically, in a topsoil cap overlying phosphogypsum (PG) tailings.

Phosphogypsum is a by-product of the production of phosphoric acid, a necessary component in the production of phosphate fertilizers. The production of phosphoric acid involves the reaction of sulfuric acid and phosphate rock. The resulting solution is a combination of gypsum ($CaSO_4$), hydrogen fluoride and phosphoric acid (Rutherford et al. 1994). Once the PG material has been filtered from the solution, it is mixed with water to form a slurry which can be pumped into settling ponds (wet stacking). These settling ponds rise as the PG settles out of suspension, forming large stacks, referred to as PG stacks (Wissa 2002). The stacks can grow to

immense scales depending on the engineered capacity and can occupy vast amounts of land.

There may be numerous impurities in the phosphate source material including radium, uranium, arsenic, barium, cadmium, chromium, lead, mercury, selenium and phytotoxic fluoride (Rutherford et al. 1995). These trace elements may accumulate in the PG by-product and in the water held within its pore space. Studies have demonstrated that concentration and mobility of most trace elements within the PG pore water decreases with time as the stack drains (Rutherford et al. 1995). However, the introduction of precipitation into the PG stack may facilitate the mobility of these trace elements as well as dissolve the PG material (SENES 1987). Therefore, the leading concerns regarding PG stacks include contamination of the environment by multi-integrated vectors such as PG leachate to groundwater, wind and water dispersion to surrounding land and radionuclide emissions from the stack (SENES 1987; Thorne 1990) and stack stability.

The main objective of this work was to investigate the temporal and spatial changes of soil ice ($\theta_i$) and liquid water ($\theta_l$) content under various snow depths and topsoil cap thicknesses to understand the influences of freeze–thaw cycles on snowmelt infiltration into the topsoil caps and subsequent drainage (if any) into the underlying PG over the course of the spring thaw period in 2011 and the following 2011 freezing period and part of the spring, 2012 thaw. The relationship between snowmelt infiltration, snow depth, topsoil cap thickness and the soil freezing characteristic will be discussed throughout the paper.

## MATERIAL AND METHODS

### Site Description

The study was conducted at the Agrium Nitrogen Operations facility, located in Fort Saskatchewan, Alberta, Canada (lat. 53°44′07″N, long. 113°11′28″W, 624 m above the sea level). The area is described as cold, semi-arid having a mean annual temperature of 2.9°C and a mean annual precipitation of 460 mm, with 355 mm in the form of rainfall mainly occurring between May and August and 105 mm as snow. The average temperature from December through February is −11.7°C and 15.8°C from June through August (Environment Canada 2011). The growing season typically starts mid- to late April as marked by a mean daily temperature of >1°C for a period of 5 consecutive days. The growing seasons for the area typically last through to early September, when the maximum duration of sunshine, calculated from latitude and Julian day, decreases below 13.5 h (Hayashi et al. 2010).

The field site is permanently located on top of a decommissioned PG stack that was operational for 8 yr before its closure in 1991. The PG stack is approximately 15 m in height and occupies a base area of 9.3 ha. Eighteen (50 m × 10 m) plots were constructed atop the decommissioned PG stack in a complete randomized design during the fall of 2006 (Jackson 2009). The plots were arranged into three replicates each containing six topsoil capping depth treatments including 8, 15, 30, 46, and 91 cm, as well as a 0-cm control; however, for the purposes of this research only replicate 2 was used for sampling due to the logistical constraints that were imposed with respect to site instrumentation. The general topography on which the topsoil was placed was relatively flat with a slope of <1%. Each topsoil depth treatment was further subdivided into five subplots (10 m × 10 m) that contained five different plant species treatments including *Agropyron trachycaulum* (Link) Malte ex H.F. Lewis (slender wheatgrass), *Agrostis stolonifera* L. (redtop), *Deschampsia caespitosa* (L.) P. Beauv. (tufted hairgrass), *Festuca ovina* L. (sheep fescue) and a mixture of 54% redtop, 2% slender wheatgrass, 28% tufted hairgrass, 8% sheep fescue and 8% alsike clover (Jackson 2009).

### Topsoil and PG Characterization

The substrate that was used as the capping soil was a sandy loam to loamy sand textured Black Chernozemic soil excavated from a nearby alfalfa field. The capping soil had an average bulk density of 1.5 g $cm^{-3}$ and an average porosity of approximately 0.44 $cm^3$ $cm^{-3}$. The saturated hydraulic conductivity of the topsoil cap was $7.4 \times 10^{-3}$ cm $s^{-1} \pm 7.9 \times 10^{-5}$ (Jackson et al. 2011). Water retention curves for the topsoil indicated that the air entry potential for the topsoil material was approximately −28 cm and that the residual water content at −15 000 cm was 0.11 $cm^3$ $cm^{-3}$ (Fig. 1).

The PG material matrix is dominated by silt sized particles that have a diameter ranging from 0.25 to 0.045 mm (Rutherford et al. 1994). Bulk density and porosity

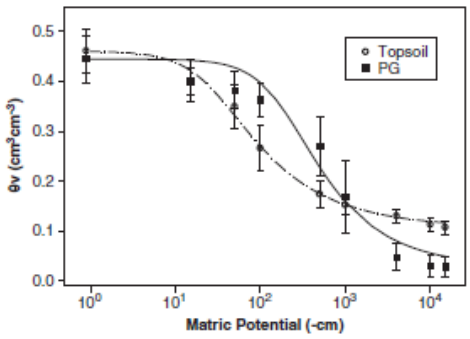


**Fig. 1.** van Genuchten (1980) model fitted to the moisture retention curves for the topsoil and PG material. van Genuchten parameters are $\alpha = 0.036$ $cm^{-1}$, $n = 1.57$, $\theta r = 0.11$ $cm^3$ $cm^{-3}$, $\theta s = 0.46$ $cm^3$ $cm^{-3}$ for topsoil, and $\alpha = 0.0054$ $cm^{-1}$, $n = 1.67$, $\theta r = 0.027$ $cm^3$ $cm^{-3}$, $\theta s = 0.44$ $cm^3$ $cm^{-3}$ for PG.

estimates for the PG material found on site averaged approximately 1.4 g $cm^{-3}$ and 0.45 $cm^3$ $cm^{-3}$, respectively. The saturated hydraulic conductivity of PG material was $3.7 \times 10^{-4}$ cm $s^{-1}$ $\pm 6.6 \times 10^{-6}$ (Jackson et al. 2011). The water retention curve for the PG material indicated that the predicted air entry potential was approximately −186 cm and that the residual water content at −15 000 cm was 0.03 $cm^3$ $cm^{-3}$; however, it is worth noting that the air entry potential is based on empirical parameters used in the van Genuchten model (Fig. 1). Some discrepancies regarding the fit of the van Genuchten model to the measured data are due in part to the finer-textured PG material and its narrow pore size distribution; therefore, the air entry potential would most likely be lower than the predicted value.

## Experimental Design

The 15-, 30- and 46-cm treatments of replicate 2 were selected for soil water investigation based on the intended final reclamation depth, that would fall within the range of 15–46 cm as suggested by previous studies, and for the close proximity of each plot to one another that was necessary given the limitation of cable length for the TDR sensors (Jackson 2009; Hallin 2009). All experimental measurements were conducted within the *Agropyron trachycaulum* subplots of the three soil treatments in order to establish a controlled plant community that would be representative of the final reclamation goals.

Within each subplot, TDR probes were installed along with dielectric water potential sensors (MPS-1, Decagon Devices Inc., Pullman, WA) and soil temperature sensors (TMC50-HD, Onset Computer Corporation, Bourne, MA) (Table 1). The TDR probes and MPS-1s were horizontally installed at the PG/soil interface as well as 7.5 cm above and below the interface. Additional TDR probes were horizontally installed at 15-cm increments from the PG/soil interface as well as a single vertical probe installed into the topsoil cap equivalent to the soil treatment depth (15, 30 and 46 cm). The horizontal TDR probes were installed into a 60-cm × 50-cm trench that was dug to a depth of approximately 1 m using a backhoe in November of 2010. Once the TDR probes were installed the substrate material was repacked in the order in which it was removed in order to avoid mixing. The soil temperature probes were installed vertically into a narrow hole that was created within 50 cm of the TDR probes in April of 2011 due to winter conditions inhibiting earlier installation. Soil temperature sensors were installed at depths corresponding to the horizontal TDR probes for each subplot and subsequently routed to HOBO U12 external data loggers and logged on an hourly basis. The MPS-1 probes were routed to a CR 1000 data logger and monitored every 2 h [Campbell Scientific (Canada) Corp. Edmonton, AB].

**Table 1. Soil sensors and placement depth below soil surface**

| Soil treatment | Sensor | Depth |
|---|---|---|
| 15 cm | TDR probe | 7.5, 0[z], −7.5, −15, −30, −45 cm, and 15 cm vertical |
| | Temp. probe | 7.5, 0[z], −7.5, −15, −30 and −45 cm |
| | MPS-1 probe | 7.5, 0[z], and −7.5 cm |
| 30 cm | TDR probe | 15, 7.5, 0[z], −7.5, −15, −30, −45 cm, and 30 cm vertical |
| | Temp. probe | 15, 7.5, 0[z], −7.5, −15, −30, and −45 cm |
| | MPS-1 probe | 7.5, 0[z], and −7.5 cm |
| 46 cm | TDR probe | 30, 15, 7.5, 0[z], −7.5, −15, −30 cm, and 46 cm vertical |
| | Temp. probe | 30, 15, 7.5, 0[z], −7.5, −15, and −30 cm |
| | MPS-1 probe | 7.5, 0[z], and −7.5 cm |

[z]Soil/phosphogypsum interface.

## TDR Measurements

The TDR probes that were used during the experiment were constructed using two stainless steel rods, each with a diameter of 0.5 cm with 4-cm inter-rod spacing attached directly to a 10-m-long RG 58/U coaxial cable. Vertically installed TDR probes varied in length corresponding to topsoil treatment depth (15, 30 and 46 cm), while the horizontally installed TDR probes were a standardized length of 30 cm. The TDR probes that were installed were routed to 3 SDMX 50 multiplexers [Campbell Scientific (Canada) Corp. Edmonton, AB] corresponding to the three subplots under investigation. The 3-SDMX50 multiplexers were subsequently routed to a central multiplexer, which was connected directly to a TDR100 and CR 800 data logger [Campbell Scientific (Canada) Corp. Edmonton, AB]. In order to reduce signal loss along the length of the cable RG 8/U coaxial cables were used to link the SDMX 50s to the central SDMX 50 multiplexer.

During spring melt and fall freeze up, electrical conductivity and the dielectric permittivity ($\varepsilon_{eff}$) were logged every 2 h, while the individual wave forms were logged every 6 h. During the mid-summer months the electrical conductivity and $\varepsilon_{eff}$ were logged every 4 h and waveforms were logged every 12 h.

## Meteorological Measurements

An on-site weather station was used to measure and record routine meteorological data on an hourly basis using a CR 10× data logger [Campbell Scientific (Canada) Corp. Edmonton, AB]. Precipitation and solar radiation were measured using a TE525WS Texas Electronic 0.254 mm tipping bucket rain gauge and a Kipp & Zonen silicon pyranometer (SP-Lite), respectively. Wind speed and direction were measured using a 05103-10 RM Young wind monitor. Finally, air temperature and relative humidity were measured using a HMP45C Vaisala probe housed in a radiation shield [Campbell Scientific (Canada) Corp. Edmonton, AB]. Snowfall data were measured at the Fort Saskatchewan

meteorological station, located 1.79 km south of the field site (Environment Canada 2012).

### Snow Survey

Snow depth and density were measured on 2011 Feb 26. The Fort Saskatchewan meteorological station, located 1.79 km away, was used after 2011 Feb. 26 to obtain further snow fall records. A snow survey was not conducted in 2012 due to the lack of cumulative snow pack; however, snowfall data were obtained from the nearby meteorological station in Fort Saskatchewan to estimate winter precipitation. For each 50 m × 10 m plot, 12 locations were selected for snow depth measurements (D, cm) using a standard ruler. Within each *Agropyron trachycaulum* subplot (10 m × 10 m) a single snow core was collected using a clear polyvinyl chloride tube (2.38-cm radius). For soil treatments with TDR probes installed the snow cores were collected within 50 cm of probe location. The snow cores were transferred to plastic sampling bags and weighed. The density of snow was used to compute snow water equivalent (mm) measurements for the plots under investigation.

### Estimation of Unfrozen Water and Ice Content with TDR-measured $\varepsilon_{eff}$

Freezing of soils affects the dielectric permittivity similarly to the drying of unfrozen soils but the drying process in an unfrozen soil involves the replacement of water with air whereas the freezing process involves the displacement of water by ice. The dielectric permittivity of ice is about 3 times greater than air (3.2 compared with 1, respectively). Therefore, the $\varepsilon_{eff}$ of a frozen soil will be greater than the $\varepsilon_{eff}$ of an unfrozen soil with the same liquid water content if there is ice present. The amount of ice present is proportional to the water content prior to freezing and any water moving into the soil volume sampled by TDR probe.

He and Dyck (2012) showed that dielectric models could be used to calibrate TDR for the measurement of unfrozen water and ice content in frozen soils. Furthermore, He and Dyck (2013) presented evidence to show that the mixing models could be parameterized using unfrozen soil at a variety of water contents and then extended to frozen soils. However, the main limitation of this calibration method is that it only remains valid if the total water content (sum of ice and unfrozen water) within the measurement volume of the TDR probe remains constant while the soil is frozen. This condition is easy to satisfy in laboratory conditions, but may not always be satisfied in the field due to translocation and percolation of water within the soil profile. How this assumption affects the estimation of unfrozen water and ice content for the field measurements presented in this paper and their interpretation will be discussed in the results and discussion section.

To estimate the liquid water and ice content, the confocal ellispsoid model initially developed by Sihvola and Lindell (1990) and further modified by He and Dyck (2013) was calibrated using unfrozen soil samples. Air-dry samples of the topsoil and PG were wetted with known quantities of deionized water to obtain various saturation levels, from air-dry to near saturation at increments of around 0.05 kg $H_2O$ $kg^{-1}$ soil and then equilibrated for at least 24 h at room temperature. The mixed soil samples at each of the prescribed moisture contents were then uniformly packed to a depth of 15 cm in a copper cylinder of 5.08-cm internal diameter in a range of bulk densities to test its influence on parameters of a specific soil. A TDR probe consisting of triple parallel stainless steel needles of 1.6 mm in diameter, 10 cm in length with 1-cm inter-rod spacing was inserted in the center of the cylinder, and connected to a TDR cable tester for measurement of $\varepsilon_{eff}$. Using this experimental data, the parameters for the mixing model were optimized using MathCad software such that the mean squared difference between TDR-measured $\varepsilon_{eff}$ and the modeled $\varepsilon_{eff}$ were minimized (Parametric Technology Corporation 2010).

Once a mixing model is parameterized, it can be used to estimate the unfrozen water content ($\theta_l$) and the ice content ($\theta_i$) given the measured $\varepsilon_{eff}$. However, the $\varepsilon_{eff}$ in a frozen soil at a given temperature is dependent on the amount of ice present. The amount of ice present during a freezing process is proportional to the liquid water content prior to freezing and the temperature of the soil. To estimate the measured $\theta_l$ and $\theta_i$, $\theta_l(\varepsilon_{eff})\varepsilon_{eff}$ and $\theta_i(\varepsilon_{eff})$ calibration curves were simulated using the parameterized confocal ellipsoid model for the field-measured water content just prior to the onset of soil freezing (i.e., the initial water content prior to freezing). To simulate the calibration curves for each initial water content, $\varepsilon_{eff}$ was calculated with the confocal ellipsoid model for a range of pairs of $\theta_l$ and $\theta_i$, such that the total water content was always equal to the initial water content:

$$\theta_l + \theta_i \frac{\rho_i}{\rho_w} = \theta_{l,init} \quad (1)$$

where $\theta_l$ is the liquid, unfrozen water content ($cm^3$ $cm^{-3}$), $\theta_i$ is the ice content ($cm^3$ $cm^{-3}$), $\theta_{init}$ is the initial unfrozen water content prior to freezing, $\rho_w$ is the density of water (assumed to be 1 g $cm^{-3}$) and $\rho_i$ is the density of ice (assumed to be 0.9167 g $cm^{-3}$). The $\theta_l(\varepsilon_{eff})$ and $\theta_i(\varepsilon_{eff})$ for each are then constructed with linear interpolation between $\varepsilon_{eff}$ and $\theta_l$, and $\varepsilon_{eff}$ and $\theta_i$. The calibration curves are presented in Fig. 2.

The data presented in this paper were measured between 2011 Mar. 07 and 2012 Apr. 17. Soil temperature was not logged until 2011 Apr. 05 because cold conditions arrived earlier than expected in the previous fall and their installation was delayed. The TDR probes were installed prior to soil freezing in the fall of 2010, but data logging did not commence until March 2011. The initial water contents required for calculating unfrozen water and ice content in the frozen soil were measured gravimetrically on soil samples taken in the

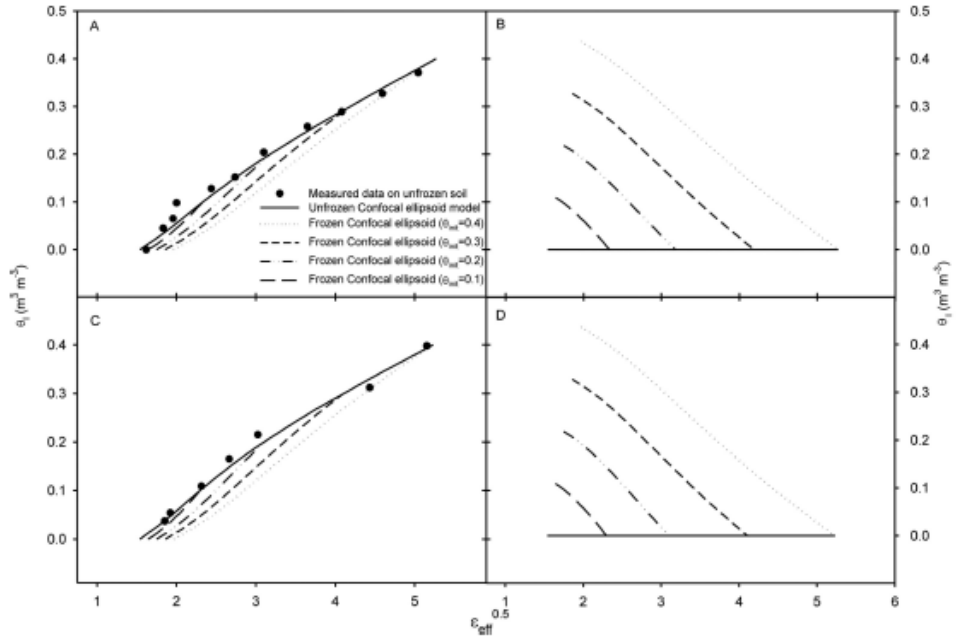


**Fig. 2.** TDR calibration curves for the estimation of liquid unfrozen water content ($\theta_l$) and ice content ($\theta_i$) for the topsoil cap (A & B) and the phosphogypsum (C & D).

fall of 2010 (Turner 2012), and with the TDR data for the winter of 2011 and 2012. It is assumed that soil freezes at temperatures $\leq 0$°C based on field tests that indicate that supercooling of soil water rarely occurs in the field (Golubev 1997). Ice contents, therefore, were only estimated when the soil temperature was $\leq 0$°C. (Miller 1980; Spaans 1996). Soil water content hereafter is referred to as liquid water content and the total water content is the sum of liquid water content and ice content. During the 2011 field season the snowmelt occurred between Mar. 29 and Apr. 15, while during the 2012 field season the snowmelt occurred between Mar. 12 and Apr. 05. The growing season for 2011 started on Apr. 23 and ended Sep. 01, the 2012 data analyzed in this paper ends prior to total soil thawing.

## RESULTS AND DISCUSSION

### Soil Freezing Processes in Different Thickness of Topsoil Treatments

For the 15-cm topsoil treatment, the time series of air temperature and precipitation, liquid water, ice, and soil temperature at six depths below the ground are presented in Fig. 3. Soil froze to a depth greater than 45 cm (Fig. 3G) below the soil/PG interface in both winters and remained frozen well into the spring following snowmelt. The PG at 45 cm below soil/PG interface had completely thawed by 2011 May 17 and had not thawed as of 2012 Apr. 17 (Fig. 3G). An increased temperature lag was observed with increasing depth. During the 2011 snowmelt event, the topsoil reached near saturated conditions for a period of about 2 wk as a result of the reduced hydraulic conductivity of the underlying frozen PG material (Fig. 3D and E). The PG material directly below the interface began thawing on 2011 Apr. 21 marked by PG temperature that was $>0$°C and an increase in liquid water content. The remaining frozen PG material at greater depths underwent similar phase changes for the following 26 d, after which point, the liquid water content stabilized at 0.35 $cm^3\ cm^{-3}$ for the remainder of the growing season. With respect to the topsoil, fluctuations in the water content above the soil/PG interface between May and November 2011 are due to periodic rainfall events followed by periods of evapotranspiration, potential drainage, and subsurface lateral flow. The summer rainfall events between mid-June and November 2011 negligibly affected the soil water content at depths greater than 7.5 cm below soil/PG interface, which indicated that limited amounts of water percolated below the topsoil/PG interface and the water losses

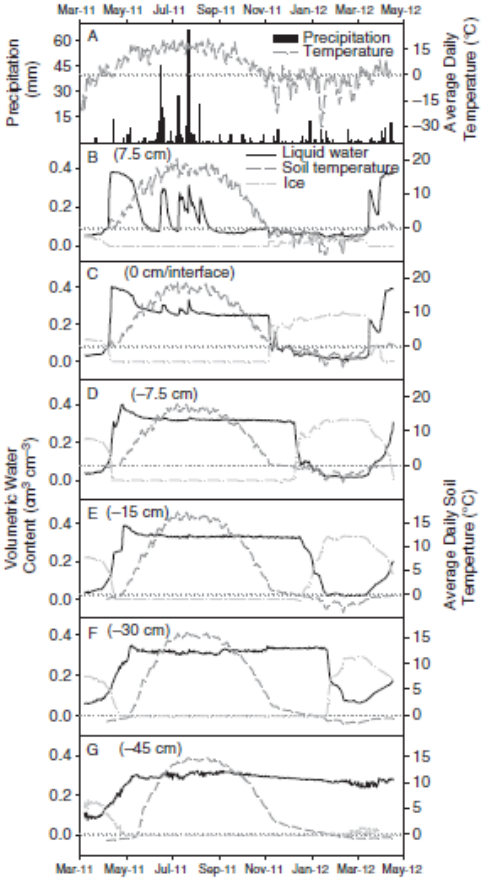


**Fig. 3.** Water and heat dynamics of 15 cm topsoil treatment during March 2011 to April 2012.

from the topsoil following precipitation events were from evapotranspiration or subsurface lateral flow. The hydraulic gradient across the soil/PG interface estimated with the matric potential sensors, however, suggests that there are discrete periods following precipitation events that could contribute to downward percolation which will be explored later in this paper.

Winter 2011–2012 was relatively warm compared with the previous 2010–2011 winter. The topsoil layer (Fig. 3B) was dry because of the low precipitation in the fall 2011 and as a result of limited winter precipitation total soil water content remained relatively constant during the winter. Total soil water content at the soil/PG interface and below (Fig. 3C–G) was much higher at the onset of soil freezing ($>0.3$ cm$^3$ cm$^{-3}$) in the fall of 2011 and a significant drop in liquid water content was observed as soil froze. As the PG material froze, the estimated liquid water content decreased and the estimated ice content increased.

The soil water content at 7.5 cm above the soil/PG interface (Fig. 3B) increased concurrently with the snowmelt events and exceeded the initial water content indicating infiltration of snowmelt. Figure 3C shows a similar pattern to Fig. 3B in that percolation appeared to be restricted by the presence of ice in the underlying PG layer, which was a result of the high water content in the fall of 2010 (Fig. 3D). Although, a few thawing–freezing cycles occurred during the winter of 2012, only the refreezing event of 2012 Mar. 27 resulted in refreezing of infiltrating water.

Figures 4 and 5 illustrate the soil water content and temperature measurements for 30- and 46-cm topsoil cap treatments, respectively. Figure 3A, Fig. 4A and Fig. 5A are the meteorological conditions at the surface, but are repeated to show the correlation between surface boundary conditions and soil water dynamics.

Figsures 4 and 5 are similar to Fig. 3 (15-cm treatment) in many respects. Steep increases in water content in the topsoil cap and PG during the snowmelt periods were observed. The date at which the snowmelt reached each depth increased with depth especially in the PG because the PG took longer to thaw. Liquid water content in the topsoil responded very rapidly to summer rainfall throughout the whole topsoil cap as indicated by the liquid water content response measured by the TDR probes at the soil/PG interface (Fig. 3C, Fig. 4D and Fig. 5E). The shallower the topsoil depth, the greater the magnitude of the response of the water content change to the rainfall events (i.e., Fig. 5B > Fig. 5C > Fig. 5D > Fig. 5E) but the PG water content did not change very much. The topsoil was relatively dry after August 2011 due to the small amounts of autumn rainfall. Total water content in the PG layers (Fig. 3D–G, Fig. 4E–G and Fig. 5F–G) remained relatively constant at approximately 0.35 cm$^3$ cm$^{-3}$ during the periods after spring snowmelt event and before winter 2011. Despite the lack of snow in the winter of 2011–2012, snowmelt infiltration into the topsoil was very efficient because it was so dry from the previous fall. There is evidence of refreezing of snowmelt in the topsoil cap in March 2012, but this refreezing only resulted in a small amount of ice formation due to the initially dry soil conditions and as a result, infiltration was not inhibited. The observed water content at the interface of the three treatments was higher than the overlying topsoil cap, but lower than the underlying PG. The interface is generally the boundary between differing materials which may disrupt vertical water movement as discussed in Dyck and Kachanoski (2009). The water content at the interface of the 15-cm plot treatment (Fig. 3C) was consistently higher than that of the 30-cm

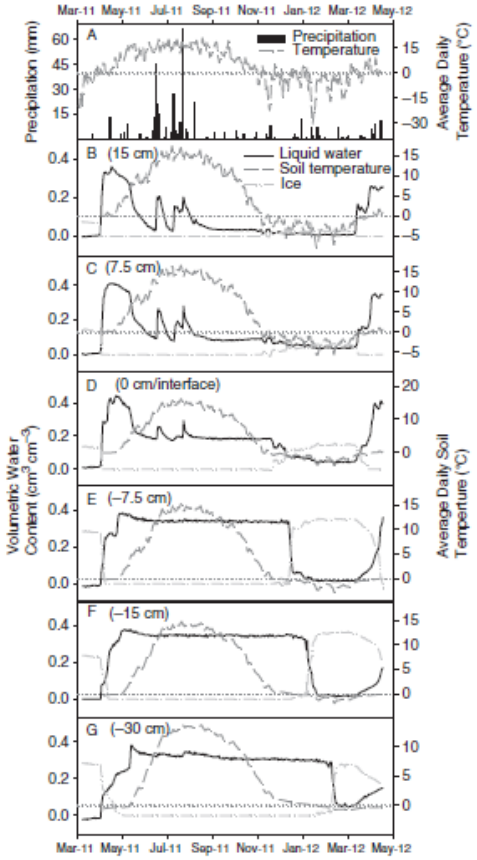


**Fig. 4.** Water and heat dynamics of 30 cm topsoil treatment during March 2011 to April 2012.

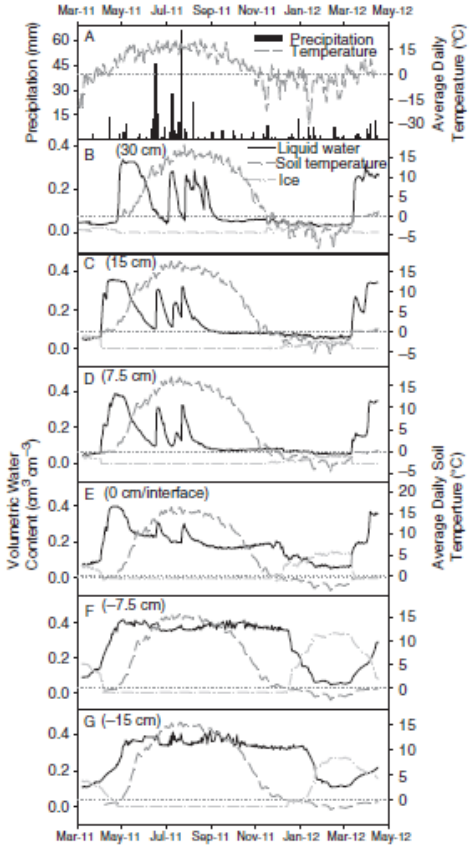


**Fig. 5.** Water and heat dynamics of 46 cm topsoil treatment during March 2011 to April 2012.

treatment (Fig. 4D) and 46-cm treatment (Fig. 5D), which could be due in part to greater evapotranspirational demand from the 30- and 46-cm plots as evident by their slightly more robust plant growth during the growing season (not shown here). The variability among total soil water contents between the various plot interfaces may be explained by multiple factors including: (1) topographical variability of soil/PG gradients resulting in convergence or divergence of lateral flow; and (2) misrepresentative proportion of soil versus PG material within the sample volume of the horizontally installed TDR probes along the soil/PG interface resulting in measurements more reflective of PG than of soil. Generally, the interface between the two layers is characterized by the very transient and variable moisture regime of the topsoil cap and very steady moisture regime in the PG.

The lack of fluctuation of water contents observed in the PG during the growing season is likely a result of the nature of the hydraulic properties between the soil and PG as well as the evapotranspirational demand of the active vegetation. However, increases in water content of the PG material at deeper depths were observed for the 30-cm plot following high magnitude precipitation events (Fig. 4G), which could be attributed to preferential flow paths. The decrease in water storage within the topsoil cap could also be attributed to plant transpiration and potential subsurface lateral flow. Utilization of pore water from the PG material by the

plants was minimal because of the lack of roots within the PG material. Field observations indicated that the majority of root material was located within the topsoil cap and concentrated on the PG/soil interface (L. Turner, unpublished data). The only time when the water content in the PG appeared to increase significantly was during soil thawing, suggesting deeper movement of snowmelt when the vegetation was still dormant.

### Estimation of Cumulative Snowmelt Infiltration into Topsoil and Net Vertical Flux within PG

To better assess the performance of the various capping depths, the net water flux within the topsoil cap and the underlying PG material was quantified using the one-dimensional soil water continuity equation:

$$\frac{\partial\theta(z,t)}{\partial t} = \frac{\partial q(z,t)}{\partial z} \quad (2)$$

Where θ is the total water content ($cm^3\ cm^{-3}$), $t$ is time (s), $q$ is the soil water flux ($cm^3\ cm^{-2}\ s^{-1}$) and $z$ is depth (m). Integration of both sides of Eq. 2 between two depths (z1 and z2) results in:

$$\frac{\partial}{\partial t}\int_{z1}^{z2}\theta(z,t)dz = -\int_{z1}^{z2}\frac{\partial q(z,t)}{\partial z}dz \quad (3a)$$

which may be expressed as:

$$\frac{\partial W_{z1,z2}(t)}{\partial t} = q(z1,t) - q(z2,t) \quad (3b)$$

where $W_{z1,z2}(t)$ is the soil water storage between depths z1 and z2 as a function of time, and $q(z1,t)$ and $q(z2,t)$ are the net vertical soil water fluxes at depths z1 and z2, respectively. In other words, the change in soil water storage between depths z1 and z2 over a period of time is equal to the net soil water flux between those two depths over the same time period. For discrete time periods that are small enough such that $q(z1,t)$ and $q(z2,t)$ do not change significantly with time, Eq. 3b may be simplified to:

$$\Delta W_{z1,z2|\Delta t} = [q(z1) - q(z2)]\Delta t \quad (4)$$

Which means the change in soil water storage between two depths measured at two discrete points in time is a result of the cumulative, net vertical flux occurring in the soil volume bounded by depths z1 and z2.

The cumulative, net vertical flux integrates fluxes affecting the change in total soil water storage between two depths such as infiltration, drainage, evapotranspiration and lateral flow over the time period in question. Positive changes in storage indicate that the cumulative flux coming into the soil volume (i.e., infiltration – evapotranspiration) bounded by z1 and z2 was greater than the net cumulative flux leaving that volume (i.e., percolation and other losses such as lateral flow), whereas decreases in soil water storage indicate the opposite. No change in soil water storage indicates a scenario where net water coming into the volume bounded by z1 and z2 was equal to the net water going out and those fluxes may or may not be zero.

Equation 3 was applied to two separate soil volumes, topsoil cap and PG, during periods of time during the snowmelt period and growing season. Estimates for the topsoil caps were calculated using the measurements from the vertically installed TDR probes and estimates for the PG material was calculated using the measurements from the horizontally installed probes at −7.5 and −15 cm for discrete time intervals during the snowmelt period of 2011. Setting z = 0 at the topsoil/PG interface with z increasing upward (Table 1) results in z1 = depth of topsoil, z2 = 0 cm for the topsoil cap, and z1 = 0 cm, z2 = −7.5 cm, z3 = −15 cm for the PG. The vertical probes spanned the entire depth of the topsoil cap. The vertical probes therefore, measured the average soil water content over the entire topsoil cap, which can then be used to estimate soil water storage by multiplying by the length of the TDR probe. For the horizontal probes in the PG, each TDR probe is assumed to represent the 3.75-cm of PG material above and below its location.

Time series of the vertical TDR probe measurements for the 2011 snowmelt period and growing season are shown in Fig. 6. Snowmelt began on 2011 Mar. 29 as marked on Fig. 6 when the average air temperature exceeded 0°C (solid grey vertical line in Fig. 6A). The start of infiltration was noted by the initial increase in volumetric water content (solid black vertical lines in Fig. 6B–D). Field observations noted that all snow had melted and infiltrated before 2011 Apr. 27.

During the spring snowmelt, the underlying PG material remained frozen limiting the amount of water able to drain from the topsoil cap. As a result of this condition the topsoil within the 15-cm plot approached near saturation during the early spring, while the 30- and 46-cm plots did not as a result of their increased storage capacity. Restrictions in flow between the soil and PG material can be attributed to the hydraulic nature of the underlying PG material, which has a saturated hydraulic conductivity that is an order of magnitude lower than that of the capping soil. However, the hydraulic conductivity is further lowered by the presence of ice-filled pore space within the PG material that had already thawed within the topsoil cap earlier in the spring. Water content in the topsoil caps began to decrease only when the underlying PG material had a temperature of >0°C, indicating that the presence of ice was restricting percolation of water from the topsoil into the PG. On 2011 Apr. 23, the 15-cm plot started to lose water and 2011 Apr. 26 so did the 30- and 46-cm plots (dashed dark grey vertical lines in Fig. 6B–D). Before these dates the PG material directly underlying the capping soil had an average temperature <0°C and can be assumed to have ice within the pore space restricting flow (Fig. 6B–D; Figs. 3–5).

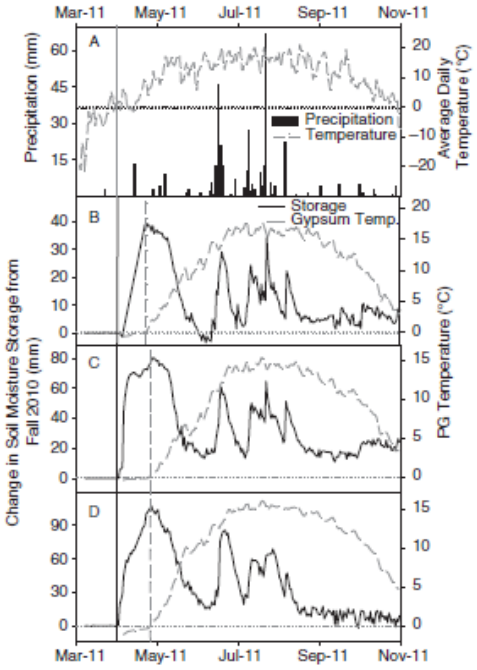


**Fig. 6.** Changes in storage within topsoil cap for the various capping soil treatments.

Snowmelt infiltration into the topsoil cap was estimated between the beginning of snowmelt (2011 Mar. 29) and the beginning of the active growing season (2011 Apr. 23). Between these dates the potential evapotranspiration is negligible due to the limited photosynthetic ability of the plants during this part of the year where the average air temperature is <1°C. The amount of infiltration into the topsoil cap as it pertains to available water from spring snowmelt (2011 Mar. 29 to Apr. 23) follows a general linear relationship with capping depth (Table 3). The estimates for infiltration for the 15-, 30- and 46-cm treatment are 38, 77 and 97 mm, respectively, indicating that an increase in soil capping depth results in an increase in infiltration of spring melt water into the capping soil. Conversely, this would suggest that the potential for runoff and/or subsurface lateral flow is highest in treatments where the topsoil is limited (i.e., ≤ 15 cm), due to the insufficient capacity of the topsoil to store the added water. Infiltration estimates for the 15- and 30-cm treatment would suggest that potential runoff and subsurface lateral flow could be occurring during snowmelt periods; however, the 46-cm treatment exhibits an excess amount of water within the topsoil cap than what was available from snowmelt and spring precipitation. (Table 3). In this regard, more water has been observed to enter the 46-cm capping soil than is available from the environment. This phenomenon could be explained by localized variability in relief underlying the 46-cm plot that could contribute to the convergence of subsurface water flow as well as runoff water from the adjacent 15-cm plot. In general, the relationship between the amount of infiltration and capping soil thickness was linearly related, whereby the thicker the topsoil cap the greater the snowmelt infiltration capacity.

Estimates of net vertical flux can be measured from the amount of total water entering and leaving the PG as measured by the horizontally installed TDR probe directly below the soil/PG interface. Integrating the changes in total water content below the soil/PG interface with depth, from 2011 Apr. 23 to Sep. 01, gives an estimation of the net vertical flux below the interface during the entire growing season. This estimation is conservative with regards to the potential drainage because it does not take into account the potential percolation that could have occurred immediately following the snowmelt infiltration as represented by the hump in the water content distributions curves (Fig. 3D, Fig. 4E, Fig. 5F). As a result of this simplification the net vertical flux estimates are reflective of the overall water balance within the PG material directly below the

**Table 2. Parameters of confocal ellipsoid models for estimating unfrozen water and ice content**

| | Parameters | | | |
|---|---|---|---|---|
| Soil type | Self-consistency | Aspect | RMSE[z] | Bulk density |
| Topsoil[y] | 0.649 | 1 | 0.809 | 1.3 |
| Gypsum[x] | 0.537 | 1 | 0.918 | 1.2 |

[z]RMSE = 1N*i* = 1N*εi* − *εi*.
[y]Topsoil is Mundare loamy sand.
[x]Gypsum is phosphogypsum tailings.

**Table 3. Estimates of cumulative spring infiltration into the topsoil cap and net storage and vertical flux within PG material over the 2011 growing season**

| Soil treatment | Available $H_2O$ (SWE[z] + Precip.[y]) (mm) | Spring[x] cumulative infiltration – topsoil (mm) | Net cumulative vertical flux[w] – PG (mm) |
|---|---|---|---|
| 15 cm | 88 | 38 | 20 |
| 30 cm | 90 | 77 | 28 |
| 46 cm | 82 | 97 | 32 |

[z]Snow water equivalent.
[y]Cumulative precipitation on site from 2011 Feb. 26 to Apr. 23.
[x]2011 Mar. 29 through to Apr. 23.
[w]15-cm-thick layer of phosphogypsum (PG) directly below soil/PG interface.
[v]2011 Apr. 23 to Sep. 01.

soil/PG interface, showcasing the net gains and/or losses during the entire 2011 growing season.

The cumulative, net vertical flux estimates (Eq. 4) over the entire growing season (2011 Apr. 23 to Sep. 01) for the PG layer directly below the interface were 20, 28 and 32 mm for the 15-, 30- and 46-cm treatments, respectively. The increase in the estimated cumulative, net vertical flux of the PG material with increasing topsoil depth is primarily due to the increased availability of infiltrating spring snowmelt water that is present within each treatment. The more water that is available within the topsoil, from infiltration, the greater the potential will be for percolation and potential drainage. Although this result is counterintuitive with respect to conventional hypotheses regarding topsoil capping depth and drainage estimates, it can be explained by the limited ability of the loamy sand material to retain water (Fig. 1) in combination with the increased amount of available water that is permitted to infiltrate into the topsoil. For example, the amount of water that infiltrated into the topsoil cap of the 15-cm treatment was 38 mm, which accounted for 43% of the available water during spring snowmelt, compared with that of the 30-cm treatment that allowed 86% of available water to infiltrate. The increased infiltration capacity of the deeper capping soils allows more water to enter into the system; however, the inability of the loamy sand material to retain the water allows for expedited redistribution of water within the reclaimed system resulting in increased estimates for net vertical flux with increased capping soil depth.

### Direction of Net Vertical Flux

Changes in soil water storage, or net vertical flux, within the PG material, between the months of April and September 2011, are positive indicating that in general the amount of soil water entering into the PG from the topsoil cap is greater than the amount of soil water leaving the PG material; however, it can only be assumed that the water is percolating from the topsoil into the PG. To estimate the direction of flow total hydraulic head was quantified using the matric potential sensors installed at +7.5 and −7.5 cm from the soil/PG interface. The difference in total hydraulic head between +7.5 and −7.5 cm was used to obtain the hydraulic gradient across the interface.

During the snowmelt of 2011, the hydraulic gradients for the 15-, 30- and 46-cm treatment were all positive, indicating that the overall water flux was in the negative direction (downward) and that drainage/percolation was occurring. For the 15-, 30- and 46-cm treatments the gradients remained positive for 32, 47 and 39 d, respectively, from early April to mid-May, 2011 (Fig. 7). During this significant period of time soil water losses within the topsoil caps, following snowmelt infiltration, is most likely primarily a function of drainage and can be minimally attributed to active evapotranspiration that was limited during the early spring. However, from

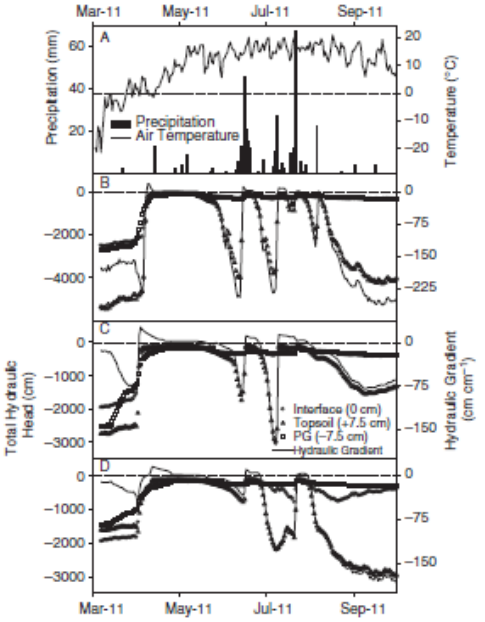


**Fig. 7.** Total hydraulic head and hydraulic gradient across soil/PG interface for various capping soil treatments during March 2011 to November 2011.

mid-May through to September 2011 evapotranspirational demand increased, resulting in periods of negative hydraulic gradient across the interface, thus indicating upward water flux from the moist PG material to the drier loamy sand topsoil. This general summer trend was interrupted by several high magnitude rainfall events on 2011 Jun. 16, Jul. 09 and Jul. 22, which produced 45, 27 and 66 mm of precipitation, respectively (Fig. 6A). During these rainfall events ( >25 mm) positive hydraulic gradients were observed across the soil/PG interface for each of the topsoil treatments, indicating that drainage/percolation was occurring. The total amount of days from the start of snowmelt to the end of the growing season (2011 Mar. 29 to Sep. 01) that were observed to have drainage/percolation events present were 49, 78 and 57 for the 15-, 30- and 46-cm treatments, respectively. No trend appears to be present with regards to capping soil treatment and duration of drainage/percolation events; however, the 30-cm capping soil treatment was observed to have the longest periods of drainage/percolation, accounting for 44% of the growing season, compared to that of the 15- and 46-cm treatments that have drainage/percolation estimates that account for 28 and 33% of the growing season (2011 Apr. 23 to Sep. 01).

### Uncertainties in Soil Water, Infiltration and Net Flux Estimates

Sources of errors in the snowmelt infiltration estimates can be traced back to the distribution of water content measurements that were used to compute storage. As a result of increasing depth computation in deriving storage terms, the errors will linearly increase with increasing capping depth; however, variability between the various water content measurements during the steady state observations was very small ($<0.01$ $cm^3$ $cm^{-3}$). Other sources of error with regards to infiltration estimates include the possibility of steady state flow within the PG material during snowmelt periods. For example, the topsoil cap of the 15-cm treatment had a very high water content that remained stable during snowmelt infiltration, we assumed the lack of water movement was due to the limited ability of the frozen PG material to transmit the water; however, under steady state flow dynamics water content distribution within the topsoil cap would not change. The result of this assumption could have been an underestimation of the potential amount of available water infiltrating into the 15-cm plot; however, the evidence for limited flow dynamics below the soil/PG interface during the early spring snowmelt event indicated that water movement below the interface was limited as evident by the minimal increase in water content within the PG material prior to PG thaw. Furthermore, the hydraulic gradient across the soil/PG interface within the 15-cm plot remained negative until 2011 Apr. 09, indicating a positive flux direction; however, after 2011 Apr. 09 the interface temperature exceed 0°C and the hydraulic gradient reversed its direction, indicating drainage (Fig. 7). This does not entirely rule out the possibility of drainage during periods where there is no observable change in soil water storage in the topsoil cap, but it is likely very small if it does occur.

As mentioned above, TDR estimates of unfrozen water and ice content during periods when the soil is frozen are based on the assumption that the total water content within the sampling volume of the TDR probe does not change. Unfortunately, it is during times of snowmelt infiltration into frozen soils that this assumption is most likely to be violated. Because soil thawing and snowmelt infiltration both increase the liquid water content of the soil, there is some uncertainty associated with the unfrozen water and ice content estimates presented, especially in the more responsive topsoil cap. However, because of the very dry fall soil water conditions in the topsoil, these uncertainties are not expected to cause a misinterpretation of the processes occurring in the field. Furthermore, the estimates of net cumulative vertical flux are based on soil water measurements in unfrozen soil where the constant total water content assumption is no longer required.

## CONCLUSION

TDR-estimated liquid water and ice contents in frozen soils were used to aid in the interpretation of hydrological processes in frozen soils at a reclaimed site. Results indicate that increases in capping soil thickness resulted in increases in infiltration of available snowmelt water into the capping soil and that lateral runoff estimates increased with decreasing capping depth. This result is primarily a response to the increase in the capacity of the deeper capping soils to infiltrate water; however, the limited ability of the loamy sand topsoil to retain water allows for the expedited redistribution of water within the reclaimed system. Therefore, greater capping soil depths appear to be associated with greater potential for percolation below the capping soil. Soil water balance estimates for the PG material directly underlying the treatment plots indicate that an increase in capping soil depth increased the net vertical flux within the first 15 cm of PG, which reflects the limited water retention characteristics of the topsoil. The estimated hydraulic gradient across the soil/PG interface indicates that during the early spring and severe precipitation events ($>25$ mm) drainage/percolation was occurring throughout all treatment depths; however, no clear trend was present in relation to treatment depth and duration of drainage/percolation events.

This research also confirms the importance of establishing very clear reclamation goals to aid in the selection of capping materials for mine tailings. At the minimum, a reclaimed tailing stack or pile should be able to support the establishment and maintenance of vegetation. It should limit exposure of environmental receptors to potential contaminants within the tailings. A soil with good infiltration and water-holding capacity should be able to aid in achieving these two goals. However, as shown in this paper, the thickness of the topsoil cap in combination with its infiltrability and water-holding capacity is a key consideration as well. Under the conditions reported in this paper a thicker topsoil cap resulted in greater water movement through the underlying PG tailings, which may or may not be desirable depending on the reclamation goals. Furthermore, moisture dynamics during freeze–thaw periods need to be taken into consideration when assessing reclamation goals and successful site reclamation.

## ACKNOWLEDGMENTS

Funding for this research was provided by the Natural Sciences and Engineering Research Council of Canada, Agrium, Inc. and the University of Alberta. Special thanks also go to Dick Puurveen and the research staff at the Ellerslie Research Station for technical support.

**Alberta Agriculture and Rural Development. 2012.** AgroClimatic information service [Online] Available: http://www.agric.gov.ab.ca/app116/stationview.jsp. [2012 Apr. 22].

**Campbell Scientific (Canada) Corp. 2007.** Products: sensors and supporting hardware [Online] Available: http://www.campbellsci.ca/Products_Sensors.html. [2011 Sep. 12].

**Cary, J. W., Campbell, G. S. and Papendick, R. I. 1978.** Is the soil frozen or not? An algorithm using weather records. Water Resour. Res. **4**: 1117–1122.

**Dyck, M. F. and Kachanoski, R. G. 2009.** Measurement of transient soil water flux across a soil horizon interface. Soil Sci. Soc. Am. J. **73**: 1604–1613.

**Environment Canada. 2011.** Canadian climate normal 1971–2000. [Online] Available: http://climate.weatheroffice.gc.ca/climate_normals/resultse.html?stnID=1886&lang=e&dCode=0&province=ALTA&provBut=&month1=0&month2=12. [2011 Mar. 15].

**Environment Canada. 2012.** National climate data and information archive. [Online] Available: http://www.climate.weatheroffice.gc.ca/advanceSearch/searchHistoricDataStations_e.html?searchType=stnName&timeframe=1&txtStationName=fort+saskatchewan&searchMethod=contains&optLimit=yearRange&StartYear=1840&EndYear=2012&Month=9&Day=21&Year=2012&selRowPerPage=25&cmdStnSubmit=Search. [2012 Mar. 20].

**Golubev, V. V. 1997.** Ice formation in freezing grounds. Pages 87–91 *in* S. Knutsson, ed. Ground freezing: frost action in soils. A. A. Balkema Publishers, Rotterdam, the Netherlands.

**Granger, R. J., Gray, D. M. and Dyck, G. E. 1984.** Snowmelt infiltration to frozen prairie soils. Can. J. Earth. Sci. **21**: 669–677.

**Gray, D. M. and Granger, R. J. 1985.** Snow management practices for increasing soil water reserves in frozen prairie soils. Proc. Watershed management in the eighties, Denver, CO.

**Gray, D. M., Toth, B., Zhao, L. T., Pomeroy, J. W. and Granger, R. J. 2001.** Estimating areal snowmelt infiltration into frozen soils. Hydrol. Process. **15**: 3095–3111.

**Hall, D. K., Foster, J. L., DiGirolamo, N. E. and Riggs, G. A. 2012.** Snow cover, snowmelt timing and stream power in the Wind River Range, Wyoming. Geomorphology **137**: 87–93.

**Hallin, I. L. 2009.** Evaluation of a substrate and vegetation cover system for reclaimed phosphogypsum stacks at Fort Saskatchewan, Alberta. M.Sc. thesis. University of Alberta, Edmonton, AB. 95 pp.

**Hayashi, M., Jackson, J. F. and Xu, L. 2010.** Application of versatile soil moisture budget model to estimate evaporation from prairie grassland. Can. Water Resour. J **35**: 187–208.

**He, H.**, and **Dyck, M. F. 2013.** Application of multiphase dielectric mixing models for understanding the effective dielectric permittivity of frozen soils. Vadose Zone J. **12**: doi: 10.2136/vzj2012.0060.

**Iwata, Y., Hayashi, M. and Hirota, T. 2008.** Comparison of snowmelt infiltration under different soil-freezing conditions influenced by snow cover. Vadose Zone J. **7**: 79–86.

**Jackson, E. M. 2009.** Assessment of soil capping for phosphogypsum stack reclamation at Fort Saskatchewan, Alberta. M.Sc. thesis. University of Alberta, Edmonton, AB. 162 pp.

**Jackson, E. M., Naeth, M. A., Chanasyk, D. S. and Nichol, C. K. 2011.** Phosphogypsum capping depth affects revegetation and hydrology in western Canada. J. Environ. Qual. **40**: 1122–1129.

**Janowicz, J. R., Gray, D. M. and Pomeroy, J. W. 2002.** Characterization of snowmelt infiltration scaling parameters within a mountainous subarctic watershed. Proc. Eastern Snow Conference, Stowe, VT.

**Kane, D. L. 1978.** Snowmelt-frozen soil characteristics for a subarctic setting. Institute of Water Resources, University of Alaska, Anchorage, AK. 6 pp.

**Kane, D. L. 1980.** Snowmelt infiltration into seasonally frozen soils. Cold Reg. Sci. Technol. **3**: 153–161.

**Kane, D. L. and Stein, J. 1983.** Water movement into seasonally frozen soils. Water Resour. Res. **19**: 1547–1557.

**Miller, R. D. 1980.** Freezing phenomena in soils. Pages 254–299 *in* D. Hillel, ed. Applications of soil physics. Academic Press, New York, NY.

**Parametric Technology Corporation. 2010.** Mathcad Software Version 15.0 Student Edition. Parametric Technology Corporation, Needham, MA.

**Rutherford, P. M., Dudas, M. J. and Arocena, J. M. 1995.** Trace elements and fluoride in phosphogypsum leachates. Environ. Technol. **16**: 343–354.

**Samek. 1994.** Environmental impacts of phosphogypsum. Sci. Total Environ. **149**: 1–38.

**SENES. 1987.** An analysis of the major environmental and health concerns of phosphogypsum tailings in Canada and methods for their reduction. Prepared by: SENES Consultants Limited. Willowdale, ON. 560 pp.

**Sihvola, A. H. and Lindell, I. V. 1990.** Polarizability and effective permittivity of layered and continuously inhomogeneous dielectric ellipsoids. J. Electromagn. Waves Appl. **4**: 1–26.

**Spaans, E. J. A. and Baker, J. M. 1995.** Examining the use of time domain reflectometry for measuring liquid water content in frozen soil. Water Resour. Res. **31**: 2917–2925.

**Stadler, D., Flühler, H. and Jansson, P. 1997.** Modeling vertical and lateral water flow in frozen and sloped forest soil plots. Cold Reg. Sci. Technol. **26**: 181–194.

**Stadler, D., Stähli, M., Aeby, P. and Flühler, H. 2000.** Dye tracing and image analysis for quantifying water infiltration into frozen soils. Soil Sci. Soc. Am. J. **64**: 505–516.

**Stähli, M. and Lundin, L. C. 1999.** Soil moisture redistribution and infiltration in frozen sandy soils. Water Resour. Res. **35**: 95–103.

**Stähli, M., Bayard, D., Wydler, H. and Flühler, H. 2004.** Snowmelt infiltration into alpine soils visualized by dye tracer technique. Arct. Antarct. Alp. Res. **36**: 128–135.

**Stein, J. and Kane, D. L. 1983a.** Monitoring the unfrozen water content of soil and snow using time domain reflectometry. Water Resour. Res. **19**: 1573–1584.

**Stein, J. and Kane, D. L. 1983b.** Water movement into seasonally frozen soils. Water Resour. Res. **19**: 1547–1557.

**Thorne, W. E. R. 1990.** Reclamation of a phosphogypsum tailings pond: an examination of the relevant issues. MEDes thesis. University of Calgary, Calgary, AB. 330 pp.

**Turner, E. L. 2012.** Influence of soil cap depth and vegetation on reclamation of phosphogypsum stacks in Fort Saskatchewan, Alberta. M.Sc. thesis. University of Alberta, Edmonton, AB. 172 pp.

**van Genuchten. M. Th. 1980.** A closed-form equation for predicting the hydraulic conductivity of unsaturated soils. Soil Sci. Soc. Am. J. **44**: 892–898.

**Wissa, A. E. Z. 2002.** Phosphogypsum disposal and the environment. Pages 195–202 *in* Proc. of an international workshop on current environmental issues of fertilizer production. Prague, Czech Republic.

**Zhao, L. and Gray, D. M. 1997.** A parametric expression for estimating infiltration into frozen soils. Hydrol. Process. **11**: 1761–1775.

**Zhao, L. T., Gray, D. M. and Toth, B. 2002.** Influence of soil texture on snowmelt infiltration into frozen soils. Can. J. Soil Sci. **82**: 75–83.